NOTICE

The quality of this microform is heavily dependent upon the quality of the original thesis submitted for microfilming. Every effort has been made to ensure the highest quality of reproduction possible.

If pages are missing, contact the university which granted the degree.

Some pages may have indistinct print especially if the original pages were typed with a poor typewriter ribbon or if the university sent us an inferior photocopy.

Reproduction in full or in part of this microform is governed by the Canadian Copyright Act, R.S.C. 1970, c. C-30, and subsequent amendments.

AVIS

La qualité de cette microforme dépend grandement de la qualité de la thèse soumise au microfilmage. Nous avons tout fait pour assurer une qualité supérieure de reproduction.

S'il manque des pages, veuillez communiquer avec l'université qui a conféré le grade.

La qualité d'impression de certaines pages peut laisser à désirer, surtout si les pages originales ont été dactylographiées à l'aide d'un ruban usé ou si l'université nous a fait parvenir une photocopie de qualité inférieure.

La reproduction, même partielle, de cette microforme est soumise à la Loi canadienne sur le droit d'auteur, SRC 1970, c. C-30, et ses amendements subséquents.

Velocity Measurements by Floats and Float Diffusion

by

Kadem El-haddi

Thesis submitted to the School of Graduate Studies
as partial fulfillment of the requirements
for the degree of M.A.Sc. in
Civil Engineering
UNIVERSITY OF OTTAWA

OTTAWA, CANADA, 1990

NOTICE

The quality of this microform is heavily dependent upon the quality of the original thesis submitted for microfilming. Every effort has been made to ensure the highest quality of reproduction possible.

If pages are missing, contact the university which granted the degree.

Some pages may have indistinct print especially if the original pages were typed with a poor typewriter ribbon or if the university sent us an inferior photocopy.

Reproduction in full or in part of this microform is governed by the Canadian Copyright Act, R.S.C. 1970, c. C-30, and subsequent amendments.

AVIS

La qualité de cette microforme dépend grandement de la qualité de la thèse soumise au microfilmage. Nous avons tout fait pour assurer une qualité supérieure de reproduction.

S'il manque des pages, veuillez communiquer avec l'université qui a conféré le grade.

La qualité d'impression de certaines pages peut laisser à désirer, surtout si les pages originales ont été dactylographiées à l'aide d'un ruban usé ou si l'université nous a fait parvenir une photocopie de qualité inférieure.

La reproduction, même partielle, de cette microforme est soumise à la Loi canadienne sur le droit d'auteur, SRC 1970, c. C-30, et ses amendements subséquents.

ISBN 0-315-60609-6

UNIVERSITÉ D'OTTAWA
UNIVERSITY OF OTTAWA

Abstract

For many centuries, streams, rivers and oceans have been used for the disposal of all kinds of man-made wastes and pollutants, of which some are extremely harmful. Studies of the spreading of these effluents require the knowledge of the velocity distribution and current patterns. A practical and alternative way to fixed current meters is the use of tracers such as combined floats or drogues.

The purpose of this laboratory investigation is to study the use of combined floats, consisting of a floating disc and a spherical weight, for velocity and discharge measurements and float diffusion. An experimental program was carried out in the hydraulics laboratory and it was found useful to investigate the effect of i) length and width of the study section, ii) float size and its depth of immersion and finally iii) the velocity itself (the magnitude). Because of the limitations involved, three float sizes were selected for which only the disc diameter varied; the sphere diameter, however, was kept constant. When compared to the velocity measured by the Pitot tube, a combination of the smallest float submerged at channel depths above 0.6d in a relatively uniform small section (width and length) was found more appropriate and consequently more accurate.

Float diffusion on the other hand was found to depend mainly on the study section length and the float size. Flow velocity was not found to be critical, especially for large floats, and the diffusion width seems to be much diminished when large floats are used.

Acknowledgements

The author is deeply indepted to his thesis advisor, Dr. Richard G. Warnock, for his assistance, professional guidance and support throughout the course of this study.

Special thanks are also due to the technician Mr. Robert Moore, for his willing assistance during the experimental stage of the project. Finally, deep appreciation is expressed to the Algerian Government for providing the financial support.

Notations

a, b	= Calibration coefficients for current meters
a_t	= Tangential acceleration
A_0	= Constant equal $\frac{1}{k}$
A_d	= Area of the disc
A_f,A_p	= Area of the body considered
A_s	= Area of the sphere
B_0	= Constant
C	= Constant or Chezy coefficient
c	= Concentration
C_b,C_w	= Constants
C_D	= Total drag coefficient
C_{D_p}	= Pressure drag coefficient
C_{D_f}	= Friction drag coefficient
C_{D_d}	= Drag coefficient for the disk
C_{D_s}	= Drag coefficient for the sphere
d	= Particle diameter
D	= Depth
$E(k)$	= Turbulent energy
f	= Depth of immersion of the sphere
F_B	= Buoyant force
Fe_d	= External forces on the disc

Fe_s = External forces on the sphere

F_D = Total drag force

F_{D_d} = Drag force on the disc

F_{D_f} = Frictional drag force

F_{D_p} = pressure drag force

F_{D_s} = Drag force on the sphere

Fr = Froude number

F_t = Total force

g = Acceleration due to gravity

H = Depth

h = Depth or head

h_d = Thickness of the disc

k = Von Karman coefficient

K = Wave number

K_l = Wave number associated with eddy size l

k_s = Coefficient

K_d = Added mass coefficient for the disc

K_s = Added mass coefficient for the sphere

K_1,K_2,K_3,K_4 = Coefficients

l,l_e,L = Distance or length scale

$\bar{l}$ = Arithmetic mean distance

m = Mass of the fluid displaced

m = A coefficient that depends on the channel roughness

M = Total mass

m_d	= Mass of the disc
m_s	= Mass of the sphere
N	= Repetitive runs
n	= Number of revolutions
p	= Pressure
q	= Flow rate
$\bar{q}$,q_*	= Arithmetic mean of the flow rate
R	= Hydraulic radius
r_p	= Particle radius
R_d	= Disc radius
R_s	= Sphere radius
$R_p(\xi)$	= Lagrangian correlation coefficient
Re	= Reynolds number
s	= Surface
t	= Time
$\bar{t}$	= Arithmetic mean of the time
T	= Tension
t_x	= Lagrangian micro-time-scale
t_*	= Lagrangian time scale for fluid velocity fluctuation
t_{*p}	= Lagrangian time scale for particle velocity fluctuation
u	= Velocity,average velocity
v_0,u_0,u_m	= Mean velocity
U_*,u_*	= Friction velocity
v	= Velocity

v_d,v_{f_d}	= Velocity of the disc
v_m	= Mean velocity
v_r	= Relative velocity
v_s,v_{f_s}	= Velocity of the sphere
v_u	= Water velocity at the surface
V	= Volume
W	= Weight of the body
Z_1,Z_2	= Lateral distance
x, y, z	= Cartesian coordinates
y_0	= Constant of integration
δ_0	= Boundary layer thickness
ϵ_x,ϵ_y,ϵ_z	= Coefficients of turbulent diffusion
$\overline{\epsilon_z}$	= Depth averaged lateral diffusivity
ϵ_{zp}	= Particle diffusivity
θ,ϕ	= Angles
μ	= Dynamic viscosity
ν	= Kinematic viscosity
ρ,ρ_w	= Water density
ρ_d	= Density of the disc
ρ_p	= Particle density
ρ_s	= Density of the sphere
σ^2	= Variance
σ_p^2	= Particle variance

τ	= Shear stress
τ_0	= Shear stress on the bottom of the channel

Contents

List of Tables

List of Figures

Chapter 1

Introduction

1.1 General

Man's first attempts at measuring velocity were undoubtedly by using free floats. This method of floats, seen as the most primitive of all velocity measuring techniques, has played over many centuries an important part in the development of hydraulic concepts and formulas.

Leonardo Da Vinci (1452-1519) was the first to use float techniques to show that the maximum velocity occurs at the free surface of the water. The float he used consisted of a rod with a bladder fixed about 5cm below the upper end and a brick attached to the bottom. This is to say that the use of floats to measure the velocity of the water dates to many years before the concept of discharge was used and even before the notion of hydrometry

was introduced.

A special application of this technique should be mentioned here. One of the fundamental requirements for the study of dispersion in rivers and oceans is the knowledge of the velocity distribution and current patterns. A common and practical way that has shown accuracy in determining this information is by using floats and determining their successive positions. Floats have also shown distinct possibilities in discharge measurement. The only disadvantage in this case is that a detailed knowledge of the geometry of the cross-section studied is required to calculate the area and consequently make the computed flow rates accurate. Their advantage on the other hand is their simplicity of construction and use, particularly in some circumstances such as excessive turbulence and low flow speed conditions where the use of current meters is unsuccessful. Finally, we notice that, historically, Da Vinci's work was the first and most comprehensive one in the subject. Since then, many other investigators recommended the use of floats for flow velocity and discharge measurements, and it is the author's belief that much can be done to improve this technique to be a most suitable and accurate alternative method for velocity and discharge measurements.

1.2 Objectives

The study described has made an investigation of the use of floats for velocity and discharge measurements.

Specifically, the items examined can be summarized as follows:

- Measurement of the velocity by means of combined floats submerged at different depths.
- Determination of the discharge from the float measurement.
- Determination of the dynamical response of the floats to accelerating and decelerating flows.
- Study of the float diffusion.
- Determination of the drag coefficients for the sphere and the discs used.

The last of the above items has been started, then discontinued after three sets of experiments because the drag coefficients for the body shapes used are well known and are available in many references.

1.3 Scope

The study deals primarily with velocity measurement using combined floats. The floats, consisting of a disc floating at the free surface of the water and a sphere submerged at a certain depth, are released in the water; the velocity is then determined by the ratio of the distance to the time the float takes to travel that distance.

More details on the description of the floats and the experiments conducted are presented in the following chapters.

The analysis of the data collected was based on the determination and comparison of the local velocities, mean velocities and discharges obtained from float measurement to those obtained by other means such as Pitot tube for the velocity, weirs and weighing tank for the discharge. Also velocities obtained using a system-balanced drag equation were compared to those obtained by floats, and finally, a theoretical study was conducted to explore the dynamical response of the floats to accelerating and decelerating flows.

Chapter 2

Theoretical Background

2.1 Velocity Distribution In Open Channel Flow

2.1.1 General

The flow in a conduit may be either open channel or pipe flow. Both kinds of flow are similar in many ways but differ in one important aspect. Open channel flow must have a free surface which is subject to atmospheric pressure while pipe flow, confined in a closed conduit, exerts hydraulic pressure only.

Due to the presence of the free surface and the friction along the channel,

velocities in an open channel are not uniformly distributed over the channel section.

Velocity distribution does not depend only on the presence of the free surface and the friction along the channel boundaries, but it depends also on many other factors, such as, the shape of the section, the roughness of the channel, the presence of bends and changes in the channel cross section.

Due to the diversity of factors influencing the velocity, it is quite difficult to establish a general pattern for the velocity distribution in the channel.

Generally speaking, the velocity distribution in the case of an open channel flow is not axisymmetric (as in pipe flow). One might therefore expect to find the maximum velocity at the free surface where the shear stress is negligible. However, the maximum velocity usually occurs below the free surface.

The Prandtl-Von Karman velocity distribution law which predicts that the maximum velocity occurs at the free surface, has been found to be consistent only in some cases such as in wide, rapid and shallow flows or in flows occurring in very smooth channels, while in some other cases such as in ordinary channels, laboratory tests and field measurements have shown that the maximum velocity usually occurs below the free surface at a distance between 0.05 and 0.25 of the depth.

Figure (2.1) illustrates the general pattern of velocity distribution over various vertical and horizontal sections of a rectangular channel and the curves of equal velocity (isovels) in the cross section.

Figure (2.2) in the other hand shows the general patterns for velocity distribution in various channel sections of other shapes.

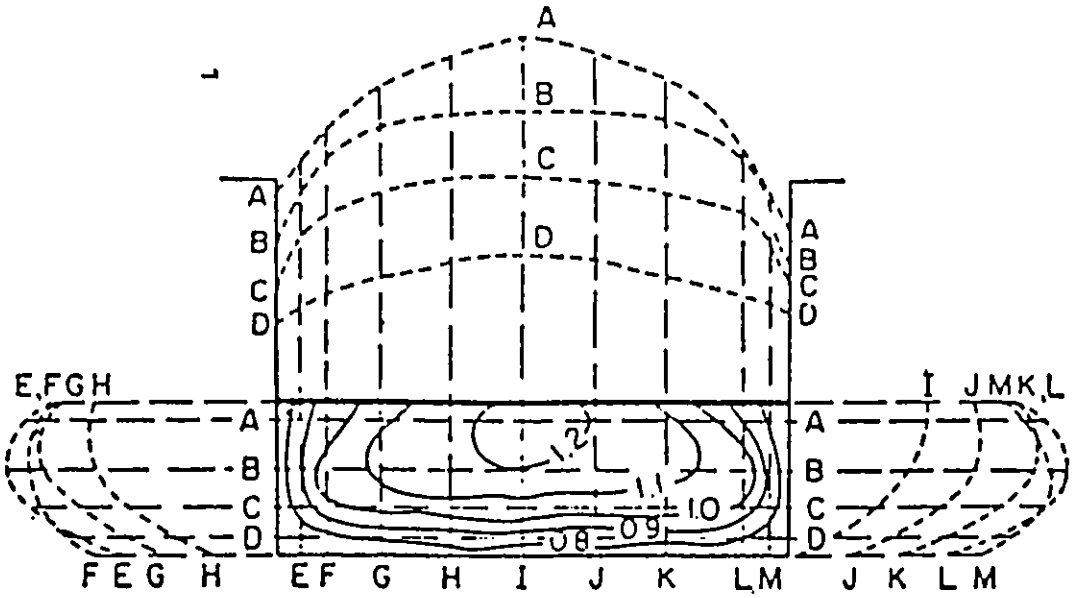

Figure 2.1: Velocity distribution in a rectangular channel.

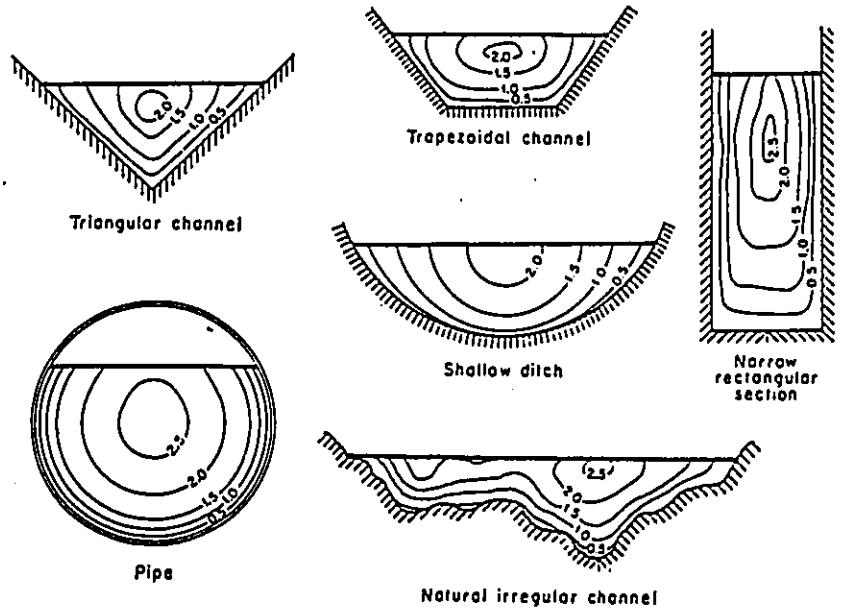

Figure 2.2: Typical curve of equal velocity in various channel sections.

The effect of the channel roughness on the velocity distribution can be seen from figure (2.3). The increase in the curvature of the vertical velocity distribution curve is highly pronounced in the case of rough channels. However, in channels with smooth bed, the velocity distribution is nearly logarithmic and the maximum velocity appears to occur at the free surface. In the literature, most of the equations governing the velocity are found to be one dimensional; that means that they consider only the variation of the velocity in the vertical direction. However, most channels encountered in practice exhibit two dimensional velocity distribution and in many other cases three dimensional ones.

Fundamental to theory development for the velocity distribution is the knowledge of its properties; these properties cannot be put on a precise basis for various channels encountered in practice. Therefore, based on extensive measurements and long experience in different kinds of open channel flow, the U.S. Geological Survey has established a standard velocity distribution curve shown in figure (2.4). The curve characteristics may be summarized in the following statements;

1. The curve may be assumed parabolic.
2. The maximum velocity does not occur at the free surface but slightly below, at a distance between 0.05 and 0.25 of the depth.
3. The mean velocity occurs at approximately 0.6y below the water surface.
4. The mean velocity is approximately 85% of the surface velocity.

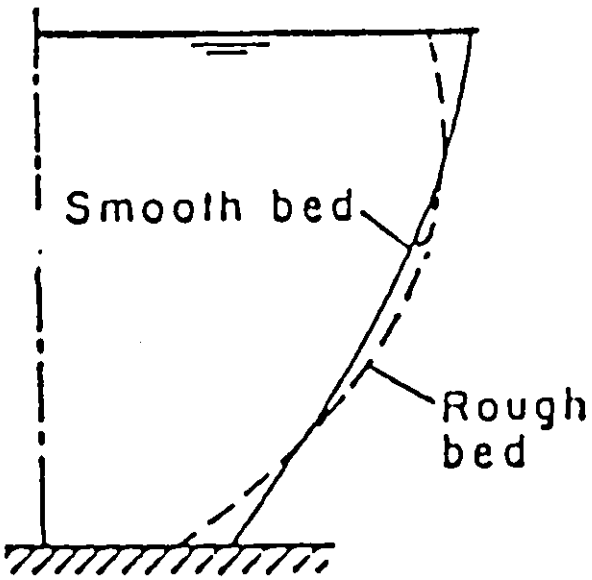

Figure 2.3: Effect of roughness on velocity distribution in an open channel.

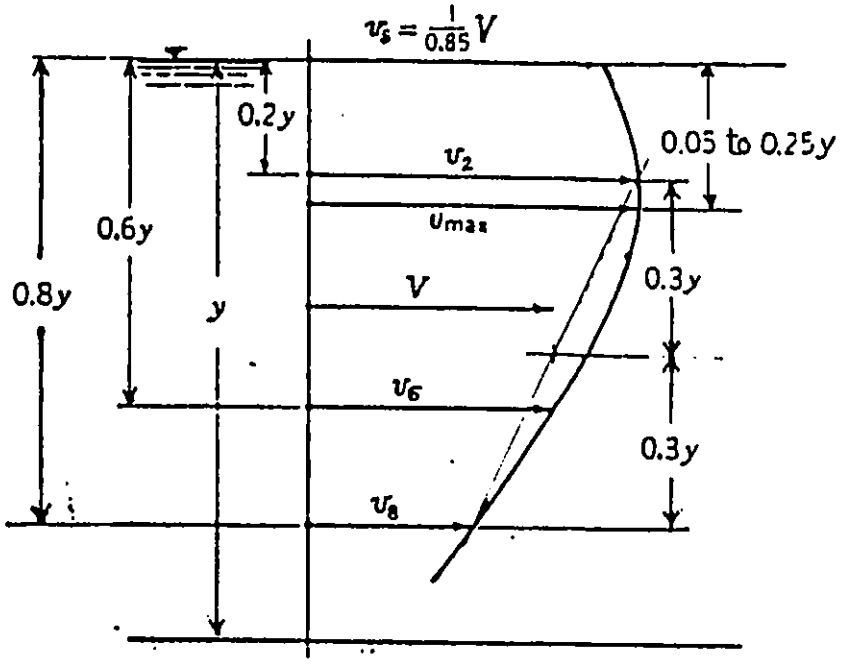

Figure 2.4: Standard velocity distribution in a vertical in open flow.

Contrary to the U.S. Geological Survey's velocity distribution curve, the other commonly used curve is based on Prandtl-Von Karman velocity distribution law; it predicts that the profile is nearly logarithmic and the maximum velocity occurs at the free surface.

Prandtl demonstrates this as follows;

Starting with the equation for the shear stress

$$\tau = \rho l^2 (\frac{du}{dy})^2 \tag{2.1}$$

where

τ = shear stress,

l = characteristic length or mixing length,

u = average velocity,

y = depth of flow.

From equation (2.1)

$$du = \sqrt{\frac{\tau}{\rho l^2}} dy \tag{2.2}$$

l is usually assumed to be proportional to the depth of the flow y.

l=ky, k is a term of proportionality called Von-Karman's universal constant and is assumed to be approximately equal 0.4.

Substituting for l in equation (2.2)

$$du = \sqrt{\frac{\tau}{\rho k^2 y^2}} dy \tag{2.3}$$

or

$$du = 2.5\sqrt{\frac{\tau}{\rho}}\frac{dy}{y} \tag{2.4}$$

Integrating we get

$$u = 2.5\sqrt{\frac{\tau_0}{\rho}}ln\frac{y}{y_0} \tag{2.5}$$

where

τ_0 = shear stress at the bottom,

y_0 = a constant of integration.

Substituting u_* for the shear velocity $\sqrt{\frac{\tau_0}{\rho}}$ yields

$$u = 2.5u_*ln\frac{y}{y_0} \tag{2.6}$$

y_0 is a constant of integration and it depends on whether the boundary is hydraulically smooth or rough.

If the boundary is smooth then, y_0 depends solely on the kinematic viscosity and the shear velocity.

$$y_0 = \frac{m\nu}{u_*} \tag{2.7}$$

Where m is a coefficient and is equal to approximately $\frac{1}{9}$ for smooth surfaces. Substituting for y_0 in equation (2.6) yields

$$u = 2.5u_*ln\frac{9yu_*}{\nu} \tag{2.8}$$

When the boundary surface is hydraulically rough, y_0 depends only on the roughness height

$$y_0 = mk_s \tag{2.9}$$

In this case m is approximately equal to $\frac{1}{30}$ for sand grain roughness. Substitution of equation (2.9) in equation (2.6) yields,

$$u = 2.5u_* ln\frac{30y}{k_s} \tag{2.10}$$

2.2 Velocity Measurements [29]

2.2.1 Hydrometric Current Meters

The standard method of river flow measurements is by means of current meters. Their principle of operation is based on the proportionality between the local flow velocity and the speed of the rotor. Types of current meters that are in wide spread use are:

1. Price or cup current meter: The most common current meter in use in the United States. It consists of six conical cups rotating about a vertical axis. Each complete revolution of the cups closes a battery operated circuit and an audible click is emitted in the headphone worn by the user (operator).

   Close attention must be given when choosing the measuring station, i.e. there should be little or no turbulence at all and current directions

should be parallel to the channel axis.

The relation between the revolutions per unit time and the velocity is

$$u = a + bn \tag{2.11}$$

where

u = flow velocity,

n = number of revolutions per unit time,

a, b = calibration coefficients.

2. Propeller current meter: In this type of meter there is a propeller which rotates around a horizontal axis. Their principle of use is the same as that of Price meter but they are not subject to rotation by vertical currents while the Price meters are. The propeller current meter can be equipped with mechanical counters or electrical counters.

3. A third type of current meter is based on the electromagnetic principle. When a fluid with a certain conductivity is moving through a magnetic field at 90° an electromotive force is induced in the fluid at right angles to both the flux of the magnetic field and the velocity of the fluid. The voltage induced by the movement of the fluid through the magnetic field is proportional to the average velocity of flow.

   These current meters are more accurate and efficient than the two other meters described above.

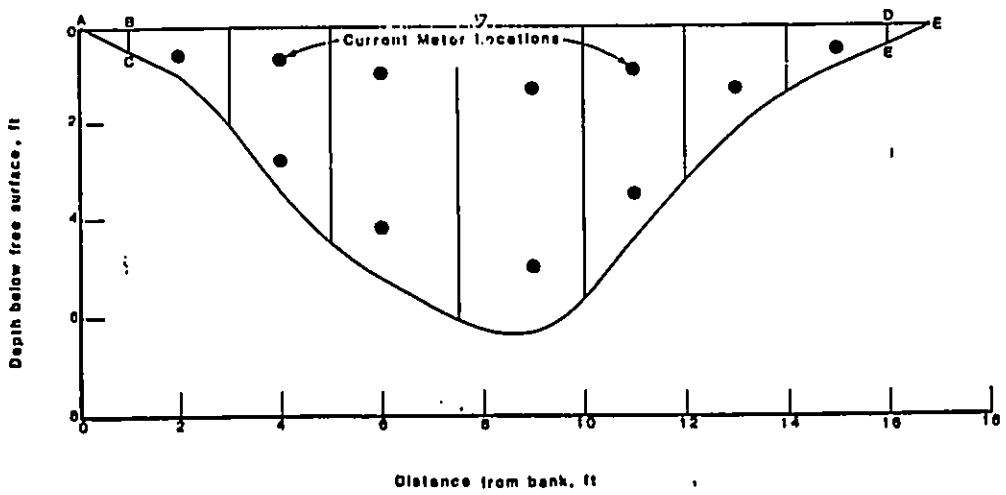

Figure 2.5: Velocity measurements by current meter.

In order to measure the discharge, the hydrometric section and the current meter should be first selected, the cross section is then divided into a number of vertical sections (see figure 2.5 above).

Each of these subsections should not include more than 10% of the total flow. The average velocity in each subsection may be determined by a variety of methods, however, the one that is widely used is based on the velocity measurement at 0.2 and 0.8 of the depth.

2.2.2 Hydrometric Floats

The principle of flow velocity measurements by means of a float depends on the proportionality between the float velocity u and the flow velocity v or

$$u \propto v$$

These two velocities can be made equal if a suitable specific weight of the float is chosen or if the weights inside the float are cleverly distributed.
Floats can be used to measure local or mean velocities of flow in open channels. Measurements of the mean velocity of flow may consist in certain cases in measuring local velocity of flow at a certain depth where the local velocity is equal to the mean velocity of flow, or by measuring the velocity of motion of a free float released at the bottom and carried by the current to the free surface.
The most commonly used types of floats are as follows:

Surface Floats

Surface floats may consist of a spherical float, a wooden disc, a stoppered bottle or any perceptible body with a density less than water and chosen so that its velocity is as near as possible to the main flow velocity.
Measurement with surface floats is simple. They are released in the river some distance upstream of the test section. The time t the float takes to travel the test section is measured by a stop-watch and the mean velocity

is then determined by dividing the distance L over the time t or

$$u = \frac{L}{t} \approx v$$

The ratio between the mean velocity of flow in the vertical plane and the velocity of a surface float varies from 0.82 to 0.92.

Subsurface Floats

This kind of float is used for measuring flow velocity at a definite depth. A variety of these floats has been used in the past from which a description for the two commonly used ones is given here;

- Canister Floats: These consist essentially of a closed canister connected by a thin line to a small surface float equipped with a flag permitting its observation during the measurement.
  The float dimensions and its depth of immersion have to be chosen so that the float velocity is equal to the flow velocity at that depth.

- Rod Floats: Wooden rods or thin walled metal tubes loaded at their lower end are widely used whenever the use of rod floats is selected. Rod floats are loaded at their lower end and the loading can be varied just by varying the amount of lead shot. This allows the worker to make the velocity of the float approximately equal to the mean velocity in the vertical plane parallel to the channel axis.

Integrating Floats

Floats of this type consist of a sphere or a ball float rising from the bottom to the free surface of the flowing stream. It enables one to measure the mean velocity of flow in the vertical plane parallel to the river axis without measuring local velocities. The determination of the mean velocity of flow in the vertical section may be determined by measuring either the depth H and the distance L to the point where the float surfaces, or, by measuring the length L and the time t from the moment of release to the moment of surfacing.

The mean velocity is determined by the relation

$$v_m = \frac{1}{H}\int_0^H v dh \tag{2.12}$$

The rate of flow per unit width can be consequently computed using the formula

$$q = v_m H \tag{2.13}$$

The operation of an integrating float is based on the principle that a body rising from the bottom to the free surface of a flowing water will integrate the horizontal velocities in its vertical path, measured by the horizontal distance travelled from the time of release to the time of surfacing.

2.3 Hydrodynamic forces

2.3.1 Drag force

A fluid moving relative to a body exerts a dynamic force on the body that is caused by two factors. First, shear stresses due to viscosity and velocity gradients at the boundary surface cause forces tangential to the surface. Second, pressure intensities which vary along the surface because of the dynamic effects result in forces normal to the boundary.
The shear force is referred to as the skin friction drag, while the pressure drag which depends largely on the shape or form of the body is known as the form drag.
The two kinds of drag may be defined as follows:

Skin friction drag

The type of resistance the fluid particles exhibit against displacement in relation to each other and with respect to the surface of solid obstacles, presents itself in the form of frictional drag. In a similar way to that of solid surfaces sliding along each other, a tangential force originates whenever a fluid moves past the surface of the body. This tangential force is defined as the skin friction drag.

Pressure drag or form drag

The distinction between the skin friction drag and the pressure or form drag is that the first one results from tangential forces, whereas, the second one results from the distribution of forces normal to the body surface. The induced drag is also a case of pressure drag and any type of wave resistance including those at the free surface of water act upon the obstacle or the body by way of pressure differentials along that body.

Bodies like airfoils, hydrofoils and slim ships have large and sometimes completely dominant surface resistance while bluff objects such as spheres, bridge piers and automobiles have large form drag relative to surface resistance.

The two kinds of drag are summed together to give the total drag, therefore one can write

$$F_D = F_{Df} + F_{Dp} \tag{2.14}$$

Each of the two components can be defined as follows:

Frictional drag: $F_{Df} = \int_s \tau \sin\phi ds$

Pressure drag: $F_{Dp} = -\int_s p\cos\phi ds$

where

s = total surface area,

ϕ = angle between the normal to the surface element and the flow direction,

τ = shear stress,

p = pressure.

Drag coefficients are given by the following relations

$$F_{Df} = C_{Df}\rho\frac{v_0^2}{2}A_f \tag{2.15}$$

$$F_{Dp} = C_{Dp}\rho\frac{v_0^2}{2}A_p \tag{2.16}$$

where

F_{Df}	= frictional drag,
F_{Dp}	= pressure drag,
C_{Dp}	= pressure drag coefficient,
C_{Df}	= frictional drag coefficient,
A_f and A_p	= areas of the bodies,
ρ	= density of water,
v_0	= mean velocity.

For surface resistance, A_f is usually the actual area over which the shear stresses act to produce F_{Df}. For form drag, however, A_f is usually the frontal area normal to the velocity v_0.

Drag coefficients C_{Df} and C_{Dp} can be computed from the previous equations and it is customary to define the total drag coefficient as the sum of the two coefficients, therefore we can write

$$C_D = C_{Df} + C_{Dp} \tag{2.17}$$

and the total drag exerted by the fluid on the body can be written as follows

$$F_D = C_D \rho \frac{v_0^2}{2} A \tag{2.18}$$

where

F_D = total drag on the body,

C_D = total drag coefficient,

ρ = density of water,

v_0 = flow velocity,

A = frontal area normal to v_0.

Notice that the dimensionless force coefficients that have been described above are functions of the body geometry and the Reynolds number Re (see figure 2.6) and they apply only for a deeply immersed bodies such as aeroplanes or submarines where there is no wave drag effect or what is called wave resistance.

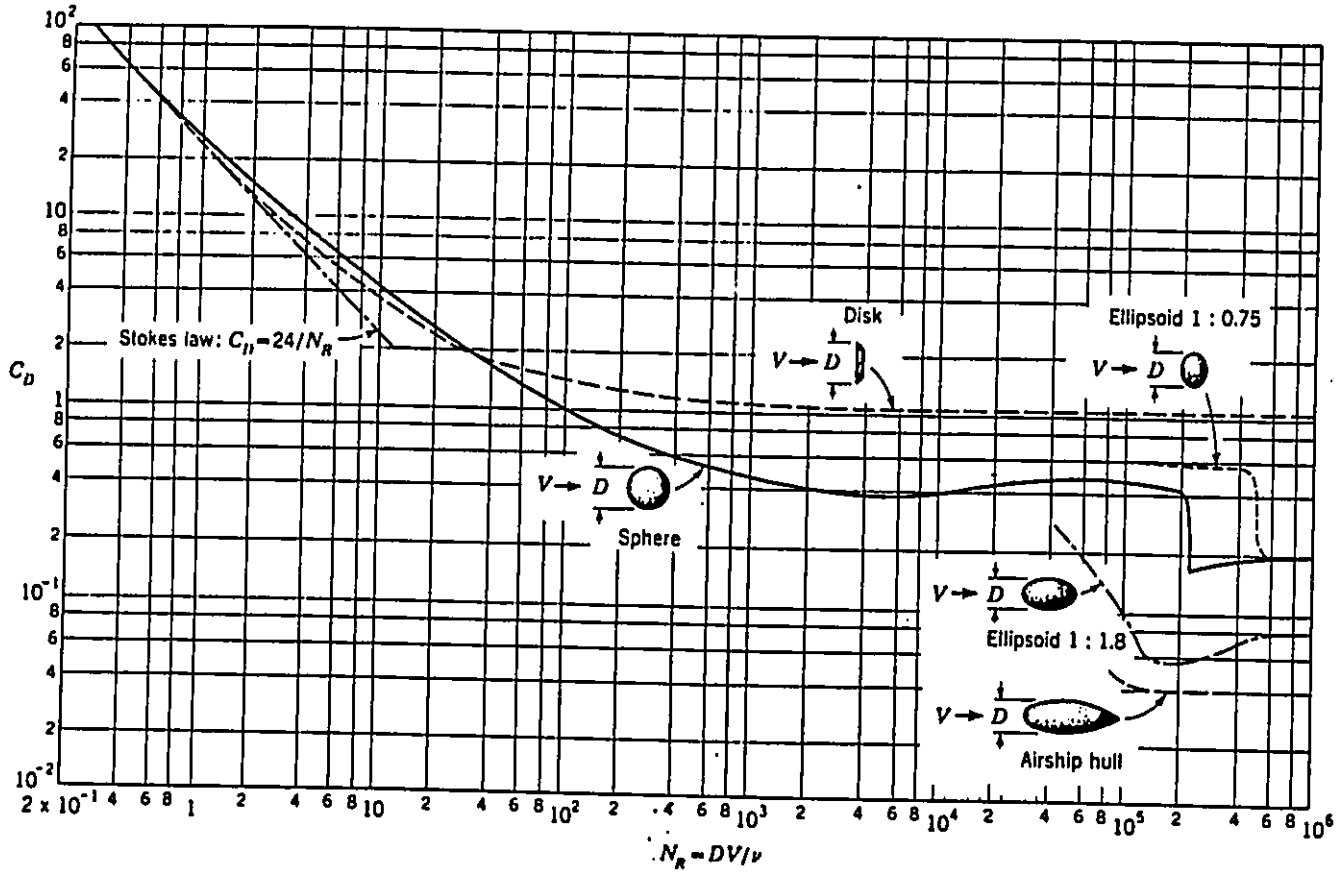

Figure 2.6: Drag coefficient for bodies of revolution.

2.3.2 Interfacial effects on resistance or wave drag effect

Compared to the cases cited above, the new factor which can be introduced when the body is moving at, or, near an interface between two fluids of different densities is the production of surface waves.

For such cases, energy is expended on the generation of interfacial wave motion. Thus, gravity influences both the flow field and the drag and also the lift, if there is any on the body.

The drag will therefore be a function of both Reynolds number $Re = \frac{ul}{\nu}$ and Froude number $Fr = \frac{u}{\sqrt{lg}}$. The first one (Re) expresses the effect of viscosity on the drag while the second nondimensional term (Fr) expresses the effect of surface wave formation on the drag.

The numerical value of the Reynolds number indicates the type of eddy pattern caused by shear stresses. In a similar way,the numerical value of the Froude number indicates the type of wave patterns caused by the passage of the body through the water.

In general, the total drag on a body is the sum of the frictional and the pressure components. In presence of surface waves, the relation still applies, however, the ratio $\frac{F_{D_f}}{F_{D_p}}$ and also the magnitude of the drag are affected by the interfacial field i.e wave formation.

2.3.3 Buoyant force

Submerged body

The resultant force exerted on a body by a fluid in which it is submerged is called the buoyant force. It is the difference between the vertical component on its underside F_z and the vertical component on its upperside $F_{z'}$.
The buoyant force acting vertically upward is denoted by F_B and equal to $F_z - F_{z'}$ and it is due to the gravity force of the volume of liquid displaced by the body.

In equation form, the buoyant force is known (from the time of Archimedes) to be

$$F_B = \gamma V \tag{2.19}$$

where

F_B = buoyant force,
γ = unit gravity force of fluid,
V = volume of fluid displaced by the body.

If the body is in equilibrium i.e $W = F_B$, this means that both the fluid and the body have the same density. If W is greater than F_B the body will sink, whereas, if W is less than F_B the body will rise. The criterion for stability of a submerged body is that the center of buoyancy must be

above the center of mass of the body.

Floating body

When a body having a weight W less than that of the same volume of liquid is present in a liquid with a free surface it will rise and float on the surface, hence W becomes equal to F_B. Therefore, one can state that a floating body displaces a volume of liquid equivalent to its weight. In equation form, the formula given for submerged bodies is applied to floating bodies, however, contrary to submerged bodies, a floating body might be stable irregardless of whether the center of buoyancy is above or below the center of mass. The only criterion in this case is that the two forces W and F_B must be equal and lie on the same vertical.

2.4 Lateral diffusion in open-channel flow

Based on the principle of conservation of mass, the equation of diffusion is known in general as

$$\frac{\partial C}{\partial t} + u\frac{\partial C}{\partial x} = \frac{\partial}{\partial x}\left(\epsilon_x \frac{\partial C}{\partial x}\right) + \frac{\partial}{\partial y}\left(\epsilon_y \frac{\partial C}{\partial y}\right) + \frac{\partial}{\partial z}\left(\epsilon_z \frac{\partial C}{\partial z}\right) \qquad (2.20)$$

where C is the time averaged local concentration of the substance, ϵ_x, ϵ_y and ϵ_z are the turbulent diffusion coefficients, u is the time averaged velocity in the main direction (x), x, y and z are Cartesian coordinates and t is the time.

Neglecting the effect of longitudinal diffusion and assuming a steady- state situation $\left(\frac{\partial C}{\partial t} = 0\right)$, equation (2.20) will be reduced to

$$u\frac{\partial C}{\partial x} = \frac{\partial}{\partial y}\left(\epsilon_y \frac{\partial C}{\partial y}\right) + \frac{\partial}{\partial z}\left(\epsilon_z \frac{\partial C}{\partial z}\right) \tag{2.21}$$

Multiplying each term of the above equation by z^2, integrating over the total width z assuming that u, ϵ_y and ϵ_z do not vary with z gives

$$\int uz^2 \frac{\partial C}{\partial x} = \int z^2 \frac{\partial}{\partial y}\left(\epsilon_y \frac{\partial C}{\partial y}\right) + \int z^2 \frac{\partial}{\partial z}\left(\epsilon_z \frac{\partial C}{\partial z}\right) \tag{2.22}$$

Introducing σ_1^2 and M defined as

$$\sigma_1^2 = \int_{-\infty}^{+\infty} z^2 C dz$$

$$M = \int_{-\infty}^{+\infty} C dz$$

Equation (2.22) can then be written as

$$u\frac{\partial \sigma_1^2}{\partial x} = \frac{\partial}{\partial y}\left(\epsilon_y \frac{\partial \sigma_1^2}{\partial y}\right) + 2\epsilon_z M \tag{2.23}$$

At a certain distance x_0 downstream from the source, the material is uniformly distributed across the depth of the channel, the variation of σ_1^2 and M in the y direction can be neglected and equation (2.23) will then have the following form

$$U\frac{\partial \sigma_1^2}{\partial x} = 2M\overline{\epsilon_z} \qquad for \qquad x > x_0 \tag{2.24}$$

U and $\overline{\epsilon_z}$ are depth averaged velocity and lateral diffusivity respectively.

Normalizing the variance $\sigma^2 = \frac{\sigma_1^2}{M}$

substituting into equation (2.24), one gets

$$\overline{\epsilon_z} = \frac{1}{2}U\frac{\partial \sigma^2}{\partial x} \tag{2.25}$$

One of the widely used relations for $\overline{\epsilon_z}$ which has fitted well the available experimental results was given by Okoye (1970); it is defined as

$$\overline{\epsilon_z} = 0.16 U_* R \tag{2.26}$$

where U_* is the frictional velocity and R is the hydraulic radius.
Assuming $\overline{\epsilon_z}$ not to be a function of the longitudinal distance, σ^2 will then vary linearly with x and the concentration over the total depth will exhibit a Gaussian distribution. Hence $\sigma^2(0) = 0$
Therefore, arranging equation (2.25) and integrating gives

$$\sigma^2 = 2\overline{\epsilon_z}\frac{x}{U} \tag{2.27}$$

Substituting for the value of $\overline{\epsilon_z}$ in equation (2.26), the variance could be evaluated

$$\sigma^2 = 0.32\frac{U_*}{U}Rx \tag{2.28}$$

2.5 Effect of particle size on the diffusion process

Observations of the diffusion of sufficiently small particles in a turbulent flow showed that they are similar to the diffusion of dissolved particles. For larger and neutrally buoyant particles, however, dimensional analysis has indicated an additional parameter. It characterizes the rate of diffusion in homogeneous turbulent field and is of the form $\frac{l}{R}$ where l represents the

length of the diffusing object whereas R represents a typical dimension of the flow field (a hydraulic radius here).

In 1952, Ogura [21] studied the relative diffusion of large balloons released in the atmosphere. He concluded that only eddies that are larger than the body dimension contribute to the diffusion, and that the field flow is not disturbed by the passage of the diffusing object.

In 1967, Iwasa and Imamoto [11] came up with a slightly different model for studying the turbulent diffusion in free surface flows. The model was obtained under the assumption that the instantaneous velocity of a particle is a volumetric mean value of the fluid velocities.

2.6 Kinematic model of Ogura [21]

In his study, Ogura [21] defined the turbulent energy as follows:

$$\frac{3}{2}\overline{u_l{}^2} = \int_0^{k_l} E(k)dk \tag{2.29}$$

where $k_l = \frac{2\pi}{l}$ is the wave number associated with eddies of size l. After introducing the Von Karman's interpolation formula, the following relation can be obtained and evaluated

$$\frac{\overline{u'_{l^2}}}{\overline{u'^2}} = f\left(\frac{l}{l_e}\right) \tag{2.30}$$

Ogura [21] argued that the $E(k)$ can be integrated with a wave number that is function of l_{max} corresponding to the largest eddies present in the turbulent field under study. To get a relation for relative diffusion, it is

required to first define σ^2 and σ_p^2; Taylor and Batchelor defined σ^2 as

$$\sigma^2 = 2\sqrt{\overline{u'^2}}.L.t = 2\overline{u'^2}.t_x.t \tag{2.31}$$

where t_x and L are the Lagrangian macro-time-scale of the turbulence and the corresponding length respectively. By analogy σ_p^2 can be defined. Finally, the following relation approximating the relative diffusivity can be defined

$$\frac{\sigma_p^2}{\sigma^2} = \frac{\sqrt{\overline{u_l'^2}}}{\sqrt{\overline{u'^2}}} = f\left(\frac{l}{l_{max}}\right) = \frac{\epsilon_{zp}}{\overline{\epsilon_z}} \tag{2.32}$$

where σ_p^2 is the mean square separation of the particle and ϵ_{zp} is its diffusivity.

2.7 Kinematic model of Iwasa and Imamoto [11]

Diffusion by continuous movements of fluid particles in a homogeneous isotropic field of turbulent flow was described by Taylor. Extending Taylor's diffusion theory to discrete particles, the variance for the displacement of a particle at a certain time is expressed as

$$\sigma_p^2(t) = 2\overline{u_{p^2}'} \int_0^t \int_0^{t_1} R_p(\xi) d\xi dt_1 \tag{2.33}$$

or

$$\sigma_p^2(t) = 2\overline{u_{p^2}'} \int_0^t (t-\xi) R_p(\xi) d\xi \tag{2.34}$$

where u'_p is the fluctuating velocity of the discrete particle and $R_p(\xi)$ is the Lagrangian correlation coefficient of u'_p and is expressed as

$$R_p(\xi) = \frac{\overline{u'_p(t_0)u'_p(t_0+\xi)}}{\overline{u'^2_p}} \tag{2.35}$$

and under the assumption made for the velocity, u'_p can be expressed as

$$u'_p(t) = \frac{1}{V}\int_V u'(t)dV \tag{2.36}$$

By introducing an averaging time τ related to the size of the particle, the above equation can be written as follows:

$$u'_p(t) = \frac{1}{\tau}\int_{t-\frac{\tau}{2}}^{t+\frac{\tau}{2}} u'(t_1)dt_1 \tag{2.37}$$

If t_* and t_{*p} are the integrated Lagrangian time scales for the fluid turbulent velocity fluctuation and the particle velocity fluctuation respectively, the analysis yields to:

$$\overline{u'^2_p}t_{*p} = \overline{u'^2}t_* \tag{2.38}$$

which predicts the absolute diffusion to be independent of the particle size. Laboratory experiments and field observations were made to verify the statistical theory. Poor agreement was found between the proposed model and the experimental observations made by Iwasa and Imamoto [11].

2.8 Literature Review

2.8.1 Use of floats

A review of literature shows different types of floats used for velocity and discharge measurements.

In 1968 Liu and Martin [16] conducted a study using integrating floats. The floats they used were accurately machined spheres with density less than water. The float released at the bottom of a stream will rise to the water surface in a time t at a horizontal distance l downstream from the release position. The velocity and the discharge per unit width can then be calculated from the relations

$$v = \frac{l}{t} \qquad and \qquad q = \frac{l}{t}h$$

where h is the depth of flow in which the float is released.
These two equations, according to what Liu and Martin [16] wrote are based on:

1. Steady flow
2. Horizontal uniform flow
3. Absence of turbulence and secondary currents
4. Float size infinitesimally small

5. The float accelerates to the horizontal speed of the stream and to a constant upward terminal velocity instantaneously after release.

In 1970 Liu and Martin [17] continued their experimental investigation on the reliability of the method in the case of low streamflow velocity. Spheres made of hollow stainless steel $\frac{5}{8}$ inches in diameter were released at the center of the flume and the corresponding discharges were computed using two different ways:

1. By taking the arithmetic mean of the values of q obtained from the measurement of l and t, in mathematical form

$$\bar{q} = \frac{\sum_{i=1}^{n} \frac{l_i h}{(t)_i}}{N}$$

2. By taking the arithmetic means of l and t first, and using these means to calculate the average discharge $\bar{q}_*$

$$\bar{q}_* = \frac{\bar{l}h}{\bar{t}}$$

Liu and Martin [17] found that the average values of q determined by the two methods differ by much less than 1% and the average difference between the discharges obtained by float measurements and those measured by other standard laboratory means was only 2.4% for the range of the studied low velocities (ranging from 0.02 to 0.3 fps).

In 1973 Dr R. G. Warnock and co-workers from Ottawa University and NRC [33,34] reported on the Ottawa river project. The portion of the project

the group undertook consisted of several aspects of which only the velocity measurement will be considered. This has been done by two means:

1. Current meters to determine the velocity variation laterally and with depth for different flow rates.

2. Float survey by aerial photographs.

The float model used by the group was made of $\frac{1}{4}$ inch thick plywood 18 inches square attached by a half inch flexaframe aluminium rod to two pieces of galvanized iron sheets 5 by 12 inches bent to form vanes.
The reliability of the data collected in the float survey may be summarized in the following: the discharges calculated from the float survey at 3 positions were compared to those measured by other means, the largest deviation from the mean value was 9.2%, also the total flow in the river was computed and found to be slightly above the daily discharge. The transverse distribution of the mean velocity (in the vertical) determined from the float survey was also compared to similar data from previous velocity measurements at the same cross-sections. It was found that float data show the transverse velocity distribution well and that the velocity distribution is altered by changing flow conditions.

Ronald E. Johnson [24] in 1975 conducted a study using different surface floats and drogue depth combinations. He used four different buoys, three were coupled to steel plates rigidly attached to each other forming a cross or plus shape, the fourth one however, was a spar type approximately 10ft

long that did not require a subsurface drag plate.

Johnson presented his work in two separate parts. The first one consists on data acquisition, methods and techniques used, while the second one, which we were not able to find (according to what Johnson wrote in the first part) will contain the analysis of the data and hopefully the formulation of a prediction equation for the relationship between the observed true current velocity at the depth of the drogue, the measured system velocity, surface current and speed.

2.8.2 Accelerated motion of particles in a liquid

The motion of particles immersed in a fluid is an important problem in many engineering applications. The free fall of a sphere from rest in a viscous fluid, or the motion of sediments in water, or the floating of dust particles in the atmosphere of an orbiting spacecraft are among the cases that have been studied to gain a better understanding of the accelerated motion of particles.

Lawrence D. Cloutman [15] examined the case of the sphere moving through a uniform fluid having a constant velocity throughout the region of study. He considered only the component of motion in the velocity direction and came up with the following relation

$$\frac{dv}{dt} = -\frac{3}{8}\rho\frac{C_D}{\rho_p r_p}|v|v \tag{2.39}$$

where

C_D = drag coefficient,

ρ = density of water,

ρ_p = particle density,

v = particle velocity in the fluid frame,

r_p = particle radius.

In this equation, the added mass effect and the Basset history integral were neglected. Assuming that the initial speed and position are known, two solutions were given depending on whether the Reynolds number is less or greater than 1000. A high speed solution was found to be:

$$v(t) = \frac{v(0)}{[1 + Av(0)t]} \tag{2.40}$$

In the low speed region however, the velocity goes exponentially to zero as t goes to infinity, in equation form

$$v(t) = \{(v_1^{-\frac{2}{3}} + C)e^{[\frac{2B(t-t_1)}{3}]} - C\}^{-1.5} \tag{2.41}$$

Using 3 different particle sizes, Cloutman concluded that the smallest particle is slowed most quickly, whereas, the largest one show the same behavior as that of the high speed solution in the early time.

The case of a sphere falling in a viscous fluid was studied by many investigators. In Stokes range, Basset [2] presented the following equation

$$(m_s + K_s m)\frac{dv_s}{dt} = (m_s - m)g - 3\mu\pi d v_s - \frac{3}{2}d^2\sqrt{\pi\rho\mu}\int_0^t \frac{\frac{dv_s}{d\tau}}{\sqrt{t-\tau}}d\tau \tag{2.42}$$

where

m = mass of the fluid displaced by the particle,

m_s = mass of the particle,

v_s = particle velocity,

K_s = added mass coefficient for the sphere.

This integro-differential equation has been accepted and used by many other authors including V. Boussinesq, C. W. Ossen C. M. Tehen and J. L. Lumley.

Lucien M. Brush et al [18] noticed that the solution presented by Basset [2] was in error. They presented a solution using Laplace transform then compared the solution obtained by a series expansion to that obtained from the numerical evaluation of equation (2.42). Good agreement was found between the two methods.

The resistance of particles above the Stokes range on the other hand is no longer a linear function of v_s. Therefore, equation (2.42) may be rewritten as

$$(m_s + \frac{1}{2}m)\frac{dv_s}{dt} = (m_s - m)g - \frac{d^2}{8}\rho C_D \pi |v_s| v_s - \frac{3}{2}d^2\sqrt{\pi\rho\mu}\int_0^t \frac{\frac{dv_s}{d\tau}}{\sqrt{t-\tau}}d\tau \tag{2.43}$$

Contrary to the case of particles in the Stokes range for which no experimental evidence is available, Moorman has presented experimental information on particles ranging from near Stokes range to well above it.

Numerical evaluation of the instantaneous fall velocity for three particles of the same density ratios ($\frac{\rho_s}{\rho} = 2.5$) and different Reynolds numbers was obtained and plotted against the experimental results of Moorman. Also, a similar plot of the fall velocity for particles with the same Reynolds number and different density ratios was presented. Close agreement between the computer solution of equation (2.43) and Moorman's experimental points on both graphs suggests that the numerical solution adopted is valid and applicable for a wide range of Reynolds numbers and density ratios.

2.8.3 Velocity distribution in rectangular channels

In a shear flow, three regions can be distinguished: viscous sublayer, inner layer and outer layer.

Viscous sublayer: characterized by a laminar flow and exists approximately up to a distance $\frac{z}{\delta_0} = 0.001$ in which δ_0 is the boundary layer thickness and z is the distance from the boundary.

Inner layer: In this layer the viscous stress is negligible and the flow is dominated by the wall. This layer extends up to a distance of $\frac{z}{\delta_0} \approx 0.15$.

Outer layer: the flow in this region is influenced by the constraints of the entire periphery of the channel geometry and it extends up to the free surface.

Turbulent flow over smooth flat plate

The basis for determining the velocity profiles in shear flows is the mixing length model. Prandtl's mixing length theory results in:

$$\frac{u}{u_*} = \frac{1}{k}\ln(z) + constant \tag{2.44}$$

in which $u_* = \sqrt{\frac{\tau_0}{\rho}}$ is the shear velocity, u is the velocity in x direction at z, k is the Von Karman's universal constant, τ_0 is the bed shear and ρ is the mass density.

Ludwieg, Tillman, Hama and many others [7] measured the mean velocity distribution across the boundary layer along a smooth flat plate with zero pressure gradient. In the inner region, the data were found to fit the equation

$$\frac{u}{u_*} = A_0 \ln(\frac{zu_*}{\nu}) + B_0 \tag{2.45}$$

known as the universal logarithmic velocity distribution.

Different values of A_0 and B_0 were suggested. Clauser [3] suggested the values for A_0 and B_0 respectively as 2.44 and 4.9. A value of $A_0 = 2.5$ is usually accepted. Townsend [28] remarked however, that many of the observed data indicate a value of B_0 nearer to 7 than 4.9. Therefore, equation (2.45) can be written as follows:

$$\frac{u}{u_*} = 2.5 \ln(\frac{zu_*}{\nu}) + B_0 \tag{2.46}$$

in which B_0 has a value in the range of 4.9 to 7.0.

In the outer region, Hama [7] proposed the following empirical formula for

the mean velocity distribution

$$\frac{u_0 - u}{u_*} = 9.6(1 - \frac{z}{\delta_0})^2 \tag{2.47}$$

in which u_0 is the free stream velocity.

For the region between $\frac{u_* z}{\nu} = 100$ and 2000, a $\frac{1}{7}$ power law was found to hold well.

$$\frac{u}{u_*} = 8.3(\frac{z u_*}{\nu})^{\frac{1}{7}} \tag{2.48}$$

Turbulent flow through wide open channels

Based on measurements in the middle verticals of eight different wide channels, Bazin obtained the following formula

$$\frac{u_m - u}{u_*} = 6.3(1 - \frac{z}{D})^2 \tag{2.49}$$

It can be easily seen that the above equation resembles the equation (2.47) except in the numerical coefficient. therefore, one can say that Bazin's law is for the outer region.

Keulegan [14] argued that equation (2.46) which is valid for smooth pipes can be extended to smooth wide open channels. He adopted such a procedure where he verified the logarithmic profile but he did not determine the constants of the logarithmic equation.

From experiments in two dimensional channels, Vanoni [30] reported that the data were found to fit the logarithmic velocity distribution some dis-

tance below the free surface and the maximum velocities occur below the free surface.

Goncharov [6] derived the local longitudinal velocity u for plane turbulent flow as

$$\frac{u}{u_s} = \frac{\ln(\frac{z+c}{c})}{\ln(\frac{D+c}{c})} \tag{2.50}$$

in which u_s is the velocity at z=D i.e., at the free surface and c is a constant.

Turbulent flow in open channels of finite widths

Keulegan [14] suggested an approach for obtaining the velocity distribution in case of channels with polygonal sections. To illustrate the method, he chose a trapezoidal section and drew the internal bisectors of the base angles. Three different zones were obtained; he assumed that at any point in any particular zone, the velocity distribution follows the logarithmic law and that the flow in any of the three zones was influenced by the wall of that zone only.

Schlichting [25] observed on the basis of Nikuradse's data that the flow at the free surface was not two dimensional for a narrow rectangular channel and that the maximum velocity occurred below the free surface.

Enger [4] conducted experiments in a trapezoidal channel with rough boundaries; he concluded that the velocity distribution was logarithmic and was unaffected by any secondary current of appreciable magnitude.

Goncharov[6], on the other hand, extended the equations given by him for the plane flow to the flow in a rectangular open channel; the equation he presented was as follows

$$\frac{u}{v} = \left(\frac{\log \frac{(\frac{B}{2}-y)+C_b}{C_b}}{\log \frac{D}{2.7C_b}} \right) \left(\frac{\log \frac{z+C_w}{C_w}}{\log \frac{B}{5.4C_w}} \right) \tag{2.51}$$

in which u is the velocity at any point (y,z) in the channel, y is the lateral distance from the side wall, C_b and C_w are constants. Measured profiles were not in good agreement with the theoretical ones and the dip (the ratio of the depth below the free surface where the maximum velocity occurs in the vertical section to the total depth of flow in the channel) was not zero as implied by the model.

Rajaratman and Muralidhar [22] conducted experiments on velocity distribution over almost the entire width of the channel. They confirmed the validity of the logarithmic law and noticed that the dip was not zero and that it was observed near the side walls.

2.9 Dynamical response of floats to accelerating and decelerating flows

The system consists of a sphere suspended from a line of length l attached to a floating disc in water flowing at velocity v_u at the free surface and at velocity v_0 at the level of the sphere some distance below the free surface. The forces consisting of weights, buoyant forces, line tension and drag forces are first in equilibrium, so that the system moves at a constant velocity v_i with the line making an angle θ_0 with the vertical. A sudden change from v_0 to v_1 in the water velocity at the level of the sphere destabilizes the system. The question which arises then is what length of time is required for the system to reach a new equilibrium condition.

The exact equations for the system were found to be complex and very difficult to solve, therefore, three simplified cases were examined as given below. The analyses of these cases yield a better knowledge of the response of the actual system.

The first case proposed is to find the time required to reach equilibrium when there is a 10% increase in the water velocity in which a freely floating sphere is moving at the initial water velocity. Assuming that the Basset integral or what is known as the historical parameter is negligible, the equation of motion of the sphere is

$$(m_s + K_s m)\frac{dv_s}{dt} = \frac{C_{D_s}\rho_w A_s}{2}(v_1 - v_s)^2 \qquad (2.52)$$

Figure 2.7: Case1: a sphere accelerating in water.

where

m = mass of the fluid displaced by the sphere,

m_s = mass of the sphere,

v_s = velocity of the sphere,

v_l = velocity of the water,

C_{D_s} = drag coefficient of the sphere,

A_s = area of the sphere,

ρ_w = density of the water,

K_s = added mass coefficient for the sphere.

The mass term is the sum of the sphere mass and the added mass. The added mass for a sphere accelerating in a liquid is equal half of the mass of the fluid displaced by the sphere.

or

$$m_s + K_s m = \frac{1}{2}\rho_w(\frac{4}{3}\pi {R_s}^3) + \rho_s(\frac{4}{3}\pi {R_s}^3) \tag{2.53}$$

or

$$m_s + K_s m = \frac{4}{3}\pi {R_s}^3(\frac{1}{2}\rho_w + \rho_s) \tag{2.54}$$

Therefore

$$\frac{4}{3}\pi R_s^3(\frac{1}{2}\rho_w + \rho_s)\frac{dv_s}{dt} = \frac{C_{D_s}\rho_w A_s}{2}(v_1 - v_s)^2 \tag{2.55}$$

After rearrangement and simplification, one gets

$$\frac{dv_s}{dt} = C(v_1 - v_s)^2 \tag{2.56}$$

which can be written as

$$\frac{dv_s}{(v_1 - v_s)^2} = Cdt \tag{2.57}$$

where C is a constant that can be evaluated from the following relation

$$C = \frac{3}{8}\frac{\rho_w C_D}{R_s(\frac{1}{2}\rho_w + \rho_s)} \tag{2.58}$$

Introducing the density ratio, C can be written as follows

$$C = \frac{3}{4}\frac{C_D}{R_s(1 + 2\frac{\rho_w}{\rho_s})} \tag{2.59}$$

To solve the equation, we proceed by variable changes

let $u = v_1 - v_s$ then $du = -dv_s$

substituting into equation (2.57), and integrating

$$\int -\frac{du}{u^2} = C\int dt \tag{2.60}$$

At $t = 0$, $v_s = v_0$, $u = v_1 - v_0$

At $t = t_1$, $v_s = 0.99v_1$, $u = 0.01v_1$

$$-\int_{v_1 - v_0}^{0.01v_1} \frac{du}{u^2} = C\int_0^{t_1} dt \tag{2.61}$$

The integration gives

$$\frac{1}{u} = Ct \tag{2.62}$$

substituting the values of u and t one gets

$$\frac{1}{0.01v_1} - \frac{1}{v_1 - v_0} = Ct_1 \tag{2.63}$$

If $v_1 = C_1 v_0$ then

$$t_1 = \frac{1}{C}\left(\frac{1}{0.01C_1 v_0} - \frac{1}{C_1 v_0 - v_0}\right)$$

$$t_1 = \frac{1}{Cv_0}\left(\frac{1}{0.01C_1} - \frac{1}{C1 - 1}\right)$$

$$t_1 = \frac{1}{Cv_0}\left(\frac{0.99C_1 - 1}{0.01C_1(C_1 - 1)}\right)$$

say $C_1 = 1.10$ (10% increase in velocity) then

$$t_1 = \frac{1}{Cv_0}\left(\frac{0.99(1.10) - 1}{0.01(1.10)(1.10 - 1)}\right)$$

$$t = \frac{80.91}{Cv_0} \tag{2.64}$$

C is typically quite large and is inversely proportional to the sphere size, therefore one can conclude that in order to minimize the time response, sphere size should be as small as practical. It can also be seen from equation (2.64) that the new equilibrium would be reached quickly in presence of high water velocity.

The second case is to consider a sphere suspended from a line of length l in water flowing at velocity v_0. The force system composed of weight, buoyant force, line tension and drag force is in equilibrium so that the line makes an angle θ_0 with the vertical.

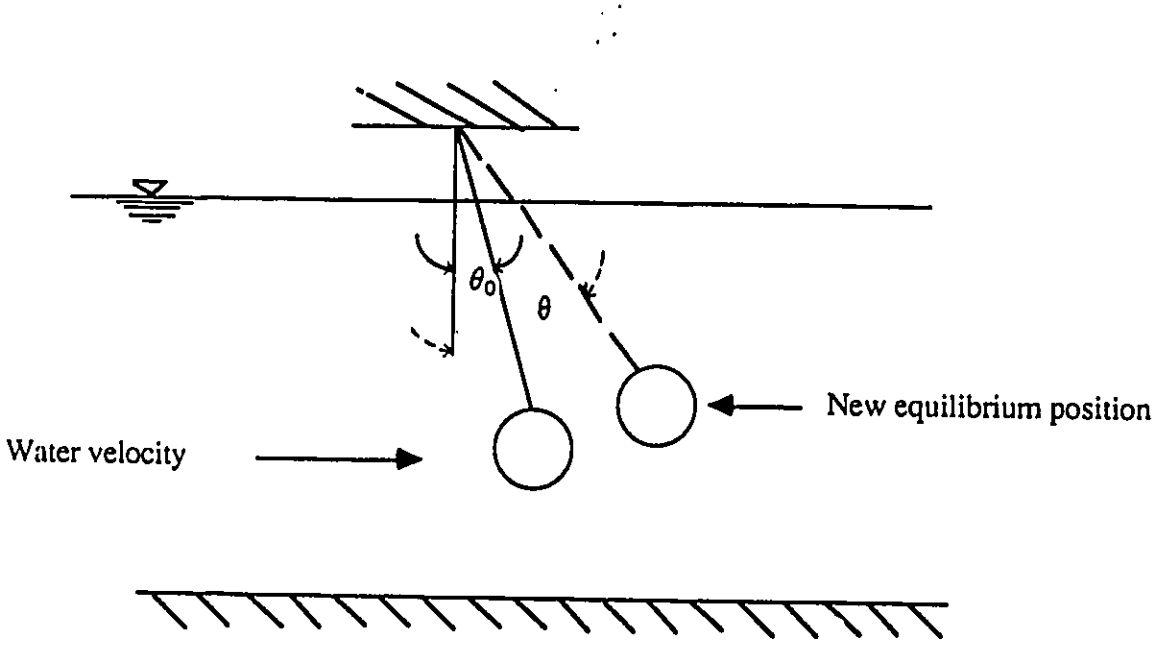

Figure 2.8: Case2: a sphere suspended from a tethered line subject to an accelerating flow.

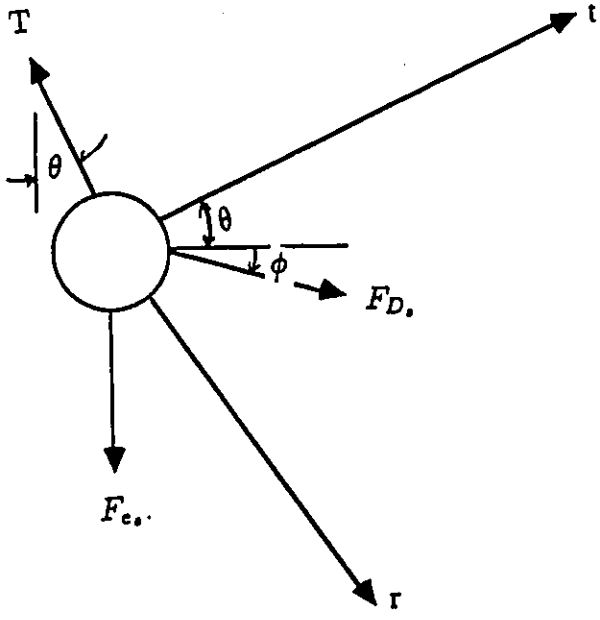

Figure 2.9: Forces on the sphere.

There is a sudden increase in water velocity to v_1 as shown in fig.2.8. What length of time is required for the sphere to reach the new equilibrium position?

The equation of motion in the tangential direction is

$$\sum F_t = -Fe_s \sin\theta + F_{D_s} \cos(\phi + \theta) \tag{2.65}$$

applying Newton's second law

$$Ma_t = \sum F_t \tag{2.66}$$

where M includes the added mass, the equation (2.66) can be written as

$$(m_s + I_s m) l \frac{d^2\theta}{dt^2} = -Fe_s \sin\theta + F_{D_s} \cos(\phi + \theta) \tag{2.67}$$

Let $F_{D_s} = Cv_r^2$, where v_r is the water velocity relative to the sphere.

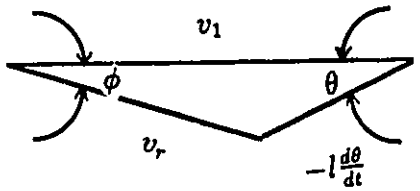

Referring to the figure above v_r can be expressed as

$$v_r^2 = \left(v_1 - l\frac{d\theta}{dt}\cos\theta\right)^2 + \left(l\frac{d\theta}{dt}\sin\theta\right)^2 \tag{2.68}$$

Using trigonometric relations, $\cos(\phi + \theta)$ can be expressed as

$$\cos(\phi + \theta) = \cos\phi\cos\theta - \sin\phi\sin\theta \tag{2.69}$$

then

$$\sin\phi = \frac{l\frac{d\theta}{dt}\sin\theta}{v_r} \tag{2.70}$$

and

$$\cos\phi = \frac{v_1 - l\frac{d\theta}{dt}\cos\theta}{v_r} \tag{2.71}$$

substituting $\cos\phi$, $\sin\phi$ and F_D, by their respective values into equation (2.67), one gets

$$(m_s + K_s m)l\frac{d^2\theta}{dt^2} = -Fe_s\sin\theta + Cv_r^2\left(\left[\frac{v_1 - l\frac{d\theta}{dt}\cos\theta}{v_r}\right]\cos\theta - \left[\frac{l\frac{d\theta}{dt}\sin\theta}{v_r}\right]\sin\theta\right) \tag{2.72}$$

which can be simplified to

$$(m_s + K_s m)l\frac{d^2\theta}{dt^2} = -Fe_s\sin\theta + Cv_r\left[(v_1 - l\frac{d\theta}{dt}\cos\theta)\cos\theta - (l\frac{d\theta}{dt}\sin\theta)\sin\theta\right] \tag{2.73}$$

The above equation is reduced to

$$(m_s + K_s m)l\frac{d^2\theta}{dt^2} = -Fe_s\sin\theta + Cv_r\left(v_1\cos\theta - l\frac{d\theta}{dt}\right) \tag{2.74}$$

with

$$v_r = \left[(v_1 - l\frac{d\theta}{dt}\cos\theta)^2 + (l\frac{d\theta}{dt}\sin\theta)^2\right]^{\frac{1}{2}} \tag{2.75}$$

or

$$v_r = \left[v_1^2 - 2v_1 l\frac{d\theta}{dt}\cos\theta + l^2(\frac{d\theta}{dt})^2\right]^{\frac{1}{2}} \tag{2.76}$$

substituting for the value of v_r in equation (2.74), one gets

$$(m_s + K_s m)l\frac{d^2\theta}{dt^2} = -Fe_s\sin\theta + C\left(v_1\cos\theta - l\frac{d\theta}{dt}\right)\left[v_1^2 - 2v_1 l\frac{d\theta}{dt}\cos\theta + l^2(\frac{d\theta}{dt})^2\right]^{\frac{1}{2}} \tag{2.77}$$

Assuming a small angle θ, then $\sin\theta = \theta$ and $\cos\theta = 1$, substituting the values, the final equation is derived and is of the form

$$(m_s + K_s m)l\frac{d^2\theta}{dt^2} = -Fe_s\theta + C\left(v_1 - l\frac{d\theta}{dt}\right)\left[v_1^2 - 2v_1 l\frac{d\theta}{dt} + l^2(\frac{d\theta}{dt})^2\right]^{\frac{1}{2}} \tag{2.78}$$

the term $[v_1^2 - 2v_1 l\frac{d\theta}{dt} + l^2(\frac{d\theta}{dt})^2]^{\frac{1}{2}}$ is equal $(v_1 - l\frac{d\theta}{dt})$. Therefore, the equation can be written as

$$(m_s + K_s m)l\frac{d^2\theta}{dt^2} = -Fe_s\theta + C(v_1 - l\frac{d\theta}{dt})^2 \tag{2.79}$$

or

$$\frac{d^2\theta}{dt^2} = \frac{1}{(m_s + K_s m)l}\left[-Fe_s\theta + Cv_1{}^2 - 2Cv_1 l\frac{d\theta}{dt} + Cl^2(\frac{d\theta}{dt})^2\right] \tag{2.80}$$

Introducing constants K_i, the final equation is written as

$$\ddot{\theta} = K_1\theta + K_2 v_1\dot{\theta} + K_3\dot{\theta}^2 + K_4 v_1^2 \tag{2.81}$$

where

$$K_1 = -\frac{Fe_s}{(m_s + K_s m)l} = -\frac{3}{2}\frac{W - F_B}{\pi R_s{}^3\rho_w\left(1 + 2\frac{\rho_s}{\rho_w}\right)l}$$

with

$$W = \rho_s g V_s = \frac{4}{3}\pi R_s{}^3\rho_s g$$

and

$$F_B = \rho_w g V_s = \frac{4}{3}\pi R_s{}^3\rho_w g$$

after substitution and rearrangement

$$K_1 = -\frac{2g}{l}\left(\frac{\frac{\rho_s}{\rho_w} - 1}{1 + 2\frac{\rho_s}{\rho_w}}\right)$$

$$K_2 = -\frac{2Cl}{(m_s + K_s m)l} = -\frac{3}{2}\frac{C_D}{R_s\left(1 + 2\frac{\rho_s}{\rho_w}\right)}$$

$$K_3 = \frac{Cl^2}{(m_s + K_s m)l} = \frac{3}{4}\frac{C_D l}{R_s\left(1 + 2\frac{\rho_s}{\rho_w}\right)}$$

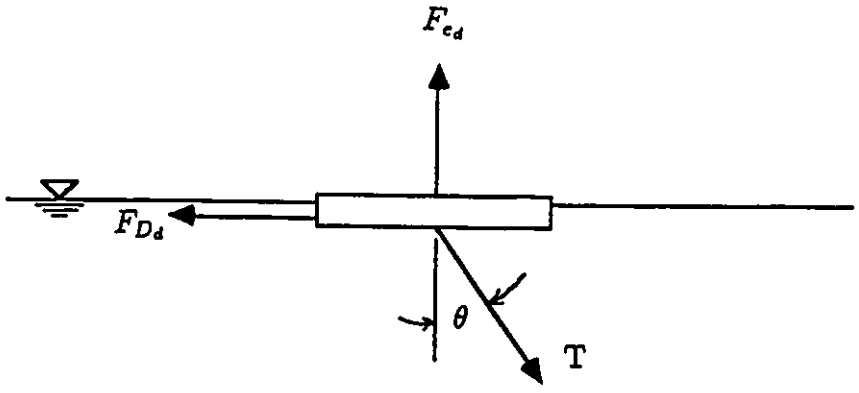

Figure 2.10: Forces on the disc.

and

$$K_4 = \frac{C}{(m_s + K_s m)l} = \frac{3}{4}\frac{C_D}{R_s\left(1 + 2\frac{\rho_s}{\rho_w}\right)l}$$

The third case proposed to complete the solution is to find the time required to reach equilibrium for case 2 if the increased horizontal tension component on the line is applied to a floating disc.

The equation of motion of the disc is as follows:

$$(m_d + k_d m)\frac{dv_d}{dt} = T\sin\theta - F_{D_d} \tag{2.82}$$

and

$$Fe_d = T\cos\theta \tag{2.83}$$

or

$$T = \frac{Fe_d}{\cos\theta} \tag{2.84}$$

Combining to eliminate T

$$(m_d + k_d m)\frac{dv_d}{dt} = Fe_d\frac{\sin\theta}{\cos\theta} - F_{D_d} \tag{2.85}$$

or

$$(m_d + k_d m)\frac{dv_d}{dt} = Fe_d \tan\theta - F_{D_d} \tag{2.86}$$

with

$$F_{D_d} = \frac{C_{D_d}\rho_w A_d}{2}(v_d - v_u)^2 \tag{2.87}$$

$$T = \frac{Fe_d}{\cos\theta} \tag{2.88}$$

and

$$Fe_d = F_B - W = \pi R_d^2 hg(\rho_w - \rho_d) \tag{2.89}$$

substituting for Fe_d and F_{D_d} in equation 2.86, one gets

$$(m_d + k_d m)\frac{dv_d}{dt} = \pi R_d^2 hg(\rho_w - \rho_d)\tan\theta - \frac{C_{D_d}\rho_w A_d}{2}(v_d - v_u)^2 \tag{2.90}$$

Neglecting the added mass effect and dividing both sides by $m_d = \pi R_d^2 h\rho_d$, developing and rearranging the above equation, one gets the equation expressing the velocity of the disc as a function of time which can be solved numerically using the Range Kutta method

$$\frac{dv_d}{dt} = g(\frac{\rho_w - \rho_d}{\rho_d})\tan\theta - \frac{C_{D_d}}{2h}\frac{\rho_w}{\rho_d}{v_d}^2 + \frac{C_{D_d}}{h}\frac{\rho_w}{\rho_d}v_u v_d - \frac{C_{D_d}}{2h}\frac{\rho_w}{\rho_d}{v_u}^2 \tag{2.91}$$

or

$$\frac{dv_d}{dt} = g(\frac{\rho_w}{\rho_d} - 1)\tan\theta - \frac{C_{D_d}}{2h}\frac{\rho_w}{\rho_d}{v_d}^2 + \frac{C_{D_d}}{h}\frac{\rho_w}{\rho_d}v_u v_d - \frac{C_{D_d}}{2h}\frac{\rho_w}{\rho_d}{v_u}^2 \tag{2.92}$$

The equation is of the form

$$\dot{v_d} = K_1 tan\theta - K_2 {v_d}^2 + 2K_2 v_u v_d - K_2 v_u^2 \tag{2.93}$$

Chapter 3

Experimental work

3.1 Introduction

Three groups of experiments were carried out. The vertical distribution of the mean velocity was first obtained using a combined float. A parametrical study was then undertaken using three different float combinations. Velocities were measured for two different study section lengths. The effect of the float size was then studied by comparing velocities so obtained to the ones obtained by Pitot tube. The third group was concerned mainly with the float migration and the effect of the float size on the diffusivity. Drag coefficients experiments were also started then discontinued after three sets of experiments because it appeared that little could be added to what was in many fluid mechanics textbooks.

3.2 Laboratory equipments

3.2.1 Description of experimental channels

Experimental investigations were conducted in the hydraulics laboratory of the University of Ottawa. The tests were performed in two different fixed horizontal flumes:

1. A small flume with a rectangular section of 12.7 cm wide, 20 cm deep and 6 m in length.
2. A big flume with a rectangular section of 38.7 cm wide, 61 cm deep and 12 m in length.

The walls of the two flumes were made of glass permitting a view of the trajectory and distance travelled by the float. The water supply tank which introduced the water was attached to the flume in both cases and the flow leaving the flume was measured by two different means: in the case of the small flume, at its end the discharge was measured by a weighing tank while at the end of the big flume, the discharge was measured by a rectangular weir. In both cases the flows were discharged back to the sump.

3.2.2 Description of floats

As shown in figure 3.1, the combined floats used in this project consisted of a circular disc floating on the surface of the water and a sphere submerged at a certain depth. The discs, having the same thickness, varied in diameter while the sphere diameter was kept constant. The two parts of the floats were connected by a monofilament fishing line.

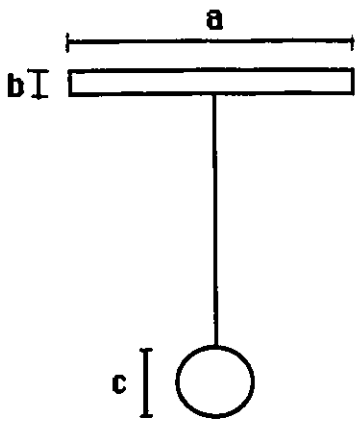

Float Type	a (cm)	b(mm)	c(cm)
Float 1	2.5	3.0	1.9
Float 2	3.1	3.0	1.9
Float 3	3.8	3.0	1.9

Shape	Material	Density (kg/m)
Disc	Wood	989
Sphere	Polyethylene	1073

Figure 3.1: Description of floats.

3.3 Velocity experiments

3.3.1 Experimental procedure

For each run, the measurements made were as follows:

1. Velocity measurements with a Pitot tube were made at three different sections within the reach. Each section was divided into six points including the surface and the bottom, the four other points were taken by incrementing the depth by 0.2D starting from the free surface down to the bottom.

2. The combined float was then released with the depths of sphere immersion: $f = 0.8D$, $f = 0.6D$, $f = 0.4D$ and $f = 0.2D$ respectively.

3. The time t the float took to travel the predetermined distance was measured using a stop watch. The stop watch was started at the time the float reached the beginning of the hydrometric section and was stopped manually when the float reached the end of the predetermined section of study.

4. The velocity at the free surface was then determined by releasing the disc in the channel and taking the time t the disc took to travel the predetermined section of study.

5. The depth of flow in the channel and the position of the Pitot tube at the points where velocities were measured were obtained by means

of a movable point gage.

6. The water temperature was measured by a thermometer at the beginning and the end of the experiment.

7. The discharge leaving the flume was measured. The rectangular weir for the big flume had been already calibrated [1] with the following rating curve:

$$Q = 1.847(l - 0.2h)h^{\frac{3}{2}}$$

where

Q = discharge of the weir,
l = length of the weir,
h = head upstream of the weir.

8. To get accurate results, velocity measurements at each depth were repeated 10 times and the arithmetic mean was taken as a result.

3.4 Drag experiments

The apparatus used is as shown in Figure 3.2. The test bodies were immersed in a flume with a rectangular section of 12.7 cm wide, 20 cm deep and having a length of 6 m. Supporting rods made of leaf spring 5 mm wide and nearly 1 mm thick were rigidly fixed to an instrument carriage.

Two strain gages were placed on the sides of the rod at 25 cm from the test bodies and were wired to a voltmeter or a digital strain indicator via the terminals.

Before testing the bodies, the relationship between the force and the strain was determined by experiment and the corresponding calibration curve was plotted.

When the force was applied to the body, the system deformed showing an output reading on the strain measuring device that was proportional to the force. The test bodies were then submerged in water at different depths and at each depth readings were taken. These readings were related to the drag on the testing body and the rod all together. The test bodies were then taken off and the supporting rod was submerged once again in water at the same depths for which readings were taken before. The strain related to the drag force on the test bodies was then obtained by subtracting readings for the supporting rod from those in presence of the test bodies. In order to calculate drag coefficients, the temperature was measured by a thermometer for each test run and flow velocities were also measured by a movable Pitot tube at nearly 1 cm upstream of the center of the testing body. The drag coefficient was determined by applying the well-known formula for the drag force

$$F_D = C_D \rho \frac{v_0^2}{2} A$$

Drag coefficient C_D is then equal to

$$C_D = \frac{2F_D}{\rho v_0^2 A}$$

where

F_D = drag on the body,

C_D = drag coefficient of the test body,

ρ = water density,

v_0 = velocity of the water,

A = frontal area of the test body.

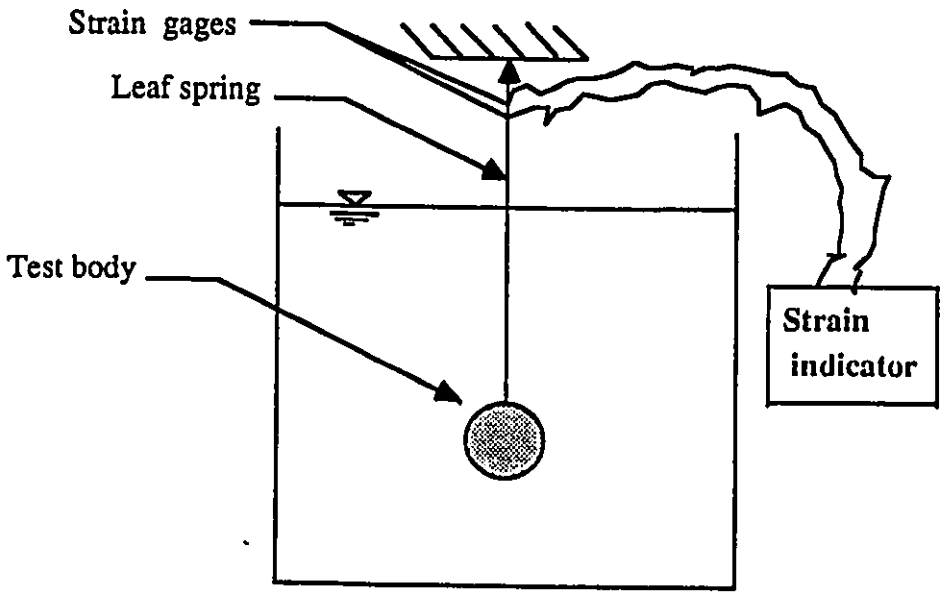

Figure 3.2: Experimental set-up for drag measurements.

3.5 Parametrical study

3.5.1 Float size effect

When the use of floats and drogues is necessary for current measurements, the size of their constituent parts then will be of great importance. In order to see the size effect on velocity measurement, a parametrical study was carried out. The experiments were conducted in the large flume and two study sections of 3.8m and 7.6m in length were selected. The floats used consisted of a combination of a disc and a sphere as previously described which are balanced to be almost neutrally buoyant. The floating part (the disc) as shown in Fig 3.1 was allowed to vary in diameter. Three diameters were selected 2.5 cm, 3.1 cm and 3.8 cm but the thickness was kept constant and equal to 3 mm. Water depths were first measured with a point gage mounted to an instrument carriage on the top of the flume, the velocity at a predetermined depth of immersion was then measured by a Pitot tube and by the three float combinations respectively. Velocities so obtained are given in Table 5.15 where they are compared to the Pitot tube ones. The results will be discussed later.

3.5.2 Section length effect

In an actual velocity measurement using floats, accurate results can be obtained if the hydrometric section is sufficiently long and uniform.
In the present investigation, uniformity was insured using the laboratory flume, the effect of the length of the reach, however, was to be examined. Ten experiments were carried out in the large flume using the three float combinations previously described. Velocities after travel distances of 3.8 m and 7.6 m were obtained for each float and compared to those obtained by Pitot tube. Results are presented in Table 5.15 and they are discussed in section 4.6.2.

3.6 Float diffusion

Float diffusion experiments were started using the same float combinations used for the parametrical study. After a few observations, the smallest float combination was excluded due to the fact that in most cases, the float reached the flume walls at mid-distance of the study section. The experiments were conducted in the large flume. Three scales were placed at about 1 to 2 cm above the water surface. These scales were used to determine the lateral float diffusion (see Figure 3.3).
The floats were released manually into the flume at a certain distance upstream from the first scale and were collected manually at the grid downstream from the third scale. In order to minimize initial disturbances, the

floats were dropped just above the water surface. To reduce any acceleration required to bring the float up to the water velocity, floats were moved at an approximately constant velocity along the surface before dropping them. The experiments were conducted for two water depths and all the floats were submerged at the same depth, hence they were exposed to almost the same conditions during the process of diffusion. For each combination of float size, travel distance, immersion depth and hydraulic conditions, three series of experiments were conducted with thirty individually repeated runs. By repeating the experiments for each float, the lateral diffusion after travel distance of 3.8 m and 7.6 m respectively can be determined from the scale readings as is shown in the next section.

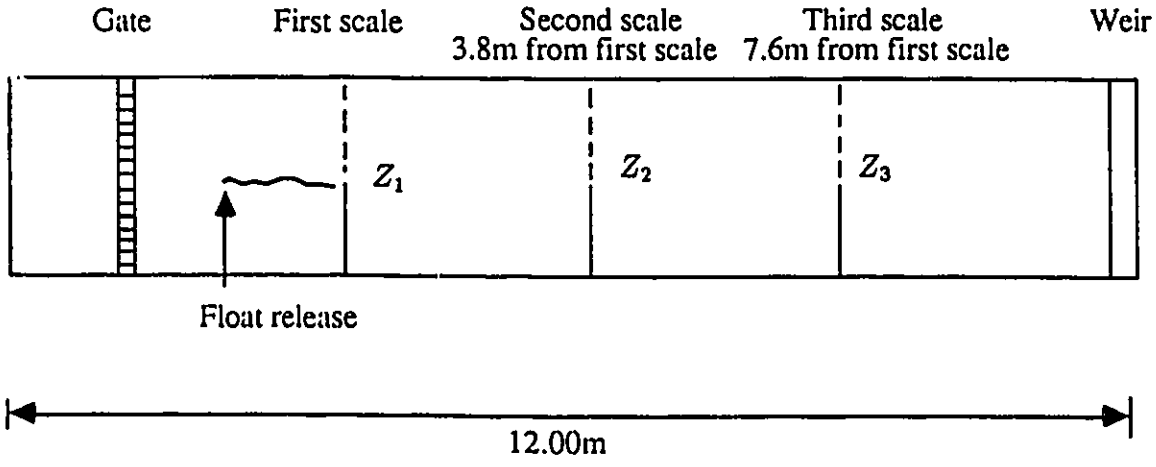

Figure 3.3: Top view of the flume and experimental set-up of the float diffusion experiments.

3.7 Experimental data reduction

The relation used for calculating the velocity by Pitot tube was as follows:

$$v = \sqrt{2g\Delta h} \tag{3.1}$$

where

g = acceleration of gravity,

Δh = dynamic pressure head.

The float velocities were then determined from the ratio of the distance to the time the float takes to travel that distance or

$$v = \frac{l}{t_0}$$

. Once velocities using the Pitot tube and the float were obtained, they were used as the input for the determination of the velocity from the drag-balance equation obtained as follows

For the disc

$$F_{Dd} = C_{Dd}\rho\frac{(v_{fd} - v_2)^2}{2}A_d \tag{3.2}$$

where

F_{Dd} = drag force on the disc,

C_{Dd} = drag coefficient for the disc,

ρ = density of water,

v_{fd} = velocity of the disc,

v_2 = velocity measured by Pitot tube at the surface,

A_d = area of the disc.

For the sphere

$$F_{Ds} = C_{Ds}\rho\frac{(v_1 - v_{fs})^2}{2}A_s \tag{3.3}$$

where

F_{Ds} = drag force on the sphere,

C_{Ds} = drag coefficient for the sphere,

ρ = density of water,

v_{fs} = velocity of the sphere,

v_1 = velocity of the water at the level of the sphere,

A_s = area of the sphere.

Equating the two drags gives:

$$C_{Dd}\rho\frac{(v_{fd} - v_2)^2}{2}A_d = C_{Ds}\rho\frac{(v_1 - v_{fs})^2}{2}A_s \tag{3.4}$$

After simplification and rearrangement, we get the equation for v_1

$$v_1 = v_{fs} + \sqrt{\frac{C_{Dd}}{C_{Ds}}\frac{A_d}{A_s}(v_{fd} - v_2)^2} \tag{3.5}$$

where

v_{fs} = velocity of the sphere,

v_{fd} = velocity of the disc,

v_2 = velocity measured by the Pitot tube at the surface.

Sphere and disc drag coefficients as a function of Reynolds number, shown in Tables 5.1 through 5.4 were obtained from the literature (Figure 2.6). Velocities, using the three different techniques, were found and the corresponding errors were calculated as shown in Tables 5.5 through 5.8. These results are discussed below.

In the parametrical study, two parameters were investigated; the length of the study section and the size of the floats. Two length reaches of respectively 3.8 m and 7.6 m were selected and three different float combinations were used in which only the diameter of the disc varied; the sphere diameter, however, was kept constant and equal to 1.9 cm. For each run, the velocity was first determined by a Pitot tube at a selected depth then each of the three float combinations was used to measure the velocity at that depth. Velocities so obtained are compared to those obtained from Pitot tube measurements.

The data from the float diffusion experiments were used to determine the properties of the distribution of the lateral migration of the floats. The frequency distribution of the variable Δz given by $\Delta z = z_1 - z_2$ in which z_1 is the reading of the upstream scale and z_2 is the reading of the downstream one, was described by calculating the three characteristics of the distribution, namely the mean, the variance and the skewness. The method of

moments was preferred and the following characteristics were calculated. The mean or the first moment

$$\mu = \frac{1}{N}\sum \Delta z_i \tag{3.6}$$

where N is the number of repetitive runs.

The second moment about the mean is the variance defined as

$$\sigma_p{}^2 = \frac{1}{N}\sum (\Delta z_i - \mu)^2 = \frac{1}{N}\sum \Delta z_i{}^2 - \mu^2 \tag{3.7}$$

and the third moment about the mean indicates the skewness of the distribution

$$\mu_3 = \frac{1}{N}\sum (\Delta z_i - \mu)^3 = \frac{1}{N}\sum \Delta z_i{}^3 - 3\mu\sigma^2 - \mu^3 \tag{3.8}$$

Theoretical variance on the other hand is given by the relation

$$\sigma^2 = 0.32\frac{U_*}{U}Rx \tag{3.9}$$

The velocity terms were eliminated as follows. The shear velocity is related to the mean velocity of the flow:

$$U_* = \frac{\sqrt{g}}{C}U \tag{3.10}$$

Assuming a steady flow and using the simpler formula stating that C varies as the sixth root of R or

$$C = \frac{R^{\frac{1}{6}}}{n} \tag{3.11}$$

substituting for the value of C in equation 3.10 leads to the relation used to determine the shear velocity

$$U_* = \frac{n\sqrt{g}}{R^{\frac{1}{6}}}U \tag{3.12}$$

or

$$\frac{U_*}{U} = \frac{n\sqrt{g}}{R^{\frac{1}{6}}} \tag{3.13}$$

in which n is the Manning's roughness coefficient equal 0.010 for the type of flume used (glass and machined metal).

Substituting for the value of $\frac{U_*}{U}$ into equation 3.9, one gets the expression for σ^2

$$\sigma^2 = 0.32n\sqrt{g}xR^{\frac{1}{6}} \tag{3.14}$$

Particle variances (equation 3.7) obtained from the method of moments were plotted together with equation 3.14.

Float diffusivities on the other hand, were calculated using the following approximate relation given by Ogura [21] :

$$\frac{\epsilon_{zp}}{\overline{\epsilon_z}} = \frac{\sqrt{\overline{u_p'^2}}}{\sqrt{\overline{u'^2}}} = f\left(\frac{l}{l_{max}}\right) = \frac{\sigma_p{}^2}{\sigma^2}$$

or simply

$$\frac{\epsilon_{zp}}{\overline{\epsilon_z}} = \frac{\sigma_p^2}{\sigma^2} = \frac{\sigma_p^2}{0.32n\sqrt{g}xR^{\frac{1}{6}}}$$

where

$\overline{\epsilon_z}$ = lateral diffusivity, and

ϵ_{zp} = Particle diffusivity.

For each experimental condition and float combination used, a ratio of the float σ_p^2 to the theoretical variance σ^2, obtained respectively from the experiments and equation 3.14, was found and then plotted against the relative float size $\frac{D}{R}$. D is the surface float or disc diameter and R is the hydraulic radius. Results are plotted in Figure 5.24 and will be discussed later.

Chapter 4

Discussion

4.1 Introduction

As discussed in chapter 1, this study was mainly an experimental one divided into three parts. The first one was the measurement of velocity by combined floats at different depths. The second part consisted of a parametrical study in which the float size and the study section length effect were examined. The third part was the study of float diffusion or lateral float migration.

The experimental data for the velocity measurement are presented in Tables 5.1 through 5.8 and the related figures are presented. The data for the parametrical study are presented in Table 5.15.

Finally, data for float diffusion are presented in Tables 5.16 and 5.17 and

plotted in Figures 5.23 and 5.24.

Besides the experimental part, a theoretical study of the response of the floats to accelerating and decelerating flows was carried out and the corresponding results are shown in Figures 5.25 through 5.28.

4.2 Results and analysis of the velocity distribution

Ten runs were performed in each of the two flumes used. In each run, the velocity was measured at the central part of the flume at different depths(from the surface to 0.8 of the depth by an increment of 0.2D) using both the Pitot tube and the float. To obtain a large range of velocities, water depths were varied . They ranged from 10 to 14 cm when the small flume was used and from 12.7 cm to 25.4 cm (5 to 10 in) when the large flume was used. Velocities so obtained ranged from 0.4 to 0.95 m/s. The floats were found to underestimate the velocity in the case of the small flume, while in case of the large flume, the floats tended to overestimate the velocity; in other words, the floats tend to move at a velocity higher than the flow velocity. This is believed to be due to the side effects and the related boundary layers.

Relative errors for the 100 point measurements were mostly below 5% except for 10 points. The location of the latter points close to the bottom of the channel (at 0.6D and 0.8D) leads one to conclude that the submerged

part of the float was affected by the boundary layer growing from the bottom. However, no boundary layer effect from the side walls was expected when the floats were released at the center of the flume.

In general, the velocity distribution evidenced a bluntness of the profile. In case of the large flume, the velocity distribution in the vertical section follows the logarithmic profile and the maximum velocity seems to occur at the surface. In case of the small flume, however, the logarithmic profile extends up from a bottom to a certain depth ranging from 0.4 to 0.2 of the flow depth; then, the velocity follows the parabolic law.

A fact that was observed when analyzing the data of both the Pitot tube and the float is that the maximum velocity does not always occur at the free surface, but sometimes occurs at a certain depth below it. This phenomenon called dip was more pronounced in case of the small flume than in the case of the large one.

Pitot tube and float measurements in most cases indicated that velocity variation with depth could not be easily detected above 0.2 and below 0.8 of the total depth. Therefore, and in an attempt to define properly the distribution of the velocity, special attention was given to the velocity measurement near the floor and the water surface.

A drag balance equation previously described was also used to calculate the velocity at the level of the sphere. It can be seen from Tables 5.4 through 5.8 that velocities obtained from the drag balance equation are very accurate and, contrary to the float case, it is hard to say that drag balance

overestimates or underestimates the velocity. Nevertheless, it is apparent that in most of the cases, velocities obtained from the drag balance equation are closer to the Pitot tube ones than the float velocities are. Notice that the drag on the tethered line was neglected and so is the wave drag.

4.3 Comparison of average velocities

The velocity distribution curves obtained from the Pitot tube were integrated over the depth of the flow to find the average velocity and so were the curves obtained from the float measurements after being extrapolated near the floor. Also, depending on whether the small or the large flume was used, an average velocity was calculated from the weighing tank or the weir respectively. The three average velocities obtained from the different techniques were compared.

The results (Table 5.9) obtained in the small flume showed the float average velocities to be slightly below the Pitot tube ones. In the large flume however (Table 5.10), float average velocities were found to be above the average velocities computed from the Pitot tube profile. When compared to the average velocities obtained by the weir and the weighing tank, float average velocities were found to be above the average velocities computed from the weighing method and the weir respectively. There was no apparent regularity to the differences in the average velocity between the floats and the other standard laboratory means used in this study, except that, in the case of the small flume, the floats did underestimate the Pitot tube average

velocity by an average of 1.46% while in the case of the large flume, floats did overestimate the Pitot tube average velocity by an average of 2.32%. On the other hand, floats were found to overestimate the weighing tank and the weir average velocities by an average of 0.99 and 2.40% respectively.

The cause of the slight difference between average velocities obtained from the float and the other techniques may be due to the integration method. The interpolation by straight lines between measured velocities and the extrapolation of the velocity curves made near the channel bottom may have resulted in a modification of the curves producing a slight change in the average velocity computed from the integration. Another source of error might be the 10 points equally weighted integration method. A smooth curve interpolation might have produced more accurate average velocities by the balancing effect.
Finally, human interaction with different equipment such as piezometers, point gages, and stop watch, may have resulted in an error in determining the local velocities on the basis of which the average velocity was computed.

4.4 Comparison between average and surface float velocity

For each of the twenty experiments performed, a surface float consisting of a disc with a 3.8 cm diameter and a density of 989 $\frac{kg}{m^3}$ was used to measure

the velocity at the surface level.

Assuming the Pitot tube average velocity to be the most accurate, surface velocities obtained from different runs by the surface float were compared to the corresponding average velocities computed from the trapezoidal integration of the Pitot tube velocity curves.

The results in Tables 5.11 and 5.12 show that from a point to point comparison, the surface float overestimates the average velocity by an amount that ranges from 0.68 to 9.77%. However, analyzing the results obtained from each of the flumes used separately, the surface float was found to overestimate the small and large flume average velocities by an average of 1.97 and 7.17% respectively. This agrees to a certain extent with what was found by other researchers even though most of them assume that the average velocity is 15% less than the surface float velocity.

4.5 Comparison of discharges

As mentioned earlier, ten runs were performed in each flume. The velocity profiles were interpolated using the trapezoidal method to get an average velocity on the basis of which the discharge was computed. Discharges so obtained were then compared to those obtained either from the weir in the case of the large flume or the weighing tank in the case of the small one.

Col.2 in Tables 5.13 and 5.14 shows the discharge measurement by one or the other laboratory equipment i.e. the weir or the weighing tank. Col.3 on the other hand, gives values of Q_I (discharge obtained from the integration

of the float velocity profile).

Assuming that the weir measurements are correct, the percentage of error for float measurements calculated from $100\frac{(Q_f - Q_w)}{Q_f}$ in the case of the large flume reveals that the floats tended to overestimate the discharge, and that, the error increases as the discharge increases. The maximum and minimum errors were found to be 11% and 0.77% respectively. Disregarding the sign, the average error for the 10 runs was 3.52%; when the sign was considered, the average error was reduced to 1.96%. In the small flume, however, the floats were found to overestimate the weighing tank discharge. The average error calculated from $100\frac{(Q_f - Q_t)}{Q_f}$ was 5.16%. Individual percentage of errors in the case of the small flume ranged from 3.37% to 9.49%. No special trend in the error was found.

The difference may have resulted from errors in measuring L, D, T and the weight in the case of the small flume and L, D, T and h of the water at the upstream end of the weir in the case of the large one. Combination of the above measured quantities may have resulted in errors in the determination of the average velocities and areas and consequently the discharge.

4.6 Parametrical study

4.6.1 Effect of the float size

By varying the diameter of the disc (the floating part) and keeping the sphere diameter constant, the size effect of the floating part on velocity measurement could be determined.

Measurements were made in the large flume. The three floats overestimate the velocity. By comparing the velocity obtained by Pitot tube to those obtained by each of the three floats at the same water depth, it was found that the smallest float size combination gives the smallest value and consequently the closest one to the Pitot tube velocity. The fact that large floats move at a velocity higher than the flow velocity can be explained as follows: If the volume occupied by the float were filled with a mass of the flowing water, then a certain part of its kinetic energy would be dissipated in eddies. Since these energy losses do not take place in presence of the float subjected to the same external forces as those acting on the equivalent fluid mass, then the float velocity is higher than the flow velocity. Thus, it is evident that small floats move at velocities nearer to the flow velocity.

4.6.2 Effect of the study section length

In order to study the effect of the section length on velocity determination, measurements were first made at the center of the large flume with the Pitot tube; then, the floats were released and the velocities were determined after a travel distance of 3.8 and 7.6 m respectively. The reason for choosing 3.8 m and 7.6 m is to investigate the effect of the length to width ratio on velocity determination. In fact, 3.8 m and 7.6 m represent the commonly used ratio of 10 and 20 times the width of the channel.
From Table 5.15, it can be seen that velocities obtained after a travel distance of 3.8 m were more accurate than those obtained after a 7.6 m travel distance. This was evident after analyzing the float diffusion data which showed the float diffusivities to be proportional to the longitudinal distance. In other words, the lateral float migration results in a timing error much larger in the case of 7.6 m than it is in the case of a 3.8 m distance. Therefore, it can be concluded that a study section length of 10 times the channel width appears to be appropriate and more suitable for average velocity measurements.

4.7 Float diffusion

As presented in Tables 5.16 and 5.17, three properties, namely, the mean, the variance and the skewness of the lateral migration of the floats were

obtained from experiments. Values of σ^2 calculated from the equation

$$\sigma^2 = 0.32n\sqrt{g}xR^{\frac{1}{6}}$$

representing theoretical values for diffusion of a dissolved substance were plotted in Figure 5.23 together with the experimental values ${\sigma_p}^2$.
Also, float diffusivities were evaluated from the equation $\epsilon_{zp} = \frac{1}{2}u(y)\frac{{\sigma_p}^2}{x}$ and normalized with the depth-averaged coefficient of transverse mixing $\bar{\epsilon_z} = 0.16u_xR$.
The relative float diffusivities so obtained were plotted against the relative float size $\frac{D}{R}$ in which D is the disc diameter and R is the hydraulic radius.

Results (see Figure 5.23) showed that for a given hydraulic condition, the float variance increases as the float size decreases. On the other hand, float variance was found to increase as the travel distance increases. No special trend indicating that the variance will increase with the increase of either the float size or the travel distance were found. Also, the figure showed that, in both cases, the lateral diffusion obtained when considering a dissolved matter is relatively higher than the float diffusion and again no regular trend was found as to how much greater the diffusion can be. Therefore, based on the above observations, it can be concluded that floats of the size used can not be treated as discrete particles or dissolved matter and that, the difference in the lateral diffusion is related to the float size. Figure 5.24, on the other hand, shows that the results obtained for the two experiments were consistent and the relative float diffusivity decreases exponentially as the relative float size increases. Also, the figure showed the same behavior and a qualitative agreement with the kinematic model

of Ogura [21]. Nevertheless, we failed to determine the largest eddy size that fits the experimental values.

4.8 Dynamical response

Three cases were studied. A sphere accelerating in water was first investigated, every single force was taken into consideration except the historical term known also as the Besset integral. The problem was first formulated and the integration was performed manually assuming an increase of 10% in water velocity and finding the time the sphere takes to reach 99% of the new velocity. The solution found suggests that the time response is inversely proportional to the flow velocity, the sphere radius and the density ratio. Even though 99% of the new velocity is really difficult if not impossible to reach, the solution shows that a few seconds are sufficient for a sphere to reach its new velocity. For spheres of diameter less than the one considered, the time response is even better.

The second case, on the other hand, was to study the time response when a submerged sphere tethered to a line is subject to an accelerating flow. The formulation of the problem led to a second order nonlinear differential equation. The equation was solved numerically since an exact solution cannot be obtained. The Runge-Kutta method was selected for this purpose. The program listing and a sample computer result are presented in

the appendix. As given in the appendix, the angular displacement and the angular velocity were determined for different density ratios and plotted against the time. This procedure was repeated for different density ratios (i.e $\frac{\rho_s}{\rho_w}$=2,3,4,5). The time required was then obtained for different combinations of parameters. As it can be seen from Figures 5.25 through 5.28, less than 2 seconds are sufficient for the system to reach its new equilibrium.

The third case is to investigate the time response when the increased horizontal component of the tension resulting from case 2 is applied to a floating disc. The formulation led to a differential equation that is a function of the angle θ, the velocity of the disc v_d and the time t. The external forces in the equation were known and an expression for the angle θ was needed. The integration of the angular velocity found in case 2 was performed as given in the appendix. The constants were then determined using boundary conditions (i.e initial and final values) and substituted into equation 2.86, a final expression was found which relates the time and the disc velocity. This equation, which was not solved, has the following form:

$$\dot{v_d} = K_1 tan\theta - K_2 {v_d}^2 + 2K_2 v_u v_d - K_2 v_u^2 \tag{4.1}$$

and the angle θ obtained from the integration is defined as:

$$-\frac{\omega}{k^2+\omega^2} X e^{-kt}\left[cos(\omega t+\phi)+\frac{k}{\omega}sin(\omega t+\phi)\right]+C \tag{4.2}$$

where

ω = frequency,

ϕ = angle,

k = coefficient for the decaying exponential response,

t = time.

Chapter 5

Conclusions

The conclusions that can be drawn from this study are:

- Combined float techniques are well suited for velocity and discharge measurements.
- Combined floats underestimated the velocity in the case of the small flume. It is believed this is due to the wall effects and the related boundary layers. In the large flume however, floats overestimated the velocity. This is thought to be possibly due to one of two effects: 1) the fact that the disc is in the zone of highest velocity or 2) the calibration of the Pitot tube used for the large flume.
- Combined floats overestimated the average velocities measured by both the weir and the weighing tank by an average of 2.40% and

0.99% respectively.

- Combined floats overestimated the Pitot tube average velocities by an average of 2.32% in the case of the large flume, in the case of the small flume, however, floats underestimated the Pitot tube average velocities by an average of 1.46%. The reasons for this are believed to be the same as mentioned for the individual velocity measurements.

- The most accurate measurements were obtained with the smallest float in a relatively small study section length (about 10 times the channel width). This is due to the lesser effects of float diffusion for this case.

- Average errors on discharge measurements were 3.52% and 5.16% in the large and small flumes respectively, for the same reasons previously given.

- For a given condition, lateral float diffusivity decreased with increasing the float size.

- Float variance increases as the float size decreases and the travel distance increases.

- The diffusion of a dissolved substance is relatively higher than the lateral diffusion of the floats (due to their size, floats of the kind used can not be treated as a dissolved matter or discrete particles).

Table 5.1: Determination of drag coefficients (Float submerged in the small flume)

Water Depth	Measurement Level	Velocity by Pitot tube	Reynolds No.		Drag Coefficient	
			Disc	Sphere	Disc	Sphere
	surface	0.536				
	0.2d	0.548		15065		
10.00	0.4d	0.551	21150	15147	1.12	0.43
	0.6d	0.548		15065		
	0.8d	0.542		14900		
	surface	0.453				
	0.2d	0.474		13030		
10.50	0.4d	0.471	17875	12948	1.12	0.40
	0.6d	0.471		12948		
	0.8d	0.464		12755		
	surface	0.562				
	0.2d	0.582		16000		0.44
11.00	0.4d	0.576	22177	15843	1.12	0.44
	0.6d	0.571		15697		0.44
	0.8d	0.556		15284		0.43
	surface	0.488				
	0.2d	0.500		13745		
11.50	0.4d	0.500	19256	13745	1.12	0.41
	0.6d	0.498		13690		
	0.8d	0.490		13470		
	surface	0.583				
	0.2d	0.608		16714		
12.00	0.4d	0.605	23005	16631	1.12	0.44
	0.6d	0.602		16549		
	0.8d	0.594		16330		

Table 5.2: Determination of drag coefficients (Float submerged in the small flume)

Water Depth	Measurement Level	Velocity by Pitot tube (m/s)	Reynolds No.		Drag Coefficient	
			Disc	Sphere	Disc	Sphere
	surface	0.621				
	0.2d	0.642		17649		0.45
12.50	0.4d	0.642	24505	17649	1.12	0.45
	0.6d	0.644		17704		0.45
	0.8d	0.629		17291		0.44
	surface	0.611				
	0.2d	0.629		17291		
13.00	0.4d	0.626	24110	17209	1.12	0.44
	0.6d	0.631		17346		
	0.8d	0.628		17264		
	surface	0.642				
	0.2d	0.652		17923		
13.50	0.4d	0.649	25333	17841	1.12	0.45
	0.6d	0.654		17978		
	0.8d	0.646		17759		
	surface	0.657				
	0.2d	0.671		18446		
14.00	0.4d	0.674	25925	18528	1.12	0.45
	0.6d	0.676		18583		
	0.8d	0.668		18363		
	surface	0.637				
	0.2d	0.660		18143		
14.00	0.4d	0.652	25136	17923	1.12	0.45
	0.6d	0.652		17923		
	0.8d	0.654		17978		

Table 5.3: Determination of drag coefficients (Float submerged in the large flume)

Water Depth	Measurement Level	Velocity by Pitot tube	Reynolds No.		Drag Coefficient	
			Disc	Sphere	Disc	Sphere
12.70	surface	0.630	24860		1.12	0.44
	0.2d	0.620		17044		
	0.4d	0.611		16796		
	0.6d	0.604		16604		
	0.8d	0.580		15944		
13.97	surface	0.663	26162		1.12	0.44
	0.2d	0.637		17511		
	0.4d	0.621		17072		
	0.6d	0.604		16604		
	0.8d	0.565		15532		
15.24	surface	0.710	28000		1.12	0.45
	0.2d	0.694		19078		0.45
	0.4d	0.682		18748		0.45
	0.6d	0.664		18253		0.45
	0.8d	0.620		17044		0.44
16.51	surface	0.735	29000		1.12	0.45
	0.2d	0.723		19875		
	0.4d	0.723		19875		
	0.6d	0.706		19408		
	0.8d	0.670		18418		
17.78	surface	0.760	29989		1.12	0.45
	0.2d	0.757		20810		
	0.4d	0.757		20810		
	0.6d	0.743		20425		
	0.8d	0.723		19875		

Table 5.4: Determination of drag coefficients (Float submerged in the large flume)

Water Depth	Measurement Level	Velocity by Pitot tube (m/s)	Reynolds No.		Drag Coefficient	
			Disc	Sphere	Disc	Sphere
19.05	surface	0.825	32550	22350	1.12	0.46
	0.2d	0.813		22404		
	0.4d	0.815		22129		
	0.6d	0.805		21250		
	0.8d	0.773				
20.32	surface	0.815	32160	22267	1.12	0.46
	0.2d	0.810		22267		
	0.4d	0.810		22129		
	0.6d	0.805		21387		
	0.8d	0.778				
21.59	surface	0.848	33462	23367	1.12	0.46
	0.2d	0.850		23422		
	0.4d	0.852		23422		
	0.6d	0.852		23284		
	0.8d	0.847				
22.86	surface	0.884	34880	24411	1.12	0.47
	0.2d	0.888		24521		
	0.4d	0.892		24604		
	0.6d	0.895		24136		
	0.8d	0.878				
25.40	surface	0.813	32000	22349	1.12	0.46
	0.2d	0.813		22349		
	0.4d	0.813		22184		
	0.6d	0.807		21552		
	0.8d	0.784				

Table 5.5: Comparison of velocity measurements by pitot tube to those obtained from drag-balance equation and floats (Small flume).

Water Depth (Cm)	Measurement Level	Velocity (m/s)			Error (%)	
		Pitot v_p	Float v_f	Drag Balance v_D	$\frac{v_p - v_f}{v_p}$	$\frac{v_p - v_D}{v_p}$
10.00	surface	0.536	0.529		1.30	
	0.2d	0.548	0.541	0.548	1.28	0
	0.4d	0.551	0.542	0.549	1.63	0.36
	0.6d	0.548	0.543	0.550	0.91	-0.36
	0.8d	0.542	0.535	0.542	1.29	0
10.50	surface	0.453	0.441		2.65	
	0.2d	0.474	0.453	0.466	4.43	1.68
	0.4d	0.471	0.458	0.471	2.76	0
	0.6d	0.471	0.457	0.470	2.96	0.21
	0.8d	0.464	0.438	0.451	5.60	1.30
11.00	surface	0.562	0.545		3.03	
	0.2d	0.582	0.567	0.584	2.57	-0.34
	0.4d	0.576	0.577	0.589	-0.17	-2.26
	0.6d	0.571	0.568	0.585	0.53	-2.45
	0.8d	0.556	0.549	0.566	1.26	-1.79
11.50	surface	0.488	0.480		1.64	
	0.2d	0.500	0.491	0.499	1.80	0.20
	0.4d	0.500	0.490	0.498	2.00	0.40
	0.6d	0.498	0.487	0.495	2.21	0.60
	0.8d	0.491	0.480	0.488	2.24	0.61
12.00	surface	0.583	0.570		2.23	
	0.2d	0.608	0.585	0.598	3.78	1.64
	0.4d	0.605	0.587	0.600	2.97	0.83
	0.6d	0.602	0.577	0.590	4.15	1.99
	0.8d	0.594	0.570	0.583	4.04	1.85

Table 5.6: Comparison of velocity measurements by pitot tube to those obtained from drag-balance equation and floats (Small flume).

Water Depth (Cm)	Measurement Level	Velocity (m/s)			Error (%)	
		Pitot v_p	Float v_f	Drag Balance v_D	$\frac{v_p - v_f}{v_p}$	$\frac{v_p - v_D}{v_p}$
12.50	surface	0.621	0.615		0.96	
	0.2d	0.642	0.640	0.646	0.31	-0.62
	0.4d	0.642	0.645	0.651	-0.47	-1.40
	0.6d	0.644	0.636	0.642	1.24	0.31
	0.8d	0.629	0.620	0.626	1.43	0.48
13.00	surface	0.611	0.591		3.27	
	0.2d	0.629	0.615	0.635	2.23	-0.95
	0.4d	0.626	0.623	0.643	0.48	-2.72
	0.6d	0.631	0.620	0.640	1.74	-1.43
	0.8d	0.628	0.596	0.616	5.10	1.91
13.50	surface	0.642	0.626		2.49	
	0.2d	0.652	0.652	0.668	0	-2.45
	0.4d	0.649	0.651	0.667	-0.30	-2.77
	0.6d	0.654	0.642	0.658	1.83	-0.61
	0.8d	0.646	0.630	0.646	2.48	0
14.00	surface	0.657	0.642		2.28	
	0.2d	0.671	0.668	0.683	0.45	-1.79
	0.4d	0.674	0.665	0.680	1.33	-0.89
	0.6d	0.676	0.662	0.677	2.07	-0.15
	0.8d	0.668	0.648	0.663	2.99	0.75
14.00	surface	0.637	0.620		2.67	
	0.2d	0.660	0.642	0.659	2.73	0.15
	0.4d	0.652	0.645	0.662	1.07	-1.53
	0.6d	0.652	0.650	0.667	0.31	-2.30
	0.8d	0.654	0.630	0.647	3.68	1.07

Table 5.7: Comparison of velocity measurements by pitot tube to those obtained from drag-balance equation and floats (Large flume).

Water Depth (Cm)	Measurement Level	Velocity (m/s)			Error (%)	
		Pitot v_p	Float v_f	Drag Balance v_D	$\frac{v_p - v_f}{v_p}$	$\frac{v_p - v_D}{v_p}$
12.70	surface	0.630	0.625		0.79	
	0.2d	0.620	0.630	0.625	-1.61	-0.81
	0.4d	0.611	0.629	0.624	-2.95	-2.13
	0.6d	0.604	0.619	0.614	-2.48	-1.66
	0.8d	0.580	0.593	0.588	-2.24	-1.38
13.97	surface	0.663	0.665		-0.30	
	0.2d	0.637	0.658	0.656	-3.29	-2.98
	0.4d	0.621	0.653	0.651	-5.15	-4.83
	0.6d	0.604	0.646	0.644	-6.95	-6.62
	0.8d	0.565	0.629	0.627	-11.33	-10.97
15.24	surface	0.710	0.691		2.68	
	0.2d	0.694	0.681	0.681	1.87	1.87
	0.4d	0.682	0.707	0.688	-3.67	-0.88
	0.6d	0.664	0.700	0.681	-5.42	-2.56
	0.8d	0.620	0.678	0.659	-9.35	-6.29
16.51	surface	0.735	0.748		1.77	
	0.2d	0.723	0.735	0.722	-1.66	0.14
	0.4d	0.723	0.744	0.731	-2.90	-1.11
	0.6d	0.706	0.736	0.723	-4.25	-2.41
	0.8d	0.670	0.735	0.722	-9.70	-7.76
17.78	surface	0.760	0.763		-0.39	
	0.2d	0.757	0.769	0.766	-1.58	-1.19
	0.4d	0.757	0.769	0.766	-1.58	-1.19
	0.6d	0.743	0.763	0.760	-2.69	-2.29
	0.8d	0.723	0.758	0.755	-4.84	-4.43

Table 5.8: Comparison of velocity measurements by pitot tube to those obtained from drag-balance equation and floats (Large flume).

Water Depth (Cm)	Measurement Level	Velocity (m/s)			Error (%)	
		Pitot v_p	Float v_f	Drag Balance v_D	$\frac{v_p - v_f}{v_p}$	$\frac{v_p - v_D}{v_p}$
19.05	surface	0.825	0.816		1.09	
	0.2d	0.813	0.804	0.813	1.10	0
	0.4d	0.815	0.812	0.820	0.37	-0.61
	0.6d	0.805	0.812	0.803	-0.86	0.25
	0.8d	0.773	0.813	0.804	-5.17	-4.00
20.32	surface	0.815	0.845		-3.68	
	0.2d	0.810	0.850	0.820	-4.93	-1.23
	0.4d	0.810	0.843	0.813	-4.07	-0.37
	0.6d	0.805	0.841	0.811	-4.47	-0.74
	0.8d	0.778	0.815	0.785	-4.76	-0.90
21.59	surface	0.848	0.871		-2.71	
	0.2d	0.850	0.859	0.836	-1.06	1.65
	0.4d	0.852	0.872	0.849	-2.35	0.35
	0.6d	0.852	0.860	0.837	-0.94	1.76
	0.8d	0.847	0.869	0.846	-2.59	0.12
22.86	surface	0.884	0.916		-3.64	
	0.2d	0.888	0.914	0.883	-2.93	0.56
	0.4d	0.892	0.905	0.874	-1.46	2.02
	0.6d	0.895	0.908	0.877	-1.46	2.02
	0.8d	0.878	0.910	0.879	-3.64	-0.14
25.40	surface	0.813	0.790		2.83	
	0.2d	0.813	0.805	0.828	0.98	-1.85
	0.4d	0.813	0.803	0.826	1.23	-1.60
	0.6d	0.807	0.805	0.826	0.25	-2.35
	0.8d	0.784	0.780	0.803	0.51	-2.42

Table 5.9: Comparison of average velocities (Small flume)

Pitot tube $\bar{V}_p$	Float $\bar{V}_f$	Weighing Tank $\bar{V}_t$	Error (%) $\frac{V_f-V_p}{V_f}$	Error (%) $\frac{V_f-V_t}{V_f}$
0.511	0.510	0.500	-0.20	1.96
0.436	0.425	0.430	-2.59	-1.18
0.535	0.530	0.505	-0.93	4.72
0.466	0.457	0.450	-1.93	1.53
0.561	0.546	0.542	-2.67	0.73
0.598	0.597	0.585	-0.17	2.01
0.587	0.575	0.578	-2.04	-0.52
0.609	0.606	0.593	-0.49	2.15
0.634	0.620	0.612	-2.21	1.29
0.611	0.603	0.620	-1.33	-2.82

Table 5.10: Comparison of average velocities (Large flume)

Pitot tube $\bar{V}_p$	Float $\bar{V}_f$	Rectangular Weir $\bar{V}_w$	Error (%) $\frac{V_f-V_p}{V_f}$	Error (%) $\frac{V_f-V_w}{V_f}$
0.569	0.577	0.582	1.39	-0.87
0.573	0.600	0.568	4.50	5.33
0.626	0.646	0.663	3.19	-2.63
0.663	0.689	0.687	3.77	0.29
0.700	0.715	0.692	2.10	3.22
0.754	0.760	0.760	0.79	0.00
0.752	0.783	0.770	3.96	1.66
0.795	0.810	0.760	1.85	6.17
0.832	0.855	0.784	2.69	8.30
0.753	0.745	0.726	-1.07	2.55

Table 5.11: Comparison between surface and average velocity (Small flume).

Run No	Velocity by surface float v_{sf}	Average velocity from Pitot tube $\bar{V}_p$	Error (%) $\frac{v_{sf}-\bar{V}_p}{v_{sf}}$
1	0.529	0.511	3.40
2	0.441	0.436	1.13
3	0.545	0.535	1.83
4	0.480	0.466	2.92
5	0.570	0.561	1.58
6	0.615	0.598	2.76
7	0.591	0.587	0.68
8	0.626	0.609	2.71
9	0.642	0.634	1.25
10	0.620	0.611	1.45

Table 5.12: Comparison between surface and average velocity (Large flume).

Run No	Velocity by surface float v_{sf}	Average velocity from Pitot tube $\bar{V}_p$	Error (%) $\frac{v_{sf}-\bar{V}_p}{v_{sf}}$
1	0.625	0.577	7.68
2	0.665	0.600	9.77
3	0.691	0.646	6.51
4	0.748	0.689	7.89
5	0.763	0.715	6.29
6	0.816	0.760	6.86
7	0.845	0.783	7.34
8	0.871	0.810	7.00
9	0.916	0.855	6.66
10	0.790	0.745	5.70

Table 5.13: Comparison of discharges (Small flume).

Run No	Discharge $*10^3(m^3/s)$		Error (%) $\frac{Q_f - Q_t}{Q_t}$
	Weighing tank Q_t	Float Q_f	
1	6.17	6.47	4.63
2	5.41	5.67	4.58
3	6.39	7.06	9.49
4	6.29	6.67	5.70
5	7.91	8.31	4.81
6	8.90	9.46	5.92
7	9.17	9.49	3.37
8	9.95	10.38	4.14
9	10.60	11.02	3.81
10	10.17	10.72	5.13

Table 5.14: Comparison of discharges (Large flume).

Run No	Discharge $*10^3(m^3/s)$		Error (%) $\frac{Q_f - Q_w}{Q_f}$
	Weir Q_w	Float Q_f	
1	28.62	27.97	-2.32
2	30.73	30.97	0.77
3	37.31	36.92	-1.06
4	40.51	39.10	-3.61
5	44.25	44.72	1.05
6	48.56	48.17	-0.81
7	51.23	53.08	3.48
8	55.50	58.60	5.29
9	61.62	65.43	5.82
10	64.23	72.17	11.00

Table 5.15: Data for the parametrical study (velocities obtained using 2 different section lengths and 3 different float sizes).

Run	Pitot tube	Travel distance = 3.80m			Travel distance = 7.60m		
No	velocity	Small size	Medium size	Large size	Small size	Medium size	Large size
1	0.500	0.508	0.515	0.525	0.520	0.536	0.538
2	0.524	0.526	0.531	0.530	0.538	0.538	0.535
3	0.543	0.537	0.550	0.552	0.550	0.558	0.562
4	0.591	0.590	0.610	0.616	0.608	0.632	0.637
5	0.611	0.618	0.623	0.630	0.628	0.636	0.636
6	0.621	0.615	0.620	0.622	0.629	0.636	0.635
7	0.631	0.630	0.630	0.638	0.636	0.638	0.642
8	0.641	0.635	0.645	0.655	0.653	0.658	0.668
9	0.651	0.660	0.667	0.670	0.660	0.665	0.670
10	0.720	0.727	0.733	0.740	0.735	0.742	0.755

Table 5.16: Data for float diffusion (Run 1)

Hydraulic Conditions	Float Type	Test Series	Travel distance = 3.80m			Travel distance = 7.60m		
			Mean	Variance	Skewness	Mean	Variance	Skewness
depth=10.8cm		1-30	0.025	53.94	-0.26	-2.87	89.65	0.18
width=38.7cm	1	2-30	-0.40	51.49	-0.001	1.20	68.90	-0.10
		3-30	-1.90	55.66	0.10	0.15	74.55	-0.16
Q=17.86l/s		mean						
U=42.5cm/s		values	-0.76	53.70	-0.06	-0.51	77.70	-0.028
U1=2cm/s		1-30	4.40	40.86	-0.69	-0.40	57.26	-0.28
	2	2-30	0.67	34.96	-0.034	-1.77	63.06	0.15
float position=0.4d		3-30	-0.27	42.66	-0.26	-2.65	65.80	0.32
R=6.93cm		mean						
		values	1.60	39.49	-0.33	-1.60	62.04	0.064

Table 5.17: Data for float diffusion (Run 2)

Hydraulic Conditions	Float Type	Test Series	Travel distance = 3.80m			Travel distance = 7.60m		
			Mean	Variance	Skewness	Mean	Variance	Skewness
depth=14cm		1-30	-3.75	29.04	0.86	-3.70	49.66	1.09
width=38.7cm	1	2-30	-4.80	33.33	0.94	0.95	49.05	-0.023
		3-30	-3.50	32.50	0.61	-0.85	52.53	-0.40
Q=27.8l/s		mean						
U=51.5cm/s		values	-4.02	31.62	0.80	-1.20	50.41	0.27
U1=2.45cm/s		1-30	4.40	36.15	0.49	-0.67	75.23	0.23
	2	2-30	0.67	41.16	0.99	-1.50	62.22	0.21
float position=0.6d		3-30	-0.27	44.03	1.42	-1.90	54.76	0.18
R=8.12cm		mean						
		values	-4.14	40.47	0.97	-1.36	64.07	0.21

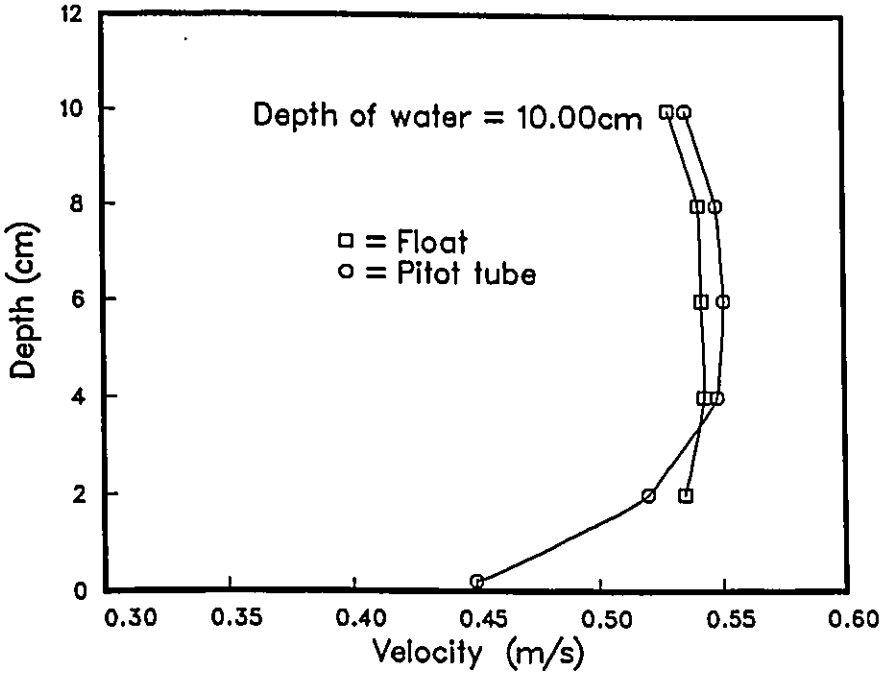

Figure 5.1: Comparison between Pitot tube and float velocity (small flume).

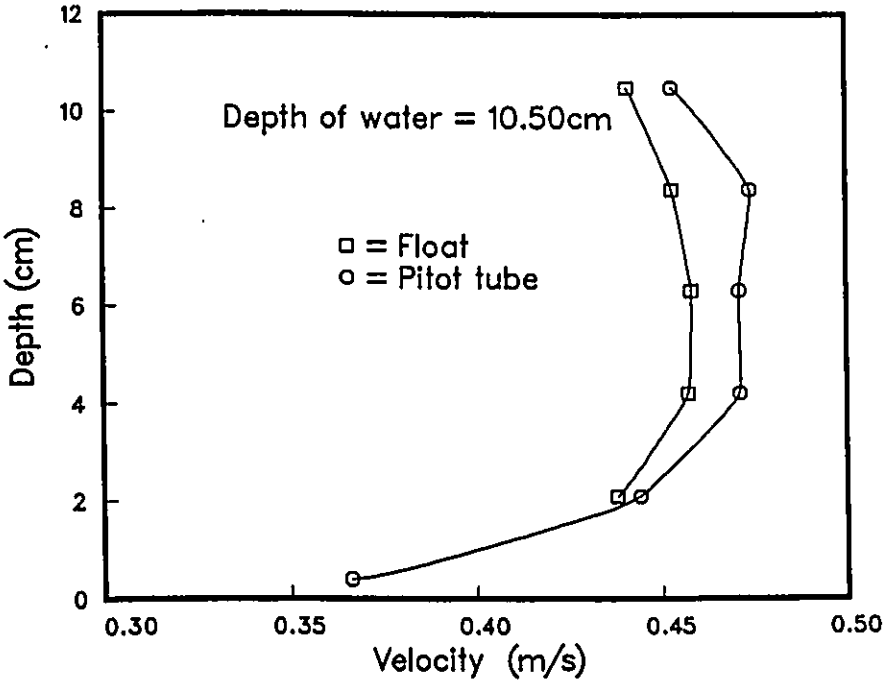

Figure 5.2: Comparison between Pitot tube and float velocity (small flume).

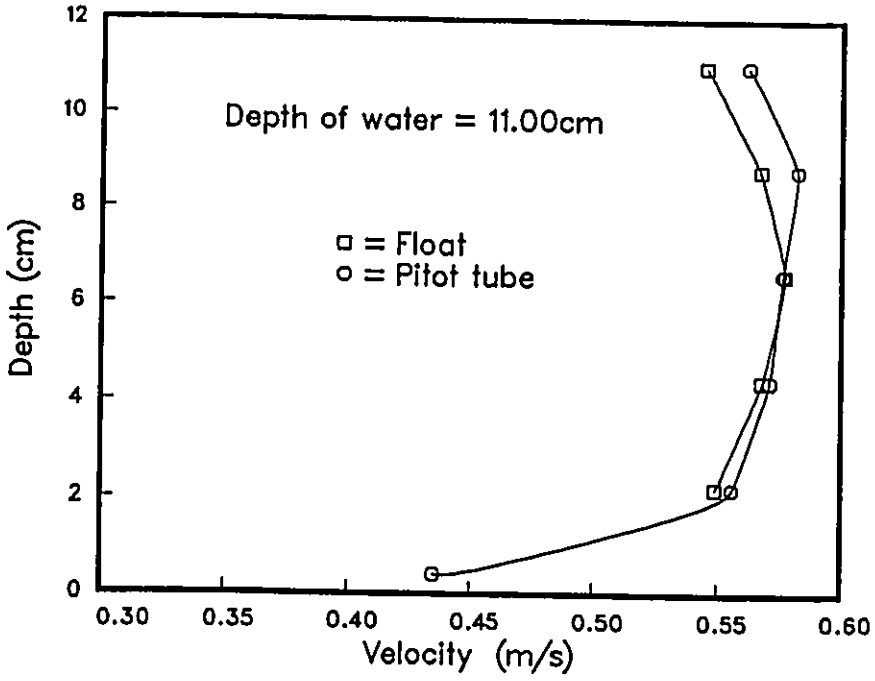

Figure 5.3: Comparison between Pitot tube and float velocity (small flume).

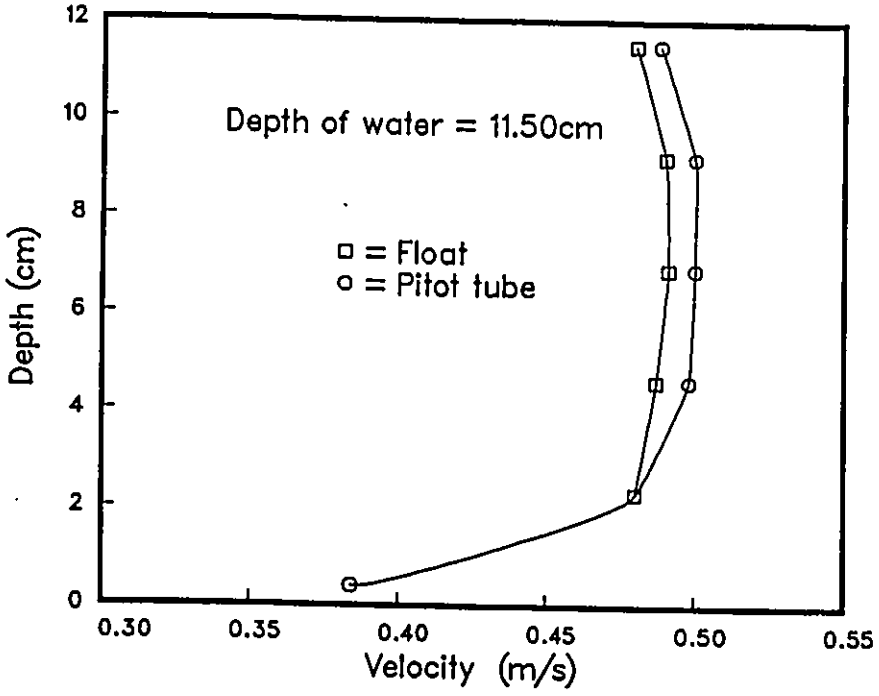

Figure 5.4: Comparison between Pitot tube and float velocity (small flume).

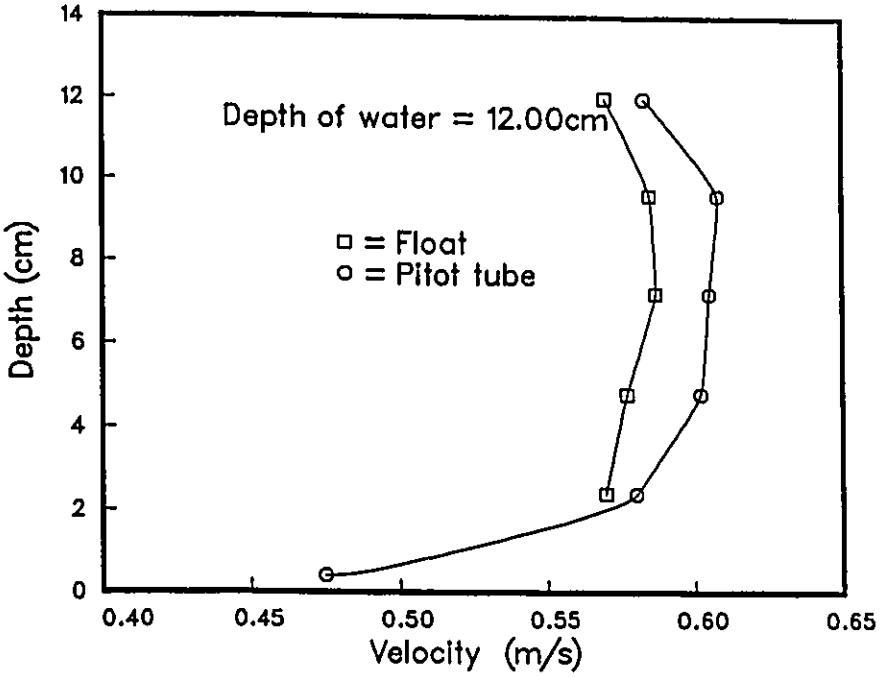

Figure 5.5: Comparison between Pitot tube and float velocity (small flume).

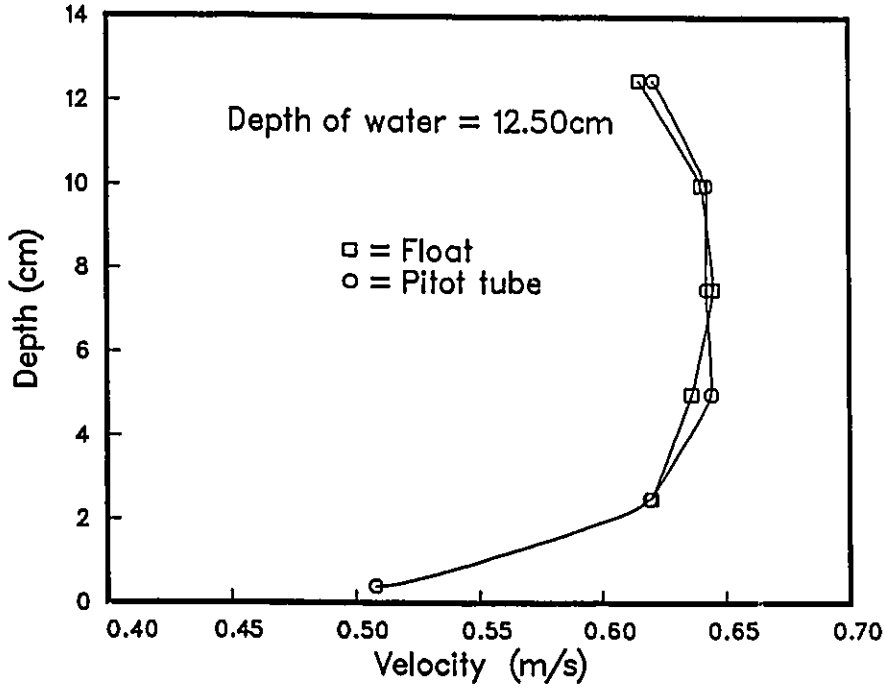

Figure 5.6: Comparison between Pitot tube and float velocity (small flume).

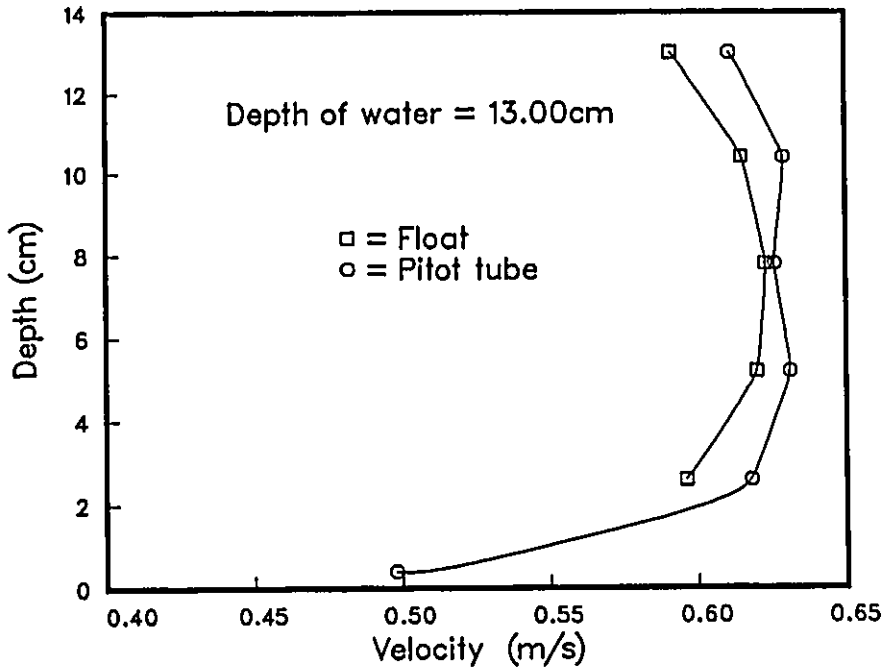

Figure 5.7: Comparison between Pitot tube and float velocity (small flume).

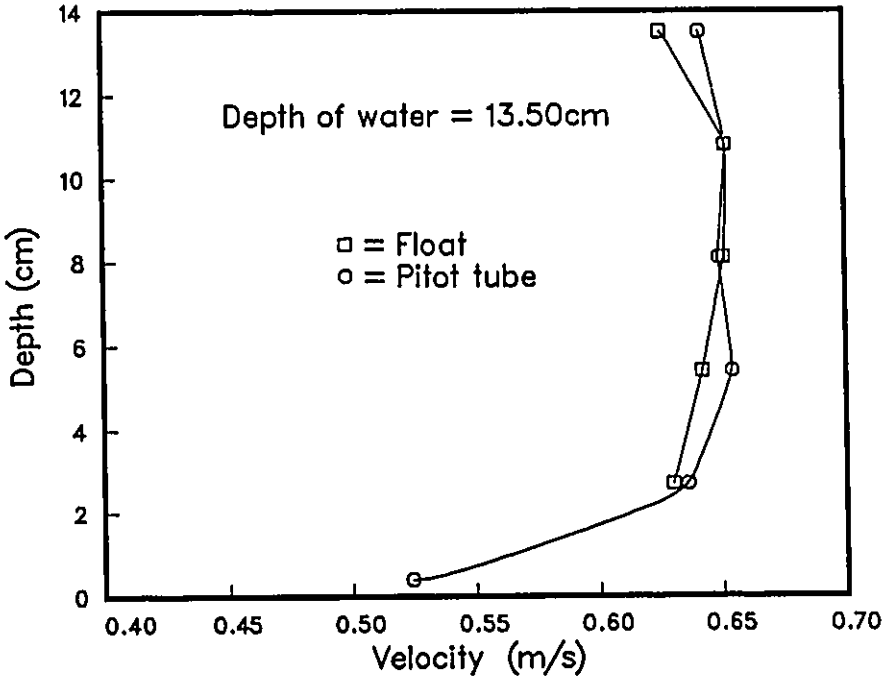

Figure 5.8: Comparison between Pitot tube and float velocity (small flume).

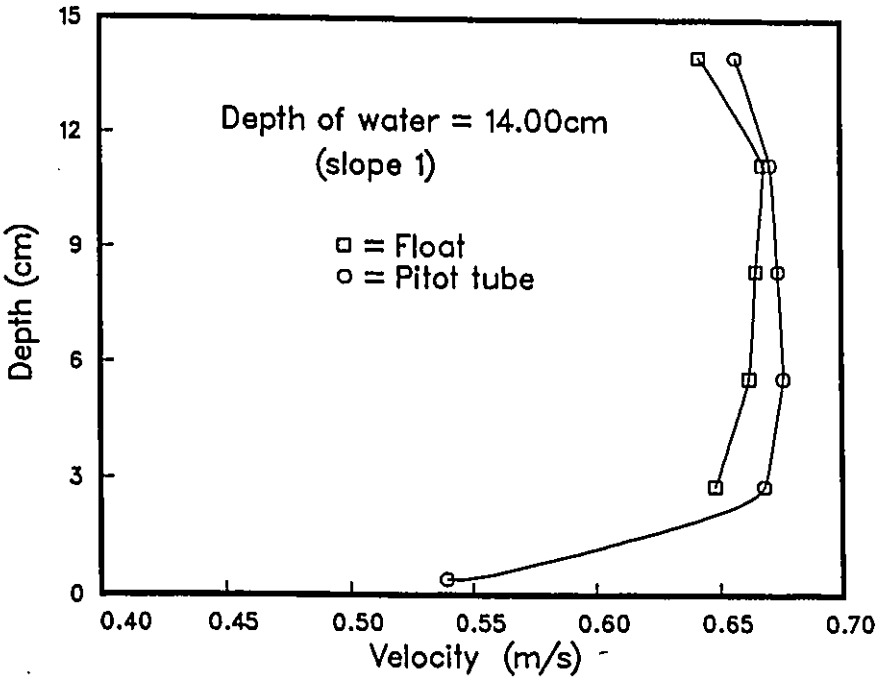

Figure 5.9: Comparison between Pitot tube and float velocity (small flume).

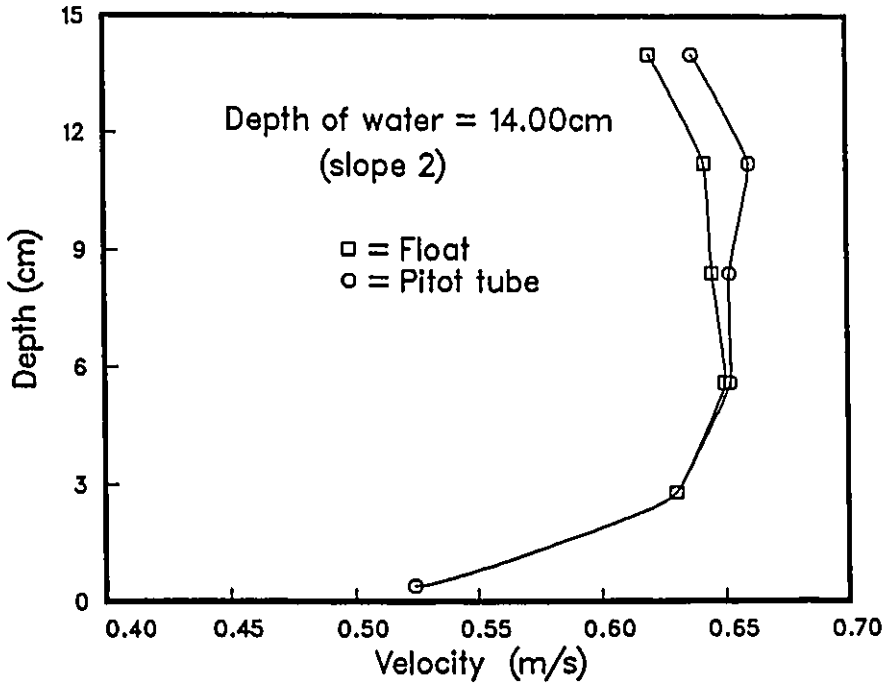

Figure 5.10: Comparison between Pitot tube and float velocity (small flume).

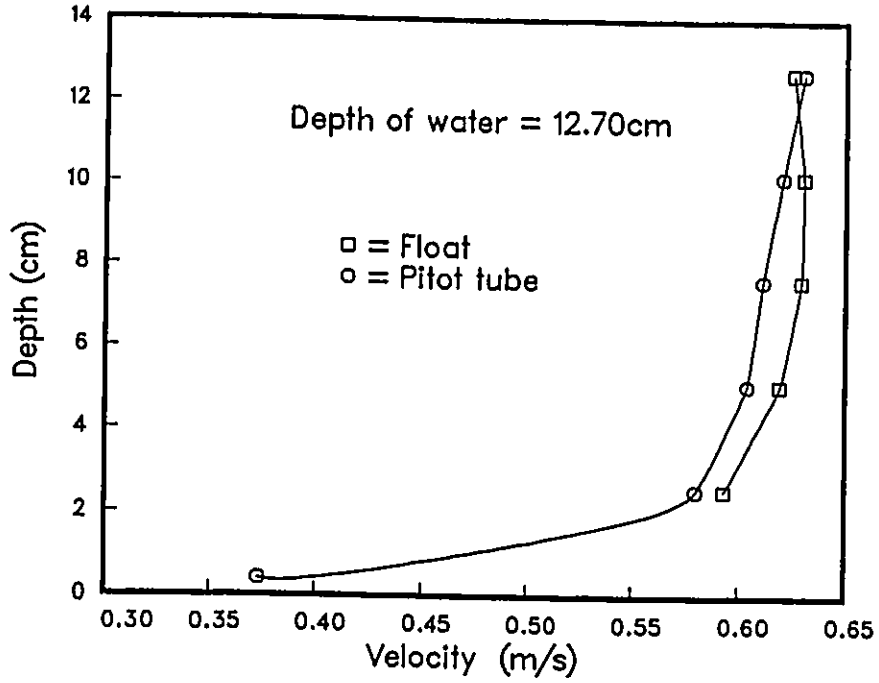

Figure 5.11: Comparison between Pitot tube and float velocity (large flume)

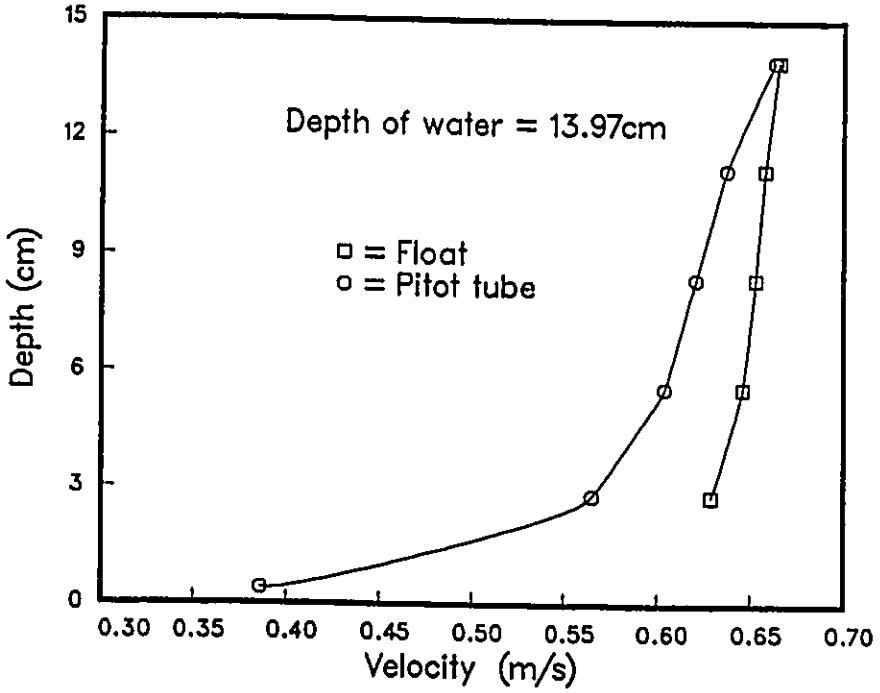

Figure 5.12: Comparison between Pitot tube and float velocity (large flume)

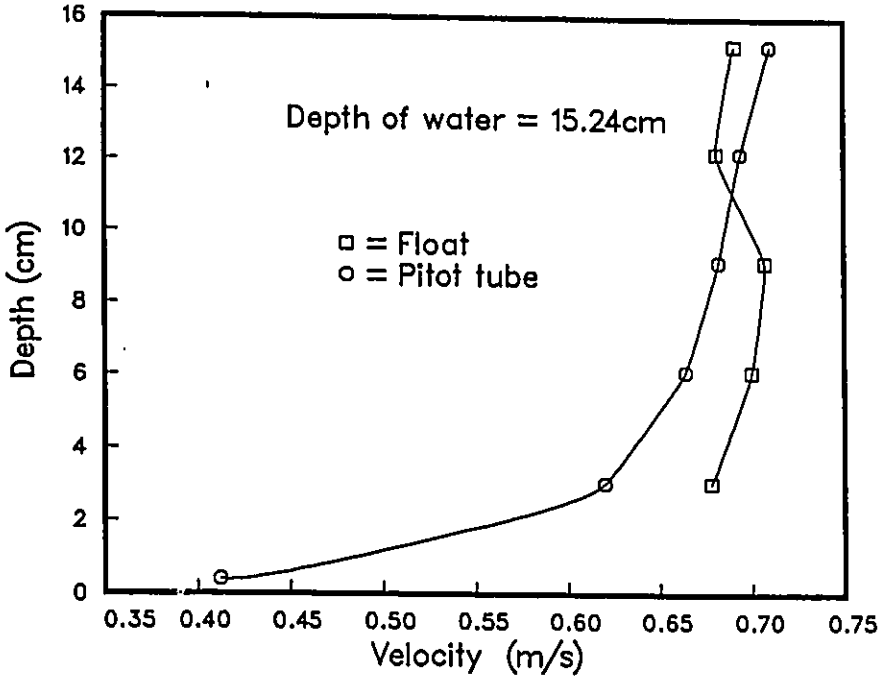

Figure 5.13: Comparison between Pitot tube and float velocity (large flume)

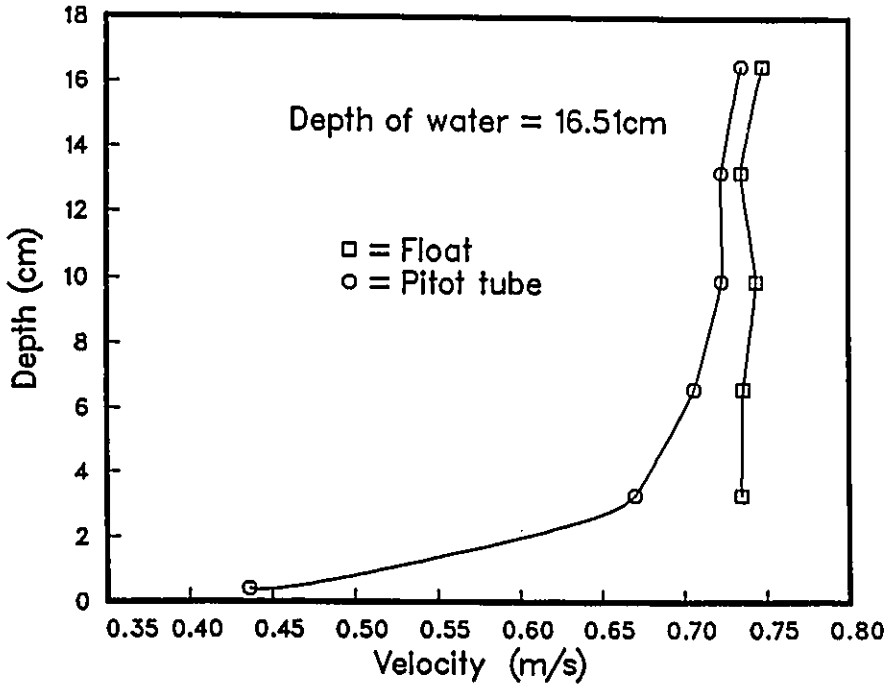

Figure 5.14: Comparison between Pitot tube and float velocity (large flume)

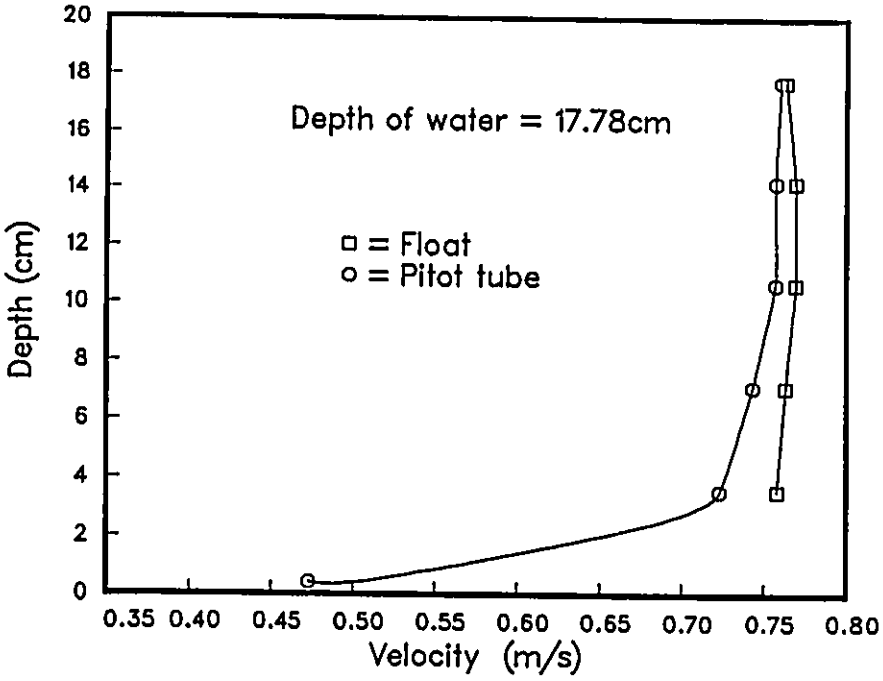

Figure 5.15: Comparison between Pitot tube and float velocity (large flume)

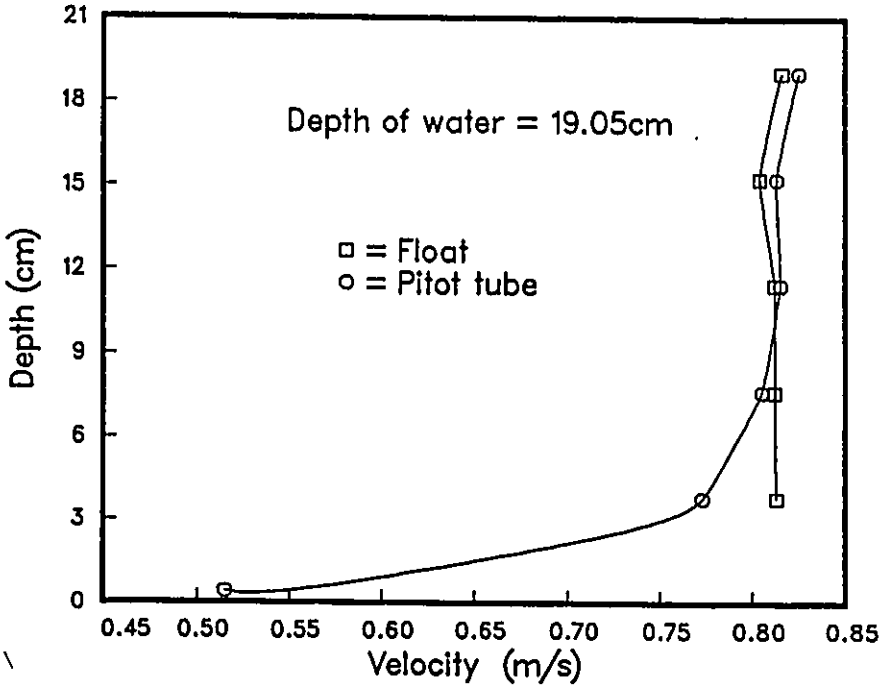

Figure 5.16: Comparison between Pitot tube and float velocity (large flume)

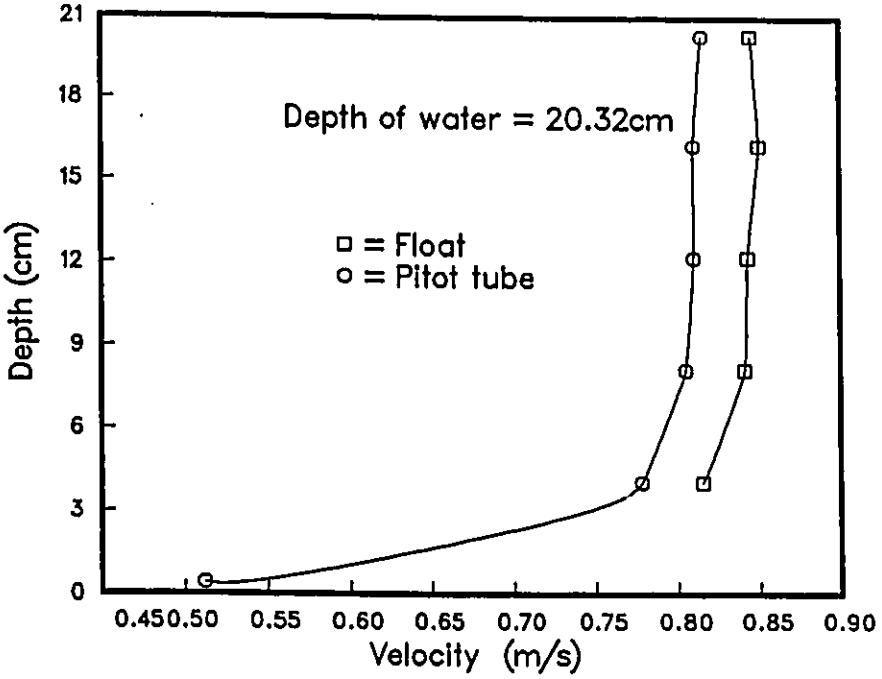

Figure 5.17: Comparison between Pitot tube and float velocity (large flume)

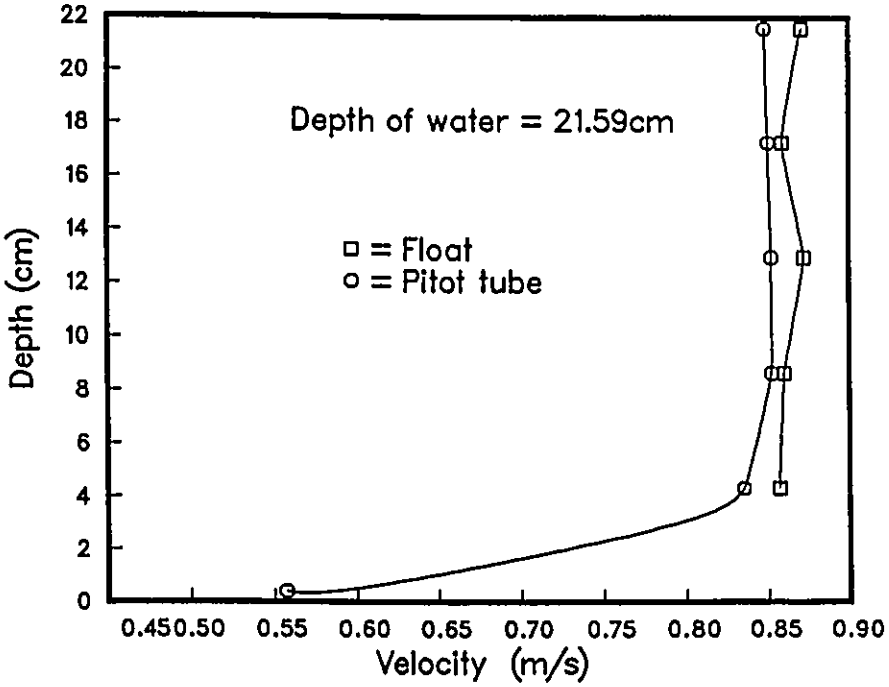

Figure 5.18: Comparison between Pitot tube and float velocity (large flume)

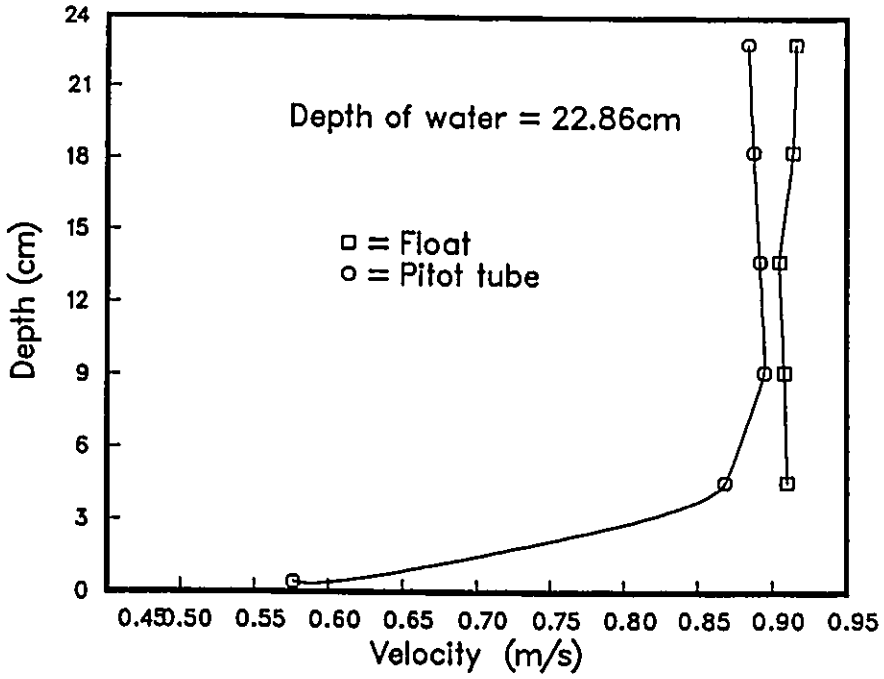

Figure 5.19: Comparison between Pitot tube and float velocity (large flume)

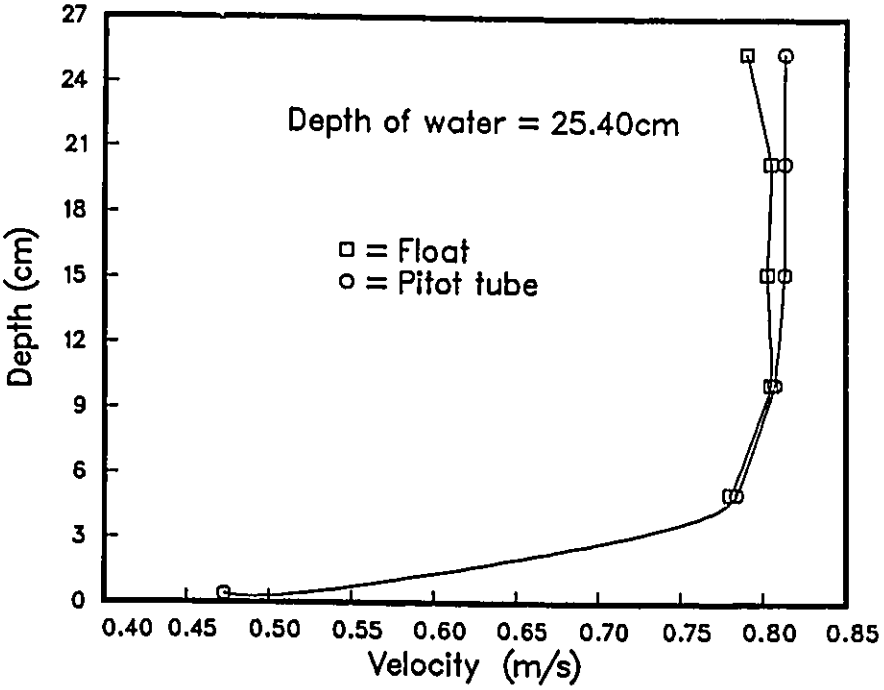

Figure 5.20: Comparison between Pitot tube and float velocity (large flume)

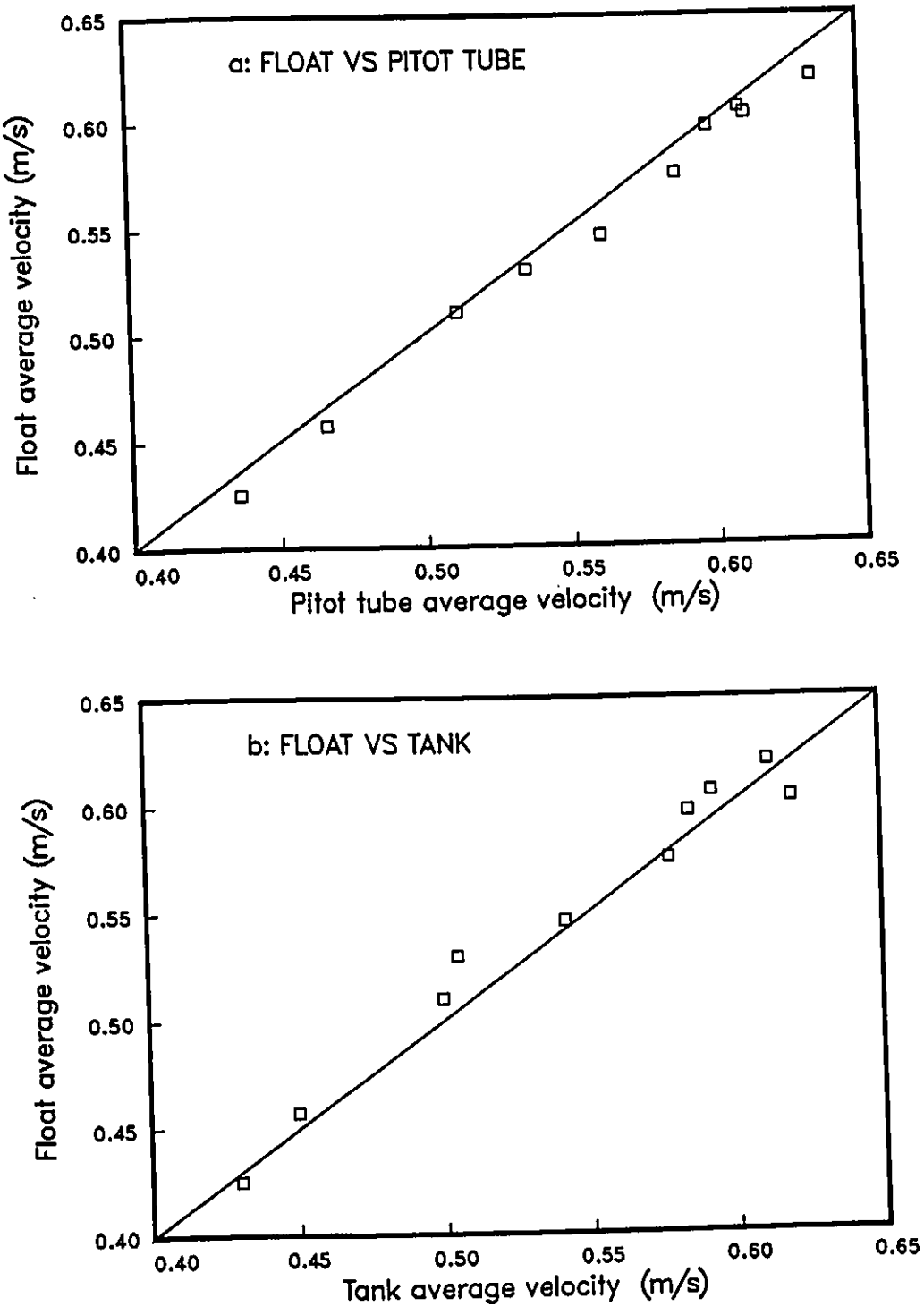

Figure 5.21: Comparison of average velocities in the small flume

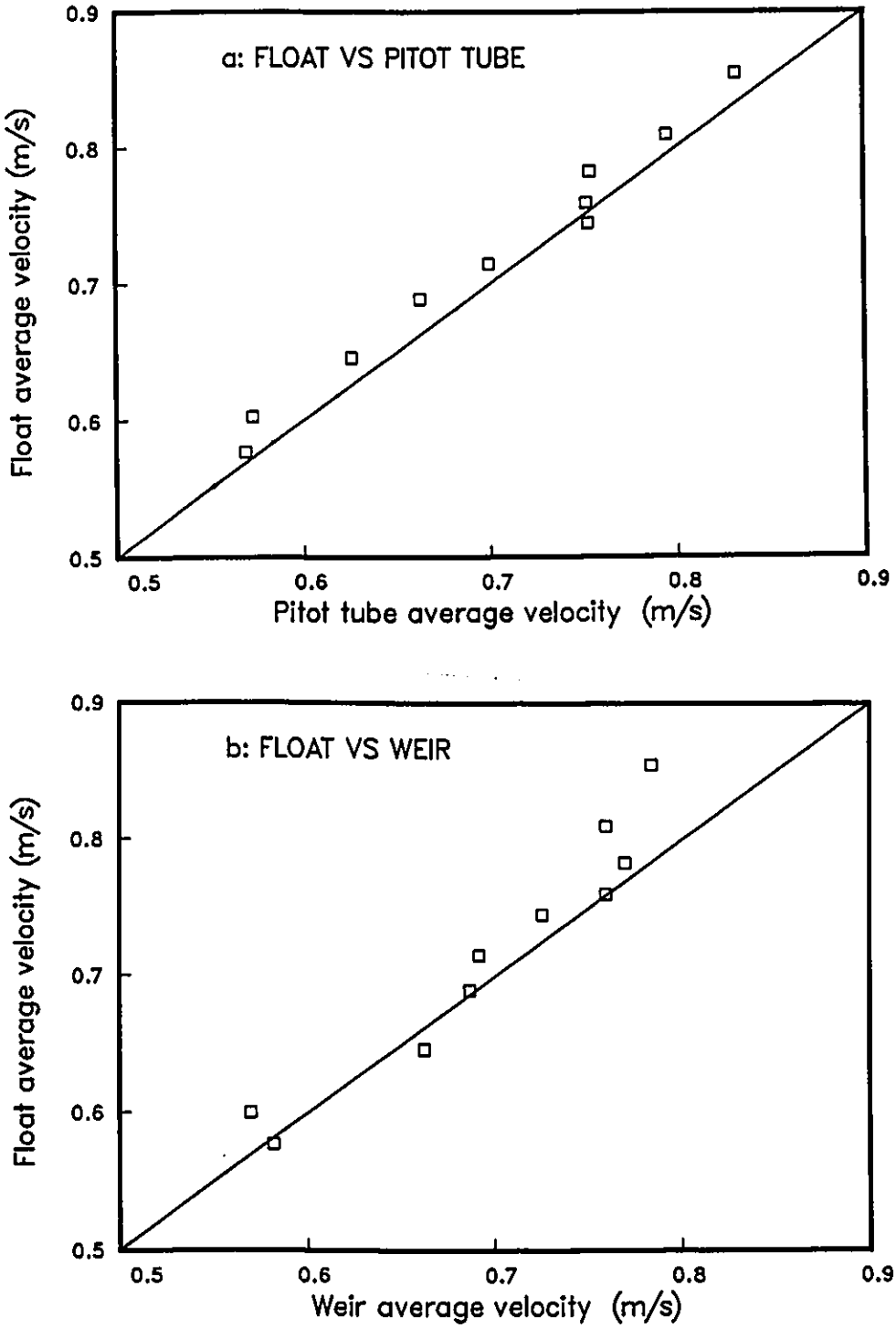

Figure 5.22: Comparison of average velocities in the large flume

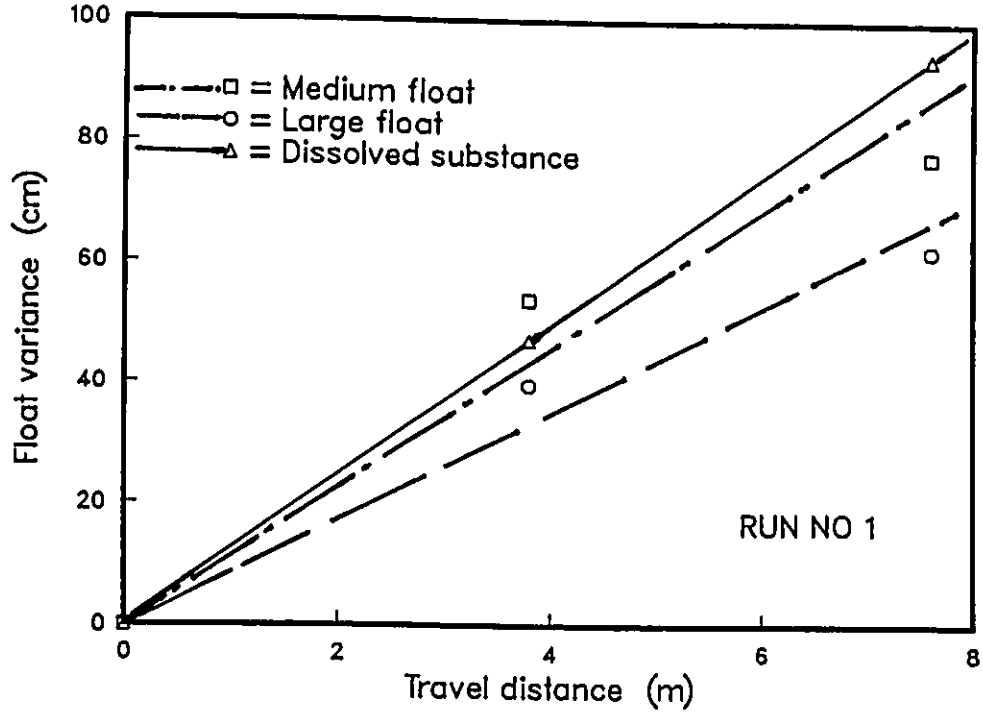

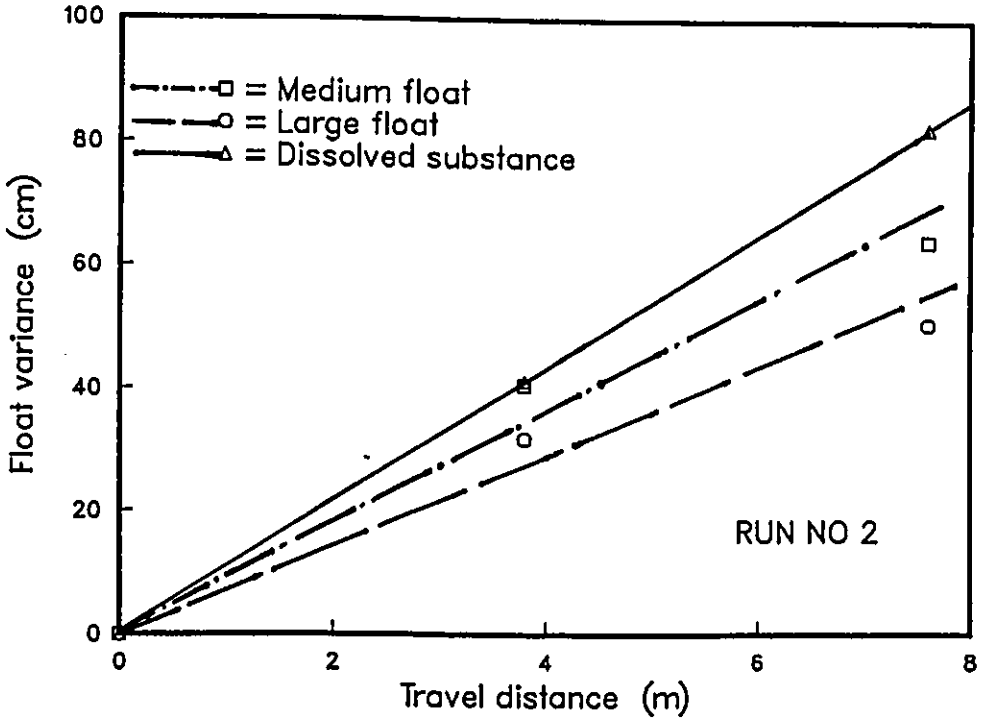

Figure 5.23: Experimental variance values plotted with the theoretical ones for a dissolved substance

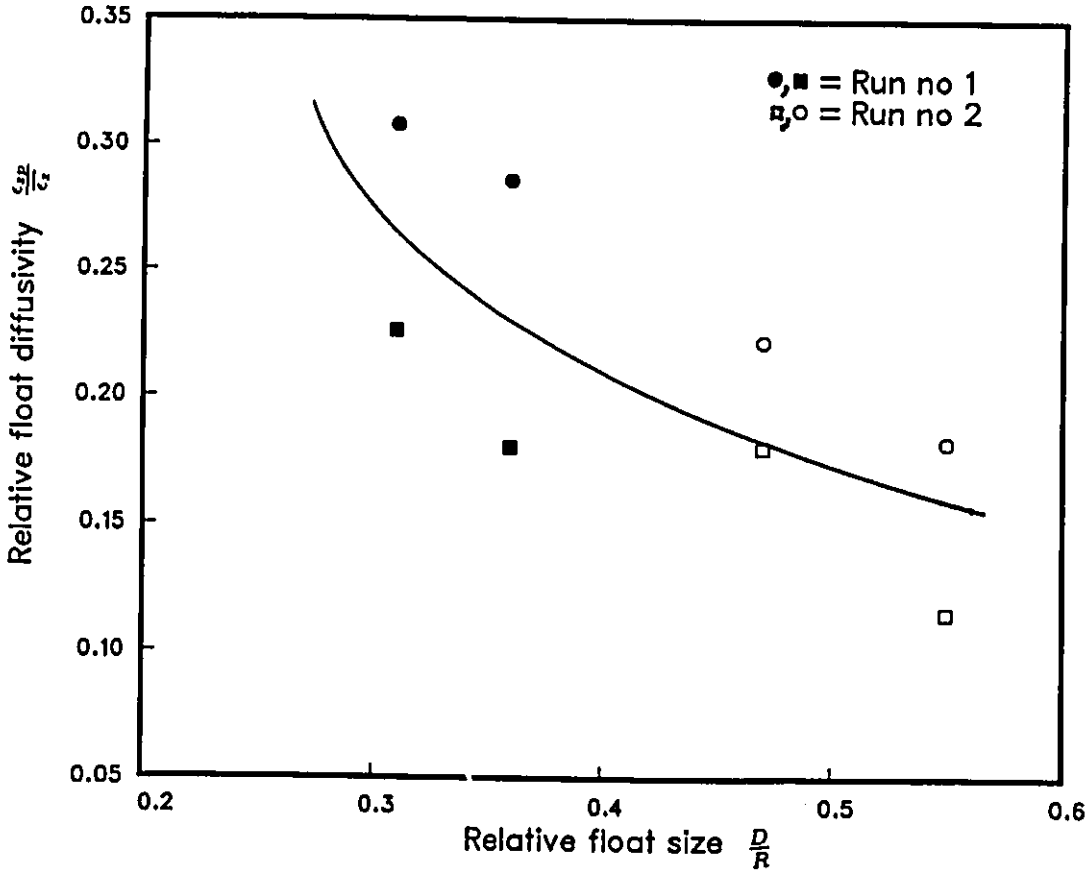

Figure 5.24: Relative float diffusivity as a function of relative float size

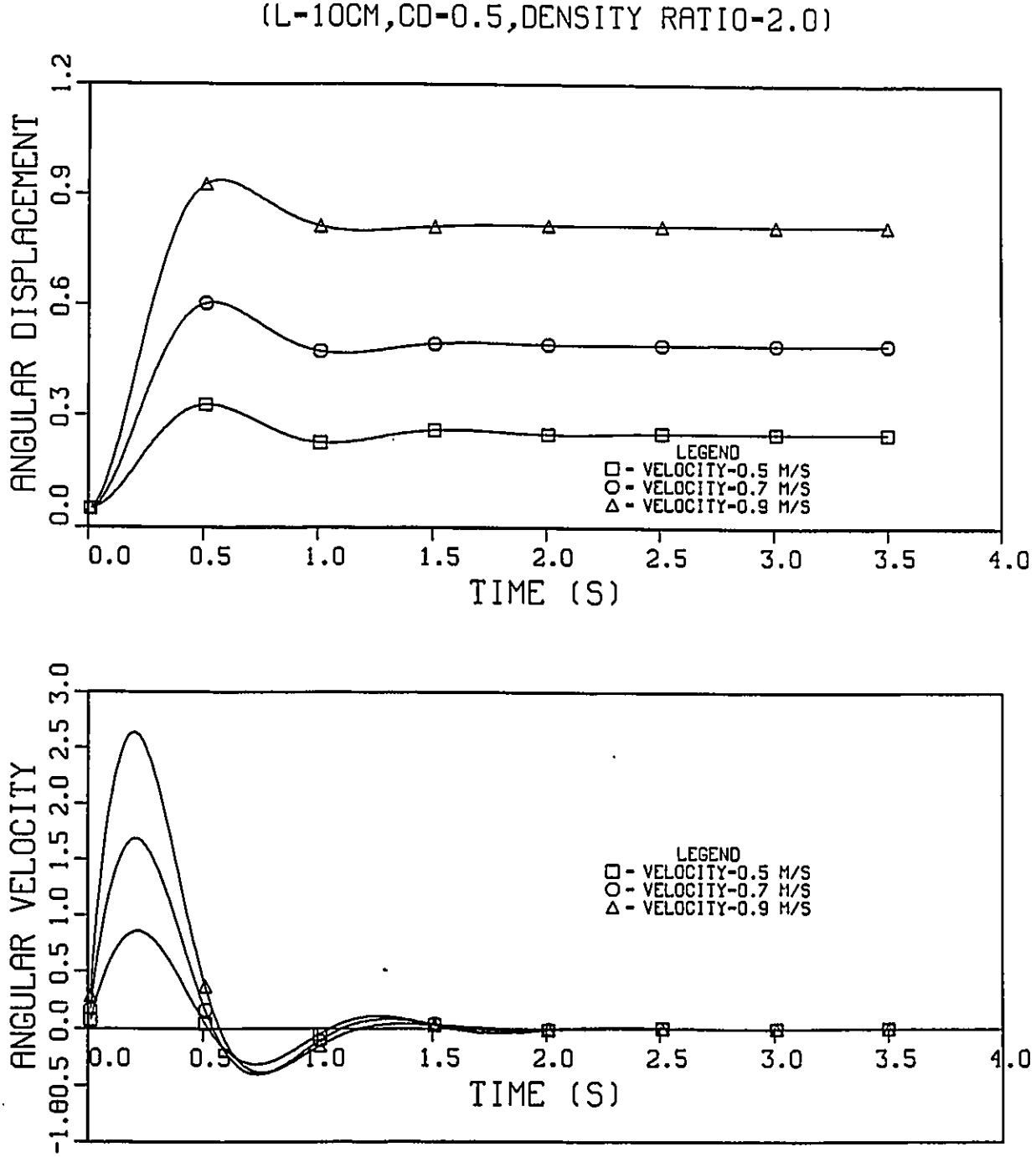

Figure 5.25: Angular velocity and displacement (case 2: density ratio=2).

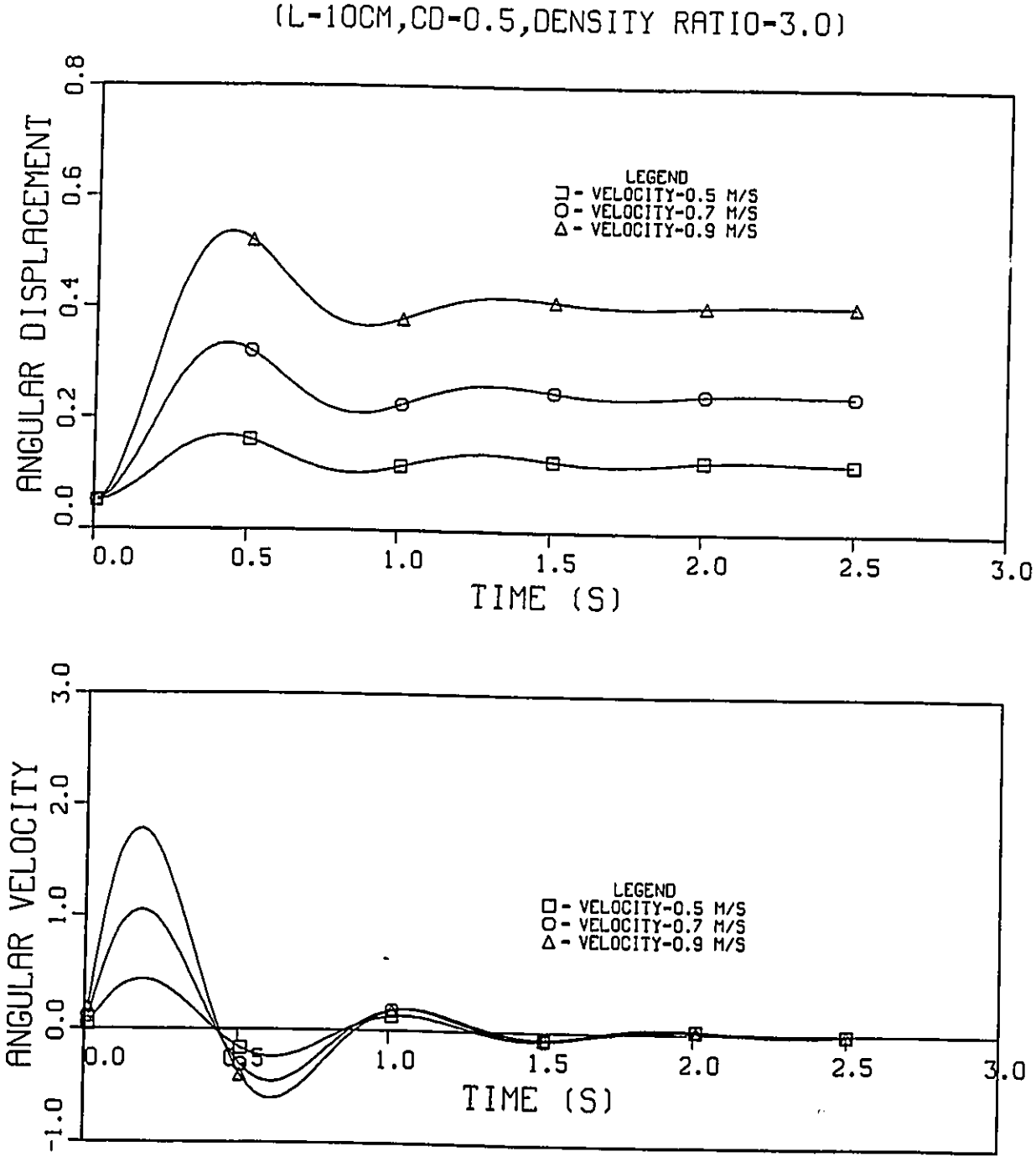

Figure 5.26: Angular velocity and displacement (case 2: density ratio=3).

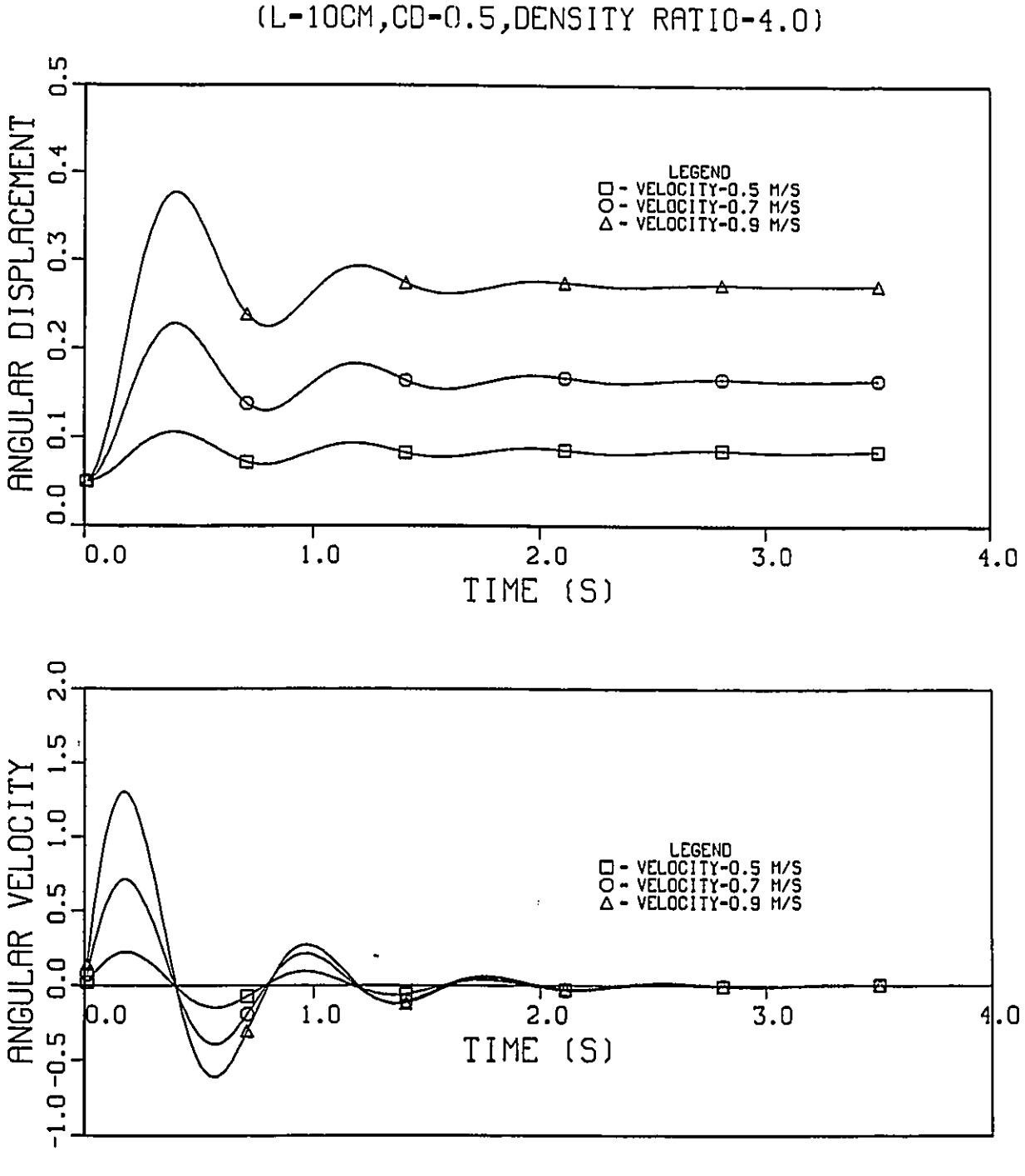

Figure 5.27: Angular velocity and displacement (case 2: density ratio=4).

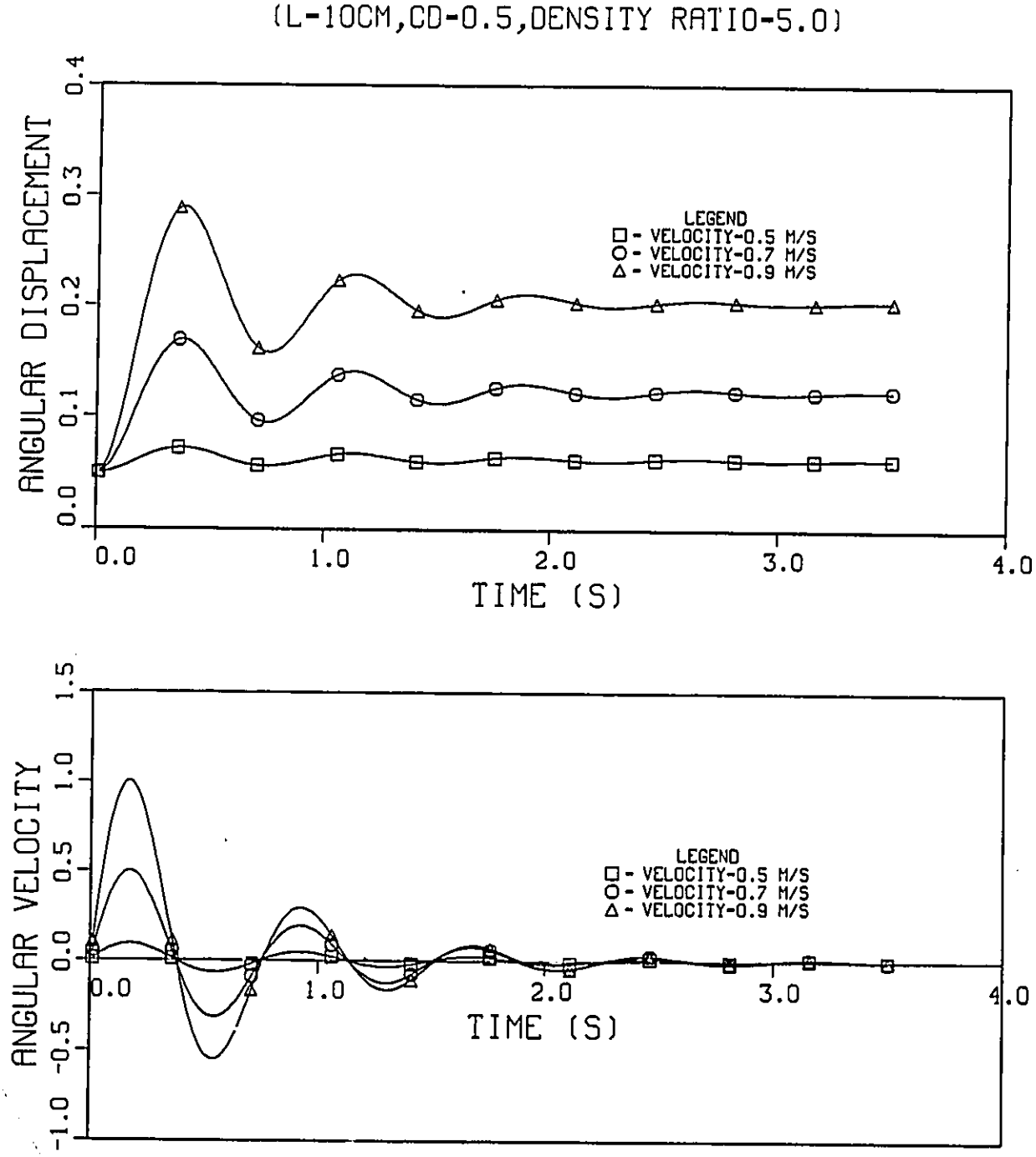

Figure 5.28: Angular velocity and displacement (case 2: density ratio=5).

Bibliography

[1] Almabruk, A. A., "Hydraulics of compound orifices.", Master's thesis, University of Ottawa, Ottawa, Ontario, 1987, p. 12.

[2] Basset A. B., "On the Descent of a Sphere in a Viscous liquid.", Quarterly Journal of Mathematics, Vol. 41, 1910, pp. 369-381.

[3] Clauser, F. H., "Advances in Applied Mechanics.", Vol. 4, New York, N.Y., 1956, p. 1.

[4] Enger, P. F., "Tractive Force Fluctuations Around an Open Channel Perimeter as Determined From Point Velocity Measurements.", presented at the April, 1961, ASCE Convention held at Phoenix, Ariz.

[5] Francis, J. R. D., and P. Minton, "Civil Engineering Hydraulics." , 1984 , Edward Arnold (publishers) Ltd .

[6] Goncharov, V. N., "Dynamics of channel flow.", 2nd ed., Israel Program For Scientific Translations, Jerusalem, 1970 (translated from Russian).

[7] Henderson, F. M., "Open-Channel Flow.", The MacMillan Co., New York, N.Y., 1966.

[8] Hoerner., S. F., "Fluid Dynamic Drag.", theoretical, experimental and statistical information, 1965 -published privately .

[9] Huffman, D. G., and Bradshaw, P., "A note on Von Karman's Constant in Low Reynolds Number Turbulent Flows.", Journal of Fluid Mechanics, Vol. 53, Part 1, 1972, pp. 55-60.

[10] Iversen., H. W. and R. Balent., "A Correlating Modulus For Fluid Resistance in Accelerated Motion.", Journal of Applied Physics, Vol. 22, No 3, March 1951, pp. 324-328 .

[11] Iwasa., Y. and Imamoto. H., "Effect of particle sizes to turbulent diffusive processes in free surface flow.", I.A.H.R, Fort Collins, Colorado, U.S.A, Vol.4, (1967).

[12] James M. Robertson, "Hydrodynamics In Theory and Application.".

[13] 11- James W. Daily and Donald R. F. Harleman., "Fluid Dynamics.",

[14] Keulegan, G. H., "Laws of Turbulent Flow in Open Channels." , Research paper RP 1151, National bureau of Standards, U.S. Department of Commerce, Washington, D.C., Vol. 21, Dec., 1938, pp. 707-741.

[15] Lawrence D. Cloutman., "Analytical solutions for the trajectories and thermal histories of unforced particulates.", American Journal of Physics, vol. 57, No. 7, July 1988, pp. 643-645 .

[16] Liu, H.,and Martin, L. D., "Analysis Of Integrating-Float Flow Measurement.", Journal of Hydraulics Division, ASCE, vol.94 No. HY5, Proc. Paper 6116, Sept., 1968, pp. 1245-1260 .

[17] Liu, H.,and Martin, L. D., "Integrating-Float Measurements at Low Velocities.", Journal of Hydraulics Division, ASCE, vol.96, No. HY1, proc. paper 7027, jan., 1970, pp. 143-151 .

[18] Lucien M. Brush, Jr., and Hau-Wong Ho and Ben-Chie Yen., "Accelerated Motion of a Sphere in a Viscous Fluid.", Journal of Hydraulics Division, ASCE, vol. 90, No. HY1, Jan., 1964, pp. 149-160 .

[19] Ludwig Prandtl., "Essentials Of Fluid Dynamics." With Applications to Hydraulics, Aeronotics, Meteorology and other subjects.

[20] Milne-Thomson, L. M., "Theoretical Hydrodynamics.", The Macmillan Company 5th ed., 1968.

[21] Ogura Y., "The theory of turbulent diffusion in the atmosphere.", Journal of meteorological science, Japan, Vol. 30,

[22] Rajaratman N., and Muralidhar D., "Boundary Shear Stress Distribution in Rectangular Open Channels.", La Houille Blanche, No. 6, 1969, pp. 603-609.

[23] Robert L. Daugherty and Joseph B. Franzini, "Fluid Mechanics With Engineering Applications.", 7th ed, 1977.

[24] Ronald E. Johnson, "Drogue Performance Evaluation. Part1: Data Acquisition.", Institute of Oceanography, Old Dominion University, Norfolk, Virginia. Technical Report No. 20, Dec. 1975.

[25] Schlichting, H., "Boundary Layer Theory.", 6th ed., McGraw-Hill Book Co., Inc., New York, N.Y., 1968.

[26] Stelson, T. E., and F. T. Mavis, "Virtual Mass and Acceleration in Fluids.", Trans. ASCE, vol 122 (1957), pp. 518-525

[27] Thomas C. Gillmer, "Modern Ship Design.", Naval Institute Press Annapolis, Maryland, Second Edition, 1977 .

[28] Townsend, A. A., "The Structure of Turbulent Shear Flow.", Cambridge University Press, New York, N.Y., 1956.

[29] Vanoni, V. A., "Velocity Distribution in Open Channels." Civil Engineering, Vol. 11, No 6, June 1941, pp 356-357.

[30] Ven Te Chow, "Open-Channel Hydraulics.", McGraw-Hill Company, Inc., New York, N.Y., 1959.

[31] Victor L. Streeter and E. Benjamin Wylie, "Fluid Mechanics." McGraw-Hill, 1981.

[32] Warnock, R. G., "Flow Characteristics and Transport of Bed Material.", Ottawa River Project, University of Ottawa-National Research Council of Canada, Report No. 2, Feb. 1974, pp. 3.1-3.47 .

[33] Warnock, R. G., "Flow Characteristics and Transport of Bed Material.", Ottawa River Project, University of Ottawa-National Research Council of Canada, Report No. 3, Jan. 1976, pp. 3.1-3.33 .

[34] Wigley., W. C. S., "Water Forces On Submerged Bodies in Motion.", Transactions Institution of Naval Architects., 95, (1953) pp. 268-279 .

Appendix

Integration of the angular velocity found in case 2

The angular velocity is of the form

$$X sin(\omega t + \phi) e^{-kt} \tag{.1}$$

The angular displacement then, can be found as follows:

$$\int sin(\omega t + \phi) e^{-kt} dt = -\frac{1}{\omega} \int e^{-kt} d(cos(\omega t + \phi)) \tag{.2}$$

$$= -\frac{1}{\omega} \left[e^{-kt} cos(\omega t + \phi) - \int cos(\omega t + \phi) d(e^{-kt}) \right] \tag{.3}$$

$$= -\frac{1}{\omega} \left[e^{-kt} cos(\omega t + \phi) + k \int cos(\omega t + \phi) e^{-kt} dt \right] \tag{.4}$$

$$= -\frac{1}{\omega} \left[e^{-kt} cos(\omega t + \phi) + \frac{k}{\omega} \int e^{-kt} d(sin(\omega t + \phi)) \right] \tag{.5}$$

$$= -\frac{1}{\omega} \left[e^{-kt} cos(\omega t + \phi) + \frac{k}{\omega} \left[e^{-kt} sin(\omega t + \phi) - \int sin(\omega t + \phi) d(e^{-kt}) \right] \right] \tag{.6}$$

$$= -\frac{1}{\omega} \left[e^{-kt} cos(\omega t + \phi) + \frac{k}{\omega} e^{-kt} sin(\omega t + \phi) + \frac{k^2}{\omega} \int sin(\omega t + \phi) e^{-kt} dt \right] \tag{.7}$$

$$= -\frac{1}{\omega} e^{-kt} cos(\omega t + \phi) - \frac{k}{\omega^2} e^{-kt} sin(\omega t + \phi) - \frac{k^2}{\omega^2} \int sin(\omega t + \phi) e^{-kt} dt \tag{.8}$$

rearranging we get

$$\int sin(\omega t + \phi) e^{-kt} dt + \frac{k^2}{\omega^2} \int sin(\omega t + \phi) e^{-kt} dt = -\frac{1}{\omega} e^{-kt} \left[cos(\omega t + \phi) + \frac{k}{\omega} sin(\omega t + \phi) \right] \tag{.9}$$

$$(1 + \frac{k^2}{\omega^2}) \int sin(\omega t + \phi) e^{-kt} dt = -\frac{1}{\omega} e^{-kt} \left[cos(\omega t + \phi) + \frac{k}{\omega} sin(\omega t + \phi) \right] \tag{.10}$$

$$\int sin(\omega t + \phi) e^{-kt} dt = \frac{-\frac{1}{\omega}}{(1 + \frac{k^2}{\omega^2})} e^{-kt} \left[cos(\omega t + \phi) + \frac{k}{\omega} sin(\omega t + \phi) \right] \tag{.11}$$

$$\int sin(\omega t + \phi)e^{-kt}dt = -\frac{\omega}{k^2 + \omega^2}e^{-kt}\left[cos(\omega t + \phi) + \frac{k}{\omega}sin(\omega t + \phi)\right] + C \tag{.12}$$

Multiplying both sides by X, one gets the expression for the angular displacement

$$X\int sin(\omega t + \phi)e^{-kt}dt = -\frac{\omega}{k^2 + \omega^2}Xe^{-kt}\left[cos(\omega t + \phi) + \frac{k}{\omega}sin(\omega t + \phi)\right] + C \tag{.13}$$

where C is the constant of integration.

```
C     SAMPLE PROGRAM TO SOLVE THE DIFFERENTIAL EQUATION OBTAIND IN CASE2 SAM00010
C     USING RUNGE-KUTTA METHOD, THEN TO PLOT THE RESULT (DENSITY RATIOS=2SAM00020
C                                                                       SAM00030
      INTEGER N,IND,NW,IER,K,IV                                         SAM00040
      REAL Y(3),C(24),W(3,9),X,TOL,XEND,T(2000),V(2000),Z(2000),U(2000) SAM00050
      COMMON VEL                                                        SAM00060
      EXTERNAL FCN1                                                     SAM00070
      CALL ANYDEV                                                       SAM00080
      DO 100 IV=1,3                                                     SAM00090
      VEL=0.5+(IV-1)*.2                                                 SAM00100
      NW=3                                                              SAM00110
      N=3                                                               SAM00120
      X=0.0                                                             SAM00130
      Y(1)=0.05                                                         SAM00140
      Y(2)=0.0                                                          SAM00150
      TOL=0.001                                                         SAM00160
      IND=1                                                             SAM00170
        DO 10 K=1,350                                                   SAM00180
          XEND=FLOAT(K)*.01                                             SAM00190
C         IF(XEND.GE.60) XEND=FLOAT(K-9)*60                             SAM00200
          CALL DVERK(N,FCN1,X,Y,XEND,TOL,IND,C,NW,W,IER)                SAM00210
C         IF (IND.LT.0.OR.IER.GT.0) GO TO 20                            SAM00220
          T(K)=XEND                                                     SAM00230
          U(K)=Y(1)                                                     SAM00240
          V(K)=Y(2)                                                     SAM00250
          Z(K)=Y(3)                                                     SAM00260
          WRITE(2,*) T(K),U(K),V(K)                                     SAM00270
   10     CONTINUE                                                      SAM00280
  100   CONTINUE                                                        SAM00290
      CALL HWROT('AUTO')                                                SAM00300
      CALL NOBRDR                                                       SAM00310
      CALL PAGE(8.5,11.)                                                SAM00320
C     CALL SWISSM                                                       SAM00330
      CALL THKFRM(0.01)                                                 SAM00340
      CALL PHYSOR(1.5,6.3)                                              SAM00350
      CALL AREA2D(6.,3.)                                                SAM00360
      CALL FRAME                                                        SAM00370
      CALL HEIGHT (.15)                                                 SAM00380
C     CALL HEADIN('ANGULAR DISPLACEMENT VS TIME$',100,1.0,1)            SAM00390
C     CALL HEADIN('FOR DIFFERENT WATER VELOCITIES$',100,1.0,3)          SAM00400
      CALL HEADIN('(L=10CM,CD=0.5,DENSITY RATIO=2.0)$',100,0.9,1)       SAM00410
C     CALL MESSAGE('(L=10CM)$',100,2.0,1.0)                             SAM00420
C     CALL MESSAGE('(L=10CM,CD=0.5,DENSITY RATIO=2.0)$',100,0.7,2.6)    SAM00430
      CALL CROSS                                                        SAM00440
      CALL XNAME('TIME (S)$',8)                                         SAM00450
      CALL YNAME('ANGULAR DISPLACEMENT$',20)                            SAM00460
      CALL GRAF(0.,0.5,4.0,0.,0.3,1.2)                                  SAM00470
      CALL HEIGHT (.08)                                                 SAM00480
      CALL LINES('VELOCITY=0.5 M/S$',IPAK,1)                            SAM00490
      CALL LINES('VELOCITY=0.7 M/S$',IPAK,2)                            SAM00500
      CALL LINES('VELOCITY=0.9 M/S$',IPAK,3)                            SAM00510
C     CALL LINES('VELOCITY=0.8 M/S$',IPAK,4)                            SAM00520
C     CALL LINES('VELOCITY=1.4 M/S$',IPAK,5)                            SAM00530
C     CALL LINES('VELOCITY=1.5 M/S$',IPAK,6)                            SAM00540
      REWIND 2                                                          SAM00550
```

```
      DO 41 JJ=1,3                                                      SAM00560
      DO 42 KK=1,350                                                    SAM00570
         READ(2,*) T(KK),U(KK)                                          SAM00580
   42 CONTINUE                                                          SAM00590
C      DO 45 I=1,500                                                    SAM00600
C         T(I)=T(I)                                                     SAM00610
C         U(I)=U(I)                                                     SAM00620
C     45 CONTINUE                                                       SAM00630
      CALL CURVE(T,U,350,50)                                            SAM00640
41    CONTINUE                                                          SAM00650
      CALL LEGEND (IPAK,3,3.4,0.1)                                      SAM00660
      CALL ENDGR(0)                                                     SAM00670
      CALL FHYSOR(1.5,2.20)                                             SAM00680
      CALL AREA2D(6.,3.)                                                SAM00690
      CALL FRAME                                                        SAM00700
      CALL HEIGHT (.15)                                                 SAM00710
C     CALL HEADIN('ANGULAR VELOCITY VS TIME$',100,1.0,1)                SAM00720
C     CALL HEADIN('FOR DIFFERENT WATER VELOCITIES$',100,1.0,3)          SAM00730
C     CALL HEADIN('(L=10CM,CD=0.5,DENSITY RATIO=2.0)$',100,0.8,1)       SAM00740
C     CALL MESSAGE('(L=10CM,CD=0.5,DENSITY RATIO=2.0)$',100,0.7,2.6)    SAM00750
      CALL XNAME('TIME (S)$',8)                                         SAM00760
      CALL YNAME('ANGULAR VELOCITY$',16)                                SAM00770
      CALL GRAF(0.,0.5,4.0,-1.,0.5,3.0)                                 SAM00780
      CALL HEIGHT (.08)                                                 SAM00790
      CALL LINES('VELOCITY=0.5 M/S$',IPAK,1)                            SAM00800
      CALL LINES('VELOCITY=0.7 M/S$',IPAK,2)                            SAM00810
      CALL LINES('VELOCITY=0.9 M/S$',IPAK,3)                            SAM00820
C     CALL LINES('VELOCITY=0.8 M/S$',IPAK,4)                            SAM00830
C     CALL LINES('VELOCITY=1.4 M/S$',IPAK,5)                            SAM00840
C     CALL LINES('VELOCITY=1.5 M/S$',IPAK,6)                            SAM00850
      REWIND 2                                                          SAM00860
      DO 51 JJ=1,3                                                      SAM00870
      DO 52 KK=1,350                                                    SAM00880
         READ(2,*) T(KK),U(KK),V(KK)                                    SAM00890
   52 CONTINUE                                                          SAM00900
      CALL CURVE(T,V,350,50)                                            SAM00910
   51 CONTINUE                                                          SAM00920
      CALL LEGEND (IPAK,3,3.4,1.5)                                      SAM00930
      CALL ENDGR(0)                                                     SAM00940
      CALL ENDPL(0)                                                     SAM00950
      CALL DONEPL                                                       SAM00960
      STOP                                                              SAM00970
      END                                                               SAM00980
      SUBROUTINE FCN1(N,X,Y,YPRIME)                                     SAM00990
      INTEGER N                                                         SAM01000
      COMMON VEL                                                        SAM01010
      REAL Y(N),YPRIME(N),X,A,B,L,D                                     SAM01020
C+++++++++++++                                                          SAM01030
      A=-39.24                                                          SAM01040
      B=-7.89                                                           SAM01050
      L=0.395                                                           SAM01060
      D=39.5                                                            SAM01070
C+++++++++++++                                                          SAM01080
      YPRIME(1)=Y(2)                                                    SAM01090
      YPRIME(2)=A*Y(1)+B*Y(2)*VEL+L*Y(2)**2+D*VEL**2                    SAM01100
```

```
      Y(3)=YPRIME(2)                                                    SAM01110
      RETURN                                                            SAM01120
      END                                                               SAM01130
```